Smart Particle Production, Characterization and Powder Forensics

By

Yuan Fang

A thesis submitted in fulfilment of the requirements of the degree

Doctor of Philosophy

Department of Chemical Engineering

Monash University

July 2010

Copyright Notices

Notice 1

Notice 2

To my family and love one

Declaration for thesis based or partially based on conjointly published or unpublished work

Monash University

Monash Research Graduate School

In accordance with Monash University Doctorate Regulation 17 / Doctor of Philosophy and Master of Philosophy (MPhil) regulations the following declarations are made:

I hereby declare that this thesis contains no material which has been accepted for the award of any other degree or diploma at any university or equivalent institution and that, to the best of my knowledge and belief, this thesis contains no material previously published or written by another person, except where due reference is made in the text of the thesis.

This thesis includes 3 original papers published in peer reviewed journals and 1 unpublished publications. The core theme of the thesis is "smart particle production, characterization and powder forensics". The ideas, development and writing up of all the papers in the thesis were the principal responsibility of myself, the candidate, working within the Department of Chemical Engineering under the supervision of Dr. Cordelia Selomulya and Prof. Xiao Dong Chen.

The inclusion of co-authors reflects the fact that the work came from active collaboration between researchers and acknowledges input into team-based research.

The following international peer-reviewed academic journal articles are presented in this thesis:

Thesis chapter	Publication title	Publication status	Nature and extent of candidate's contribution
2	On Measurement of Food Powder Reconstitution Properties	Published	Initiation, Key ideas, Literature review, Writing up [90%]
3	Characterization of Milk Protein Concentrate (MPC) Solubility using Focused Beam Reflectance Measurement (FBRM)	Published	Initiation, Key ideas, Experimental work, Development, Results interpretation, Writing up [85%]
4	On Quantifying the Dissolution Behavior of Milk Protein Concentrate	Accepted	Initiation, Key ideas, Experimental work, Development, Results interpretation, Writing up [85%]
5	Functionality of Milk Protein Concentrate: Effects of Spray Drying Temperature	In preparation	Initiation, Key ideas, Experimental work, Development, Results interpretation, Writing up [80%]

Signed: ……

(YUAN FANG)

Date: ……

Acknowledgement

This thesis is an important milestone in my life journey. It is not only a brief summary of my PhD research which consists of the experimental results and scientific discussions but also is also a gathering of all the love, friendship, guidance and help I gained in the past three years.

It is not easy to find the appropriate words to express my great gratitude to my supervisors Dr. Cordelia Selomulya and Professor Xiao Dong Chen. Their guidance, patience, understanding, encouragement, advice and support got me through many difficulties and obstacles. Their doors are always open for discussion and advice. Their feedback is always prompt to clarify doubts. Their inspiration never fails to show new ways to approach problems. Their enthusiasm showed me an inspired attitude towards life and work. They are the best supervisors I could ever ask for and I am truly honoured to be one of their students.

Many thanks go to the Monash Research Graduate School (MRGS) and Gardiner Foundation for Dairy Research for funding this project. Thanks to Dairy Innovation Australia Ltd for in-kind support of this work.

I would like to thank Dr. Sean Lin for his help in setting up the experimental setups, Dr. Yan Jin and Dr. Meng Wai Woo for the keen discussion on mathematical questions and Mr Samuel Rogers for his help with the spray drying experiments. I would also like to thank Dr. Palatasa Havea for his kind assistance with the TEM and micro XCT analysis, Dr. Jenny Ho for her advice on the Malvern Mastersizer, Dr. Sandra Ainsworth and Ms. Nicole Barnes for samples acquisition, Mr David Vowles for training on SEM, Dr. Dan Li for her help with FTIR, Dr. Peggy Chan for her advise on SDS-PAGE, Dr. Wei Shen for sharing his views and advise. My thanks also extend to all the current and former members of Biotechnology and Food Engineering Group (BFE) and Monash Advanced Particle Engineering Lab (MAPEL).

My sincere appreciation to my friends from both near and far; special thanks to Wang Ning, Wang Jian Chao, Dr. Anita Venkatanarayanan, Ying Khosravi, Hue Chen Au Yong, Thanh Nguyen, Hui Ling Tay, Amanthi Jayemanne, Ria Amelia, Xiao Pei Hoo, Rothman

Kam, Alice Yuen, Carrie Chen, Viqqi Tan. Thanks for being such great companies and the comfort whenever needed.

Finally yet important, my sincere gratitude also goes to my beloved father, mother, boyfriend and all my family members, for their unconditional love and support. Thank you for having belief in me and for encouraging me to pursue my dreams.

TABLE OF CONTENTS

ABSTRACT I

LIST OF PUBLICATIONS III

ABBREVIATIONS IV

NOMENCLATURE V

LIST OF FIGURES VII

LIST OF TABLES XI

CHAPTER 1 INTRODUCTION 12

1.1. BACKGROUND 12

1.2. RESEARCH AIM AND THESIS OUTLINE 13

1.2.1. RESEARCH AIMS 14

1.2.2. THESIS OUTLINE 15

1.3. REFERENCES 16

CHAPTER 2 LITERATURE REVIEW 18

2.1. MILK COMPOSITION 20

2.1.1. PROTEINS 20

2.1.2. LACTOSE 25

2.1.3. LIPIDS 27

2.1.4. SALTS 29

2.2. PHYSICAL AND FUNCTIONAL PROPERTIES OF MILK POWDER 30

2.2.1. DENSITY 30

2.2.2. MOISTURE CONTENT 31

2.2.3. FLOWABILITY 32

2.2.4. HEAT STABILITY 32

2.2.5. RECONSTITUTION PROPERTIES 33

2.3. STANDARD METHODS TO MEASURE POWDER DISSOLUTION IN INDUSTRY 38

2.4. Measurement techniques in the laboratories **41**
2.4.1. Wettability 41
2.4.2. Dispersibility 44
2.4.3. Solubility 45
2.5. Summary and remarks **54**
2.6. Investigation and assessment of characterization techniques **55**
2.7. References **57**

CHAPTER 3 CHARACTERIZATION OF MILK PROTEIN CONCENTRATE POWDER (MPC) SOLUBILITY USING FOCUSED BEAM REFLECTANCE MEASUREMENT (FBRM) **69**
3.1. Introduction **69**
3.2. Materials and Methods **72**
3.2.1. Materials 72
3.2.2. Experimental set up and procedure 72
3.2.3. Relative particle counts (RPC) and initial particle size 74
3.3. Results and Discussion **75**
3.3.1. Reproducibility of the solubility measurement of MPC 75
3.3.2. The effect of external factors on FBRM's MPC chord length 76
3.3.3. Defining solubility for MPC 77
3.3.4. Establishing the dissolution profiles of MPC 81
3.3.5. Particle size population analysis 82
3.3.6. Characterization of dissolution parameters with FBRM 86
3.4. Conclusion **91**
3.5. References **92**

CHAPTER 4 ON QUANTIFYING THE DISSOLUTION BEHAVIOUR OF MILK PROTEIN CONCENTRATE POWDER **95**
4.1. Introduction **95**
4.2. Material and methods **98**
4.2.1. Materials 98
4.2.2. Methods 99
4.2.2.1. Characterisation 99
4.2.2.2. Dissolution studies 99
4.2.2.3. Dissolution kinetics 101

4.3. RESULTS AND DISCUSSION **103**

4.3.1. MPC DISSOLUTION PROFILES 103

4.3.2. DISSOLUTION MODELS 106

4.3.3. DISSOLUTION PARAMETERS 108

4.3.3.1. Dissolution rate constant 108

4.3.3.2. Final particle size in suspension 111

4.4. FURTHER DISCUSSION **113**

4.5. CONCLUSION **116**

4.6. REFERENCES **118**

CHAPTER 5 FUNCTIONALITY OF MILK PROTEIN CONCENTRATE: EFFECTS OF SPRAY DRYING TEMPERATURE 122

5.1. INTRODUCTION **122**

5.2. MATERIAL AND METHODS **125**

5.2.1. MATERIAL 125

5.2.2. LABORATORY-SCALE PRODUCTION OF MPC POWDERS 125

5.2.3. PHYSICAL CHARACTERIZATION 125

5.2.4. DISSOLUTION TEST 126

5.2.5. POLYACRYLAMIDE GEL ELECTROPHORESIS 126

5.2.6. MICRO XCT 127

5.2.7. TRANSMISSION ELECTRON MICROSCOPE (TEM) 127

5.3. RESULTS AND DISCUSSION **127**

5.3.1. PHYSICAL CHARACTERIZATION 127

5.3.2. PARTICLE MORPHOLOGY 131

5.3.3. PARTICLE SOLUBILITY CHARACTERIZATION 134

5.3.4. DEGREE OF PROTEIN DENATURATION 136

5.3.5. PROTEIN-PROTEIN INTERACTION 139

5.4. CONCLUSION **140**

5.5. REFERENCES **141**

CHAPTER 6 CONCLUSIONS AND RECOMMENDATIONS 144

6.1. CONCLUSIONS **144**

6.2. RECOMMENDATIONS **145**

Appendix A Understanding Wetting Behaviour of Dairy Powder using a Flow Channel 147

A.1. Introduction 147
A.2. Experimental procedure 149
A.3. Results and discussion 154
A.4. Conclusion 157
A.5. References 157

Appendix B Understanding Milk Powder Dispersion using Turbiscan 159

B.1. Introduction 159
B.2. Experimental Setup 161
B.3. Results and Discussion 162
B.4. Conclusions 165
B.5. References 166

Appendix C Application of FBRM to Characterize the Solubility of Different Dairy Powders 168

C.1. Introduction 168
C.2. Experiment 168
C.3. Results and discussion 169
C.4. Conclusion 173
C.5. References 174

Abstract

Powdered food ingredients are common yet important in our daily life. The most well-known method to produce these powdered products is via spray drying. Nowadays, it is possible to customize the spray dried products with desired nutrition/physiochemical properties according to the requirements and demands of the consumer market. Powders resulting from different processes (or different process conditions) vary significantly in composition and the functional behaviours. This renders traditional measurement techniques for characterising spray dried products to be insufficient and inadequate. Therefore, an effective and reproducible technique to benchmark different dairy powder functionality for both manufacturers and end-users usage is necessary and remains a challenge. This thesis reports the exploration of a possible 'toolkit' to characterize dairy powder functionality, benchmarking powder dissolution kinetics, and investigate the effects of spray drying conditions on powder functionality.

A range of techniques applied in both industrial and laboratory for powder functionality characterization were reviewed, investigated and evaluated. A methodology to characterize the solubility of milk protein concentrates (MPC) using the technique Focused Beam Reflectance Measurement (FBRM) was established and presented. FBRM provides the ability to monitor *in situ* the changes in chord length with time over a wide range of suspension concentrations, which directly reflected the solubility of the investigated powder. A faster rate of the chord length reduction implied a better solubility as more particles break down and dissolve in solution. Using this protocol, the effect of water temperature for MPC powders was investigated and a characteristic dissolution profile for different MPC powders was subsequently established. Importantly, the measuring protocol of using FBRM to characterize dairy powder dissolution behaviour was established and validated.

Using the established protocol, FBRM was used to monitor the dissolution process of MPC powder, with the data applied in the development of a kinetic dissolution model based on the Noyes-Whitney equation. The model was used to estimate two key benchmarking parameters, namely the dissolution rate constant k and the final particle size in suspension d_{∞}, describing dynamic dissolution behaviors and final solubility respectively of a particular powder. The effects of dissolution temperature, storage

duration and storage temperature on dissolution properties of an MPC powder were also investigated and a quantitative understanding of relationship between process and storage conditions with powder functionality were achieved from the k and d_{∞} profiles.

Furthermore, the relationship between drying conditions and the functionalities and microstructure properties of the resulting products were established by investigating the effects of production drying air temperature on the functionality of MPC. To achieve this objective, mono-dispersed MPC particles were produced using a specially constructed dryer at selected drying air temperatures. Dissolution properties of the resulting MPC product were characterized using the established FBRM protocol, and the differences in microstructure examined from transmission electron microscopy images and micro XCT. A direct relationship between the drying air temperature and solubility was established whereby the solubility of MPC particle decreased with increasing drying air temperature. The degree of protein denaturation at different drying air temperatures was also established using gel electrophoresis. The knowledge could be used to establish a better understanding of the relationship between drying conditions and microstructures, and the corresponding influence on the functionality for different powder types.

This PhD work established the basis measurement and protocol for characterising different powder types with varying functional and physical properties, the basis modelling fundamental approach to elucidate the mechanism of powder dissolution as well as demonstrated how the application of these protocols and approaches by establishing the relationships between powder production conditions to resultant product functional and physical properties. This work is the first step to establishing a standardised toolkit to establish a powder characteristic profile library to be use for production optimisation and rapid powder functionality analysis.

List of Publications

Journal Publications:

1. Fang, Y., Selomulya, C. and Chen, X. D. (2008) On measurement of food powder reconstitution properties. *Dry. Technol.*, 26 (1): 3-14.
2. Fang, Y., Selomulya, C. and Chen, X. D. (2008) Characterization of milk protein concentrate (MPC) solubility using focused beam reflectance measurement (FBRM). *Dairy Sci. Technol.*, 90 (2-3): 253-270.
3. Fang, Y., Ainsworth, S., Palmer, M., Selomulya, C. and Chen, X. D. On quantifying the dissolution behaviour of milk protein concentrate. Food Hydrocolloids, Accepted.
4. Fang, Y., Rogers, S., Havea, P., Selomulya, C. and Chen, X. Functionality of milk protein concentrate: Effects of spray drying temperature. (In preparation for submission to Food Hydrocolloids).

Refereed Conference Proceedings:

1. Fang, Y., Selomulya, C. and Chen, X. D. On Techniques of food powder reconstitution measurements. Proceedings of CHEMECA 2007. Sofitel Melbourne, Victoria, Australia, 23-26 September, 2007.
2. Fang, Y., Selomulya, C. and Chen, X. D. Characterization of milk protein concentrate (MPC) solubility using focused beam reflectance measurement (FBRM). 4th International Symposium on Spray Dried Dairy Products. Melbourne Convention Centre, Victoria, Australia, 15-17 April, 2009.
3. Fang, Y., Ainsworth, S., Palmer, M., Selomulya, C. and Chen, X. D. Modelling dissolution kinetics of milk protein concentrate—Influence of dissolution temperature. World Congress on Particle Technology (WCPT6). Messe, Nuremberg, Germany, 26-29 April, 2010.
4. Fang, Y., Rogers, S., Selomulya, C. and Chen, X. Functionality of milk protein concentrate: Effect of spray drying temperature. Submitted to CHEMECA 2010. Hilton Adelaide, South Australia, Australia, 26-29 September, 2010.

Abbreviations

α-La	α-lactalbumin
β-Lg	β-lactoglobulin
BSA	Blood serum albumin
FBRM	Focused beam reflectance measurement
FTIR	Fourier transform infrared
IDF	International Dairy Federation
Ig	Immunoglobulins
ISI	Insolubility index
Micro XCT	X-ray microtomography
MPC	Milk protein concentrate
NaCl	Sodium chloride
NMR	Nuclear magnetic resonance
NSI	Nitrogen solubility index
PC	Particle counts
PDI	Protein dispersibility index
PVM	Particle vision and measurement
RPC	Relative particle counts
SDS-PAGE	Sodium dodecyl sulphate polyacrylamide gel eletrophoresis
SEM	Scanning electron microscopy
SLS	Static light scattering
SMP	Skim milk powder
TEM	Transmission electron microscopy
WDP	Water dispersible protein
WMP	Whole milk powder
WPC	Whey protein concentrate
WPI	Whey protein isolate
XPS	X-ray photoelectron spectroscopy

Nomenclature

$\boldsymbol{a}$	Diameter of occluded air (m)
A	Cross-section area of the flow channel (m^2)
B	Width of channel (m)
$\boldsymbol{C}$	Instantaneous concentration ($g \cdot m^{-3}$)
$\boldsymbol{C_s}$	Solubility at the end of investigation ($g \cdot m^{-3}$)
$\boldsymbol{D}$	Diffusion coefficient ($m^2 \cdot s^{-1}$)
D [v, 0.9]	The particle size that 90% (v/v) of the particles below
$\boldsymbol{d}$	The measured particle size at time t (m)
$\boldsymbol{d_0}$	The initial particle size (m)
$\boldsymbol{d_\infty}$	The final particle size at the end of the investigation (m)
$\boldsymbol{d_h}$	Hydraulic diameter
$\boldsymbol{h}$	Thickness of the diffusive boundary layer (m)
$\boldsymbol{k}$	Dissolution rate constant (s^{-1})
$\boldsymbol{k_1}$	A proportionality, $k_1 = k/S$ (s^{-1})
$\boldsymbol{l}$	Water penetrating distance
p	Wetted perimeter (m)
$\boldsymbol{r}$	Capillary radius
Re	Reynolds number
$\boldsymbol{S}$	Surface area of solute (m^{-2})
$\boldsymbol{u}$	Mean velocity ($m \cdot s^{-1}$)
$\boldsymbol{V}$	Volume of the liquid solution (m^3)
$\boldsymbol{v}$	The particle volume (m^3)
$\boldsymbol{V_{ia}}$	Volume of interstitial air
$\boldsymbol{W}$	Dissolved mass of solute at time t (g)
$\boldsymbol{W_E}$	Dissolved mass of solute at the end of the investigation (g)
$\boldsymbol{W_0}$	The initial mass of the solute particle (g)
$\boldsymbol{W_\infty}$	The mass of undissolved particle at the end of the investigation (g)
$\boldsymbol{W_t}$	The mass of undissolved particle at time t (g)
$\boldsymbol{\rho}$	Mass density of fluid ($kg \cdot m^{-3}$)
$\boldsymbol{\rho_{bulk}}$	Bulk density ($g \cdot mL^{-1}$)

$\rho_{particle}$	Particle density ($g \cdot mL^{-1}$)
γ	Surface tension of the liquid
η	Viscosity of the liquid
θ	Contact angle
μ	Dynamic viscosity (Pa·s)
T_2	Transverse relaxation time

List of Figures

Figure 1-1 Schematic illustrating the scope of the project (light arrows). Development of a protocol to characterise different types of powders produced by spray drying. This was achieved *via* experimental and modelling approaches investigating the relationships between drying and dissolution conditions, as well as the product functional properties and microstructures. The knowledge gained will aid in the product testing and optimization efforts to further improve the process and the end products. 14

Figure 2-1 Flow diagram of processing different dairy powders (Schuck, 2008) 19

Figure 2-2 Proposed casein micelle models (Fox and McSweeney, 1998b, Holt, 1992) 23

Figure 2-3 Schematic of heat-induced whey protein/κ-casein complexes in heated milk 24

Figure 2-4 α-lactose and β-lactose structure (Fox and McSweeney, 1998a) 25

Figure 2-5 Schematic of dissolution timeline for different powder types showing overlaps between different phases with time 33

Figure 2-6 IDF Method to measure wettability, dispersibility and solubility of dairy powder (Varnam and Surherland, 1994) 39

Figure 2-7 The customized device to measure the sinkability of whole milk powder 42

Figure 2-8 Schematic view of the wetting time testing device (Hla and Hogekamp, 1999) 42

Figure 2-9 Flow channel to measure the dynamic wettability (Freudig et al., 1999) 43

Figure 2-10 Using optical fibre sensor to measure dispersibility 44

Figure 2-11 Experiment setup for monitoring the reconstitution process of powders by NMR 49

Figure 2-12 Schematic of the FBRM probe 51

Figure 2-13 Schematic of a chord length (Hartman, 2007) 52

Figure 3-1 A single MPC powder rehydration (3 hours duration) .... **Error! Bookmark not defined.**

Figure 3-2 A single skim milk particle dissolution (10 second) ..... **Error! Bookmark not defined.**

Figure 3-3 Schematic of the experimental setup 73

Figure 3-4 Chord length of powder A at 20 ℃ (repeat measurement) 76

Figure 3-5 The effect of stirring speed on chord length of powder A at 50 ℃ 77

Figure 3-6 The effect of concentration on chord length of powder A at 50 ℃ 77

Figure 3-7 Results of powder A-F obtained from FBRM 78

Figure 3-8 Powder A-F chord length / insolubility against temperature 80

Figure 3-9 Chord length of the supernatant from different powders at 20°C 81

Figure 3-10 Particle population counts for fine/big particles of Powder A and Powder F 84

Figure 3-11 SEM images of powder A and F 85

Figure 3-12 Light microscopy images of Powder A and F dissolved at 20°C.....85

Figure 3-13 Normalized particle size of powder A-F 88

Figure 3-14 Normalised parameters of powder A-F (CL: chord length, ISI: insolubility index) 90

Figure 4-1 Proposed dissolution mechanism 101

Figure 4-2 FBRM results of MPC powder size change with time under different storage duration and temperatures (tested at 20 and 50 ℃ respectively) 104

Figure 4-3 Equation 4-15 and Equation 4-16 fitted with experimental data.....107

Figure 4-4 Microscopy images of fresh MPC dissolved at 20 ℃ (reference bar: 200 μm).....107

Figure 4-5 Fresh powder tested under different temperatures fitted with Equation 4-16 108

Figure 4-6 Testing temperature effect on k.....109

Figure 4-7 Storage temperature and duration effects on k (■: tested at 20 ºC; ▲: tested at 50 ºC)110

Figure 4-8 Δk for different dissolution and storage condition 110

Figure 4-9 Testing temperature effect on d_∞ (◆: fresh MPC; ■: MPC stored at 35 ºC for 2 weeks; ▲: MPC stored at 35 ºC for 2 months).....112

Figure 4-10 Storage temperature and duration effects on d_∞ (a: tested at 20 ℃; b: tested at 50 ℃)113

Figure 4-11 Fine and large particle counts over dissolution process (fresh MPC tested at 20 ℃).114

Figure 4-12 Particle size distributions of fresh powder and aged powder.....115

Figure 4-13 SEM images of fresh powder and aged powder.....116

Figure 5-1 Moisture content and particle size of powders spray dried at different temperatures...128

Figure 5-2 Light microscopy images of powders spray dried under different temperatures before dissolution and after dissolution (10 wt%, reference bar: 200 μm) 130

Figure 5-3 SEM images of 10 wt% and 20 wt% particles (dried at 90 ℃) 131

Figure 5-4 Micro XCT images of powder spray dried at 90 ℃ and 177 ℃ 132

Figure 5-5 SEM images of particles with different morphology as a result of different drying conditions 133

Figure 5-6 Schematic showing some of the different particle morphologies that may result when drying from different temperatures 134

Figure 5-7 Dissolution profile of MPC particles spray dried at different temperatures tested at 50 ℃ 135

Figure 5-8 Reducing and non-reducing SDS-PAGE gel 137

Figure 5-9 Relative change in solubility measured from integrated band intensities for the major caseins and whey proteins in the supernatants 138

Figure 5-10 TEM results of 10 wt% MPC dried at (a). 80 ℃; (b). 156 ℃; (c). 177 ℃ 140

Figure A-1 Two dimensional Wetting Distance Experimental Design by Freudig *et al.* (Freudig et al., 1999) 148

Figure A-2 Schematic setup of flow channel 149

Figure A-3 Extension of experimental setup from 2D (Wetting distance) to 3D observation (Wetting Distance and Dispersing Distance) in addition to observing the dispersion angles α 149

Figure A-4 Major component setup of designed flow channel 152

Figure A-5 Calibration plot for flow sensor with has an inconsistent output 153

Figure A-6 Calibration results of powder feeder 153

Figure A-7 Preliminary results (side camera recording image stills) of the test run for SMP and WMP at two different particle size sample groups 155

Figure A-8 Preliminary results (top down camera recording image stills) of the trial run for SMP and WMP at two different particle size sample groups 156

Figure B-1 Working principle of Turbiscan MA 2000 (Sci-Tec, 2008) 160

Figure B-2 Typical readout from Turbiscan for backscattering intensities at different time points where the x-axis denotes length of the tube from bottom (left) to top (right), y-axis denotes backscattering intensity reading and individual curves denoting independent scans at specific dissolution time-points. 161

Figure B-3 Turbiscan transmission intensity readout for SMP 163

Figure B-4 Turbiscan transmission intensity readout for WMP 164

Figure B-5 Transmission intensity of lactose solution compared with water 164

Figure B-6 Average delta-backscattering for different particle size groups in time 165

Figure C-1 Reproducibility of measuring the MPC solubility using FBRM 170

Figure C-2 Dissolution profile of SMP measured by FBRM 170

Figure C-3 Dissolution profile of WMP measured by FBRM 171

Figure C-4 Dissolution profile of MPC measured by FBRM 171

Figure C-5 Dissolution profile of WPC measured by FBRM 172

Figure C-6 Comparison of dissolution profiles of different powders measured by FBRM 173

Figure C-7 Sedimentation amounts of MPC and WPC 173

List of Tables

Table 2-1 Composition of lipids and total phospholipids in Bovine milk (weight % of total lipids) (Fox and McSweeney, 1998a) 27

Table 2-2 Main Constituents of Milk Salts 29

Table 2-3 Wettability of Different Powders with Different Particle Size Fractions 40

Table 2-4 Summary of measurements of food powder reconstitution properties 53

Table 4-1 Testing matrix for the effects of testing temperature, storage duration and temperature .99

Table 5-1 Drying conditions of 10% and 20% solids concentration 125

Table A-1 Mean feed rate, standard deviation and error percentage of the powder feeder 153

Table A-2 Testing conditions 154

Table A-3 Results of the wetting distance and the calculated wetting time 154

Table B-1 Dispersible fraction and particle size for different powder types (Fox and McSweeney, 1998) (Walstra and Jenness, 1984) (Sci-Tec, 2008) 164

Chapter 1

Introduction

1.1. Background

Dairy products are very common yet important component of our daily diet, particularly in the western world. There are many consumer food products that use different forms of dairy products in our daily life, including cheese, butter, yogurt, ice cream, infant food, instant milk powder, chocolate, energy bar, coffee, and bread. It is therefore not surprising that the worldwide demand on dairy products have been increasing over the years.

The most common form of dairy ingredients in the market is the powder form for ease of storage and transport. A widely used method to manufacture powdered products is *via* spray drying, as it is an effective process to rapidly remove water content from liquid droplets, usually within seconds (Písecký, 1997, Varnam and Surherland, 1994, Chen and Patel, 2008). It started to become popular in the dairy industry from the 1970s (Schuck, 2008). However for many years, the drying operations were predominantly based on trial and error due to the lack of scientific or technical studies and knowledge.

With the advancement in technologies, it is now possible to produce different forms of powdered products, not only in food and dairy products, but also in chemical, ceramic, polymers and pharmaceutical products (Niro, 2010). In the dairy industry, the emergence of advanced filtration technology (such as nano-filtration, micro-filtration, ultra-filtration and reverse osmosis) led to the production of a wide range of different powdered products with tailored nutritional/physicochemical properties (Písecký, 1997, Schuck, 2008). These new constituents allow the manufacturing of formula products, substitutes and adapted raw materials. These products were usually developed to meet specific consumer needs such as high protein content;

however this could alter the composition of the product leading to variations in physical and functional properties. These differences in properties potentially cause issues for both powder production and product characterization.

Furthermore, with the increase in demand, the production capacity has been significantly improved in the past decades. Improvement in production output of powdered products is now in the orders of several tons per hour per dryer using large-scale equipment (Chen and Patel, 2008, Langrish et al., 2006). It has been noted that by using the largest capacity drier available, production of up to 30 tons of powder per hour (personal communication with Dr. David Pearce) can be achieved. However, this improvement in capacity does not directly translate to an increase in efficiency, thus the optimization of the process becomes imperative under such circumstances.

With increasing varieties of product mixes and the need to improve efficiency of production, optimization in drying process requires both the improvement of the production efficiency and the resultant powder quality. To achieve these improvements, an understanding of the substrate (pre-dried powders) and product (resultant powders) properties together with the mechanisms of the processes are necessary. One critical aspect is the knowledge of the resultant product properties as powders resulting from different processes vary greatly in their functionality behaviours.

Over the years, numerous techniques have been developed to characterize powder functionality. Among the functionalities, dissolution of these products is of utmost importance to their usage (specifically as a food ingredient) as it directly affects the efficiency of the manufacturing process, quality of final products, as well as the end-user satisfaction. Current standard methods for characterizing powder dissolution properties employed in the dairy industry are developed based on ‘traditional’ powders like skim milk powder and whole milk powder. With the recent development of new powders including milk protein concentrate, caseinate powder, and whey protein isolate, the standard testing methods usually fail to distinguish between the different functionalities. Therefore the development of a robust and reproducible method for powder characterization for both traditional and newly developed powders is essential to evaluate the rehydration properties of these powders.

1.2. Research aim and thesis outline

The objective of this project was to develop a set of protocols for efficient and reproducible characterization of powder functionality. This would serve as a basis to develop a standardised method for generic benchmarking of the functional and physical characteristics for different powder types. The aim was achieved *via* both experiments and modelling to enhance the

understanding of powder dissolution kinetics. The protocols developed could be used to rapidly test newly produced powders and verify their functionality, thus reducing the time required to run various standard tests for newly produced powders while increasing the reliability of the results, which would assist in process optimization.

1.2.1. Research aims

The specific research aims were:

1) To develop a set of protocol to quantify and establish functional profiles for different powder types and conditions.
2) To quantify the dynamic behaviours of powders thus enhancing the understanding of their dissolution mechanisms. This was done by establishing the procedures for modelling the dissolution kinetics for different powder types and conditions, particularly for newly developed powders like Milk Protein Concentrates.
3) To study the effects of processing/storage conditions on powder functionality and changes in microstructure. Understanding of this relationship is useful for optimizing the drying process and to potentially reduce the production cost and improve product quality (as shown in Figure 1-1).

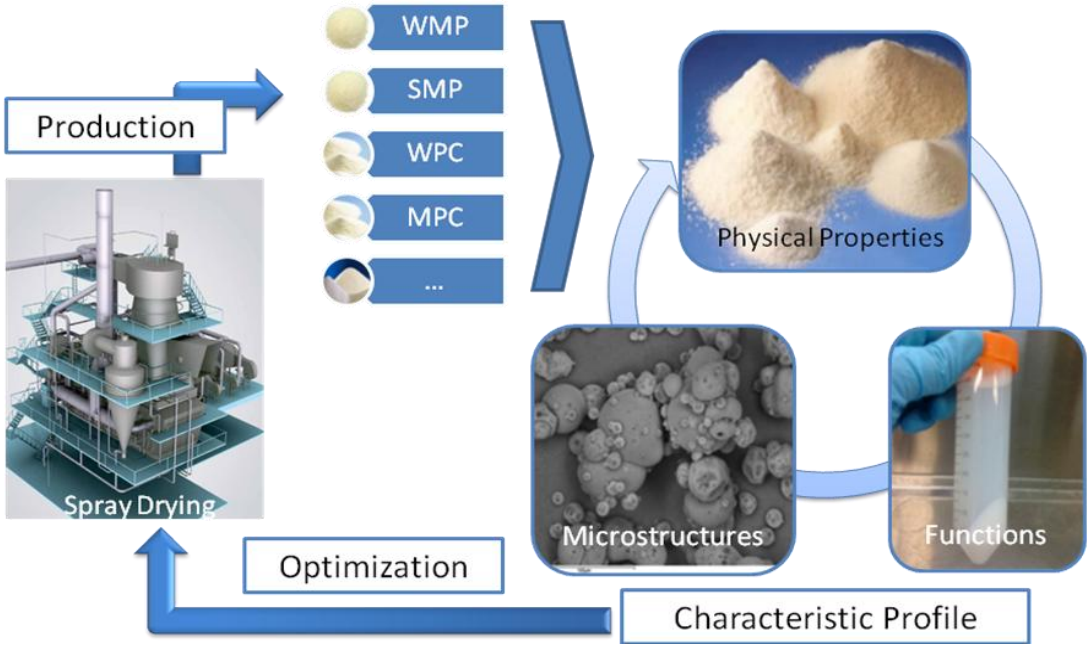

Figure 1-1 Schematic illustrating the scope of the project (light arrows). Development of a protocol to characterise different types of powders produced by spray drying. This was achieved *via* experimental and modelling approaches investigating the relationships between drying and dissolution conditions, as well as the product functional properties and microstructures. The knowledge gained will aid in the product testing and optimization efforts to further improve the process and the end products.

1.2.2. Thesis outline

The thesis is organized into 5 sections:

Chapter 2: Literature Review. This section presents a comprehensive review of the composition and physicochemical properties of milk, and an evaluation of the different testing methods employed in both industry and laboratory.

Chapter 3: Characterization of Milk Protein Concentrate (MPC) Solubility Using Focused Beam Reflectance Measurement (FBRM). In this section, a protocol to characterize the solubility of MPC using Focused Beam Reflectance Measurement (FBRM) was presented. FBRM provides the ability to monitor *in situ* the changes in chord length with time over a wide range of suspension concentrations, which directly reflects the solubility of MPC. Specifically the effect of dissolution water temperature was investigated for different MPC powders and their respective characteristic dissolution profiles were established.

Chapter 4: On Quantifying the Dissolution Behaviour of Milk Protein Concentrate. Using the measurement protocol established in Chapter 3, this section looked into modelling the milk protein concentrate dissolution kinetics. The data obtained from FBRM were applied to develop a kinetic dissolution model. The kinetic dissolution profiles for MPC under different storage and dissolution conditions were outlined and benchmarked.

Chapter 5: Functionality of Milk Protein Concentrate: Effects of Spray Drying Temperature. Using the measurement protocol established in Chapter 3, this section investigated the effect of spray drying temperature on the resultant MPC particle's functionality and microstructure. Mono-dispersed MPC particles were produced and applied in this work to improve the comparability by removing the variability in terms of surface area and particle size between the samples. The relationship between the manufacturing conditions, resultant powder microstructure and resultant functionality were established.

Chapter 6: Conclusion and future work. This section summarized the major findings of this PhD project. Recommendations for the further exploration in the field of dairy powder characterization were proposed.

1.3. References

CHEN, X. D. & PATEL, K. C. 2008. Manufacturing Better Quality Food Powders from Spray Drying and Subsequent Treatments. *Drying Technology: An International Journal,* 26**,** 1313 - 1318.

LANGRISH, T. A. G., MARQUEZ, N. & KOTA, K. 2006. An Investigation and Quantitative Assessment of Particle Shape in Milk Powders from a Laboratory-Scale Spray Dryer. *Drying Technology: An International Journal,* 24**,** 1619 - 1630.

NIRO. 2010. *Spray Drying Information from GEA Niro* [Online]. Søborg, Denmark: GEA Niro. Available: http://www.niro.com/niro/cmsdoc.nsf/WebDoc/ndkk5hmc6zSprayDryersSprayDryers [Accessed 7th July 2010].

PÍŠECKÝ, J. 1997. *Handbook of Milk Powder Manufacture,* Copenhagen, Denmark, Niro A/S.

SCHUCK, P. 2008. Effects of drying on milk proteins. *In:* ABBY, T., MIKE, B. & HARJINDER, S. (eds.) *Milk Proteins.* San Diego: Academic Press.

VARNAM, A. H. & SURHERLAND, J. P. 1994. *Milk Powder Technology: Evaporation and Spray Drying,* Copenhagen, Denmark, NIRO A/S.

Monash University

Declaration for Thesis Chapter Two

In the case of Chapter 2, the nature and extent of my contribution to the work was the following:

Name	% contribution	Nature of contribution
Yuan Fang	90%	Initiation, Key ideas, Literature review, Writing up
Dr. Cordelia Selomulya	5%	Initiation, Key ideas, Review
Prof. Xiao Dong Chen	5%	Initiation, Key ideas, Review

Declaration by co-authors

The undersigned hereby certify that:

(1) they meet the criteria for authorship in that they have participated in the conception, execution, or interpretation, of at least that part of the publication in their field of expertise;
(2) they take public responsibility for their part of the publication, except for the responsible author who accepts overall responsibility for the publication;
(3) there are no other authors of the publication according to these criteria;
(4) potential conflicts of interest have been disclosed to (a) granting bodies, (b) the editor or publisher of journals or other publications, and (c) the head of the responsible academic unit; and
(5) the original data are stored at the following location(s) and will be held for at least five years from the date indicated below:

Location(s)	**Department of Chemical Engineering, Monash University** **Clayton campus, Australia**

Signature		
Signature		
Signature		

Chapter 2

Literature Review

With the advancement of modern technologies (such as ultra-filtration, nano-filtration, to name a few) in recent years, it is now possible to customize different types of dairy powders to meet the requirement of end-users, both functionally and nutritionally. Consequently, powders with different compositions have since been produced using different manufacturing processes (Figure 1). The differences in chemical composition between these powders lead to greatly distinctive physical properties and functional behaviours between powder types and thus, rendering traditional testing methods inadequate to sufficiently characterize these powders. Therefore, to be able to characterize these new generation powders, it is necessary to firstly understand the importance of the powder's individual particle composition (on the micro scale-level) and correlate this with the respective functional behaviours (on the macro scale-level). Secondly, current and recent methods of particle measurements and characterization techniques were reviewed and investigated in an attempt to establish an integrated technique(s) which will allow the full range of reconstitution profiles of these new powders to be measured and predicted.

This chapter is divided into the following sections:

1) Milk composition
2) Physical and functional properties of milk powder
3) Measurement techniques employed in industry
4) Measurement techniques employed in laboratories
5) Summary and remarks
6) Investigation and assessment of characterization techniques

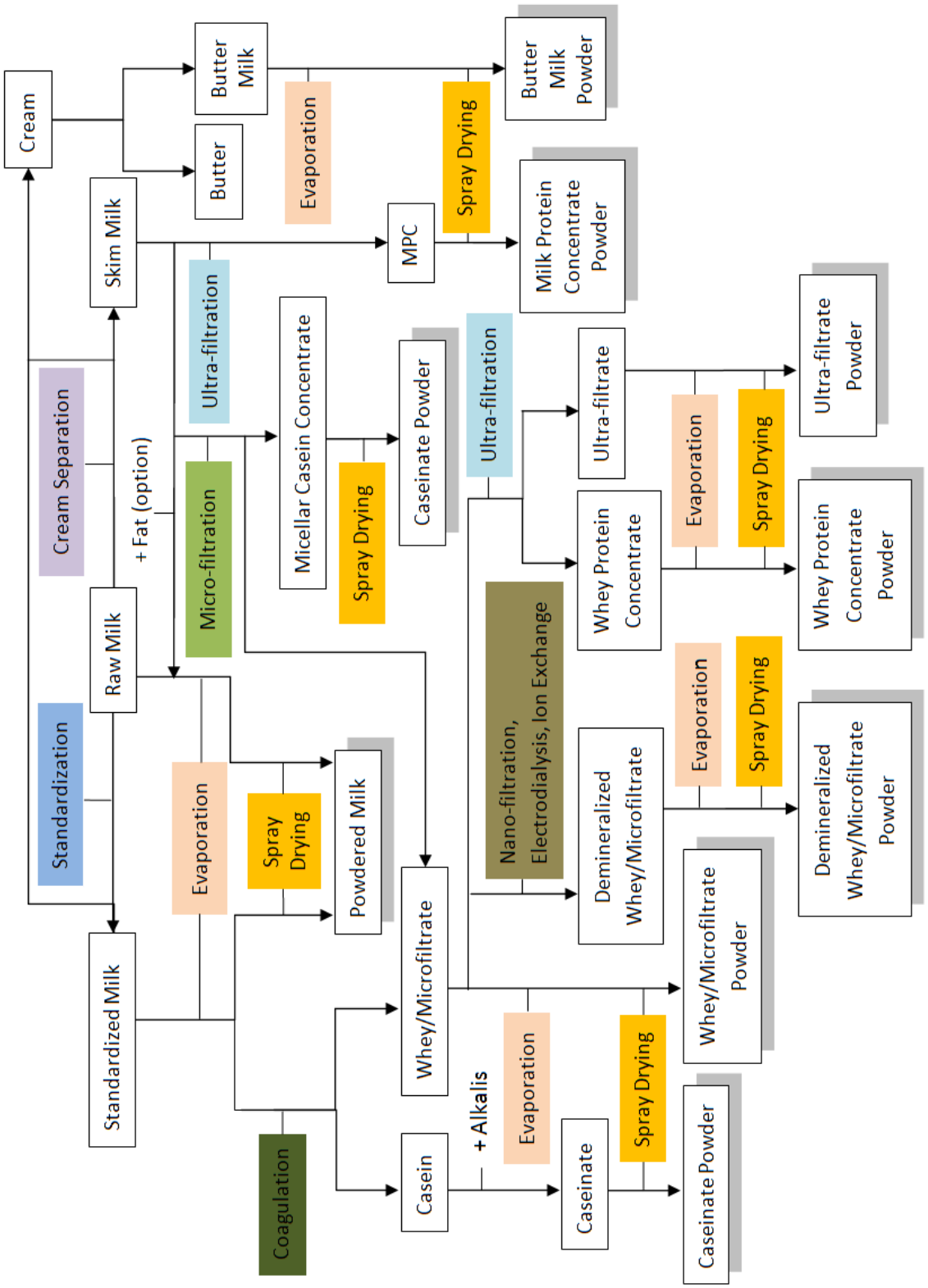

Figure 2-1 Flow diagram of processing different dairy powders (Schuck, 2008)

2.1. Milk composition

Milk is a very complex system consisting of many components in several states of dispersion. The understanding of milk composition is of key importance for both the manufacturing process as well as end-user value. Previous studies have emphasized that milk's natural variation involves differences in their chemical composition, physical properties, size and stability of structural elements. These variations are due to the following (Walstra and Jenness, 1984):

- Genetic: between different species or between individuals.
- Physiological: particularly stage of lactation, as well as age, estrus, and gestation.
- Environmental: particularly feed, and also climate and stress.

In spite of the complexity, raw milk is still made up of basic components comprising water, protein, lipid, lactose and traces of salts. In order to extend the shelf life of milk and reduce transportation cost, the raw milk is subjected to spray drying, so that the water can be rapidly removed from the solid (within seconds) without excessive heating of the product. This rapid dehydration process minimizes the degree of degradation of protein and fat contents, which in turn, helps to extend the shelf life of the powdered products without affecting the nutritional and functional value. The stability of milk powder is governed by the physical state of its component chemical compounds. The properties of different components have varying effects on milk powder properties. For example, protein is heat sensitive, and denatured when subjected to high temperatures even for a short period of time, and consequently affects the heat stability of milk. High moisture content promotes lactose crystallization, which directly affects the dissolution properties of milk. Lipid has a wide range of melting point which promotes caking of milk powders. These examples of key components affecting milk powder properties highlight the need to understand their roles and functions in milk powders which will in turn help in the understanding of the resulting powder functionality behaviours.

2.1.1. Proteins

Different types of dairy products have different properties and nutritional value which gives these products their quality and value. These specific properties of dairy products are mainly dependent on the properties of the protein content they possess, although other

components, such as fat, lactose and salts, do play very significant modifying roles (Fox and McSweeney, 1998a). For example, bovine milk contains about 5.3 g of nitrogen per kilogram, among this, about 95% is in the form of proteins—approximately 32 $g.kg^{-1}$ (Walstra and Jenness, 1984). Milk proteins have interesting functional properties, including emulsification of milk fat globule, stabilization of ionic and colloidal minerals, pH buffering, rennet action in cheese curd formation, foaming expansion and gelation in cultured and sterile milk products, etc. Therefore, milk proteins are widely used as ingredients in many applications, such as bakery products, confectionary food and beverages (Morr, 1985, Thomas et al., 2004). Recently, with the development of new technologies like ultra-filtration, micro-filtration, nano-filtration and reverse osmosis, several customized dairy products based on milk protein have been developed, such as milk protein concentrate (MPC), whey protein concentrate (WPC), micellar casein concentrate (MCC), whey protein isolate (WPI) and sodium caseinate (NaCas) etc. Most of these products are used as nutritional or functional ingredients in different applications (Schuck, 2008).

Generally, milk proteins can be classified into two main groups. When milk is subjected to conditions of pH 4.6 at 20^{o}C, about 80% of the **total protein** in bovine milk will precipitate out of solution (Fox and McSweeney, 1998b, Fox, 2001, Fox and McSweeney, 2003a, Walstra and Jenness, 1984). The fraction that precipitates out is known as **casein** while the rest of the protein remaining in solution is known as **whey protein**. Both caseins and whey proteins have widely varied nature and very different molecular and physicochemical properties. The following is a brief summary of key properties of casein and whey protein (Fox and McSweeney, 1998b, Fox, 2001, Fox, 2008):

i. **Solubility** *at pH 4.6*: caseins are insoluble whereas whey proteins remain in the solution;
ii. **Heat stability**: caseins are highly heat stable whereas whey proteins are heat sensitive;
iii. **Amino acid composition**: caseins contain high level of proline and they are phosphorylated, whereas the principal whey proteins are not;
iv. **Physical state in milk**: whey proteins exist as monomers or as small quaternary structures, whereas caseins exist in large aggregates known as micelles;
v. **Heterogeneous**: both caseins and whey proteins contain several different proteins.

Therefore, there are significant differences between caseins and whey proteins; more details on casein and whey protein are as follows.

2.1.1.1. Casein

Casein can be considered a critical component as it is the protein that is attributed to most of the characteristics of milk (P śeck ý, 1997). It is relatively hydrophobic in nature, amphipathic with randomly or flexibly structured molecule and has relatively low levels of secondary and tertiary structures (Fox and McSweeney, 1998b). The primary structural characteristic of casein is that polar and apolar residues are not uniformly distributed but rather occur in clusters, giving rise to hydrophobic and hydrophilic regions which makes caseins good emulsifiers (Fox and McSweeney, 1998b).

The casein family has four distinct forms, namely α_{s1}-, α_{s2}-, β- and κ-caseins which are approximately 37, 10, 35 and 12% of the whole casein mass respectively (Fox and McSweeney, 1998b, Fox and McSweeney, 2003b). In milk, caseins occur naturally and associate with themselves and with each other, forming supramolecules called casein micelles (Fox, 2001, Fox and McSweeney, 1998a, Walstra and Jenness, 1984, Donato and Guyomarc'h, 2009). These micelles are large colloidal particles which make up about 95% of casein in milk (Fox and McSweeney, 1998b). The main function of casein micelle is to fluidize the casein molecules and solubilise the calcium and phosphate (Qi, 2007).

In many years of dairy research, there are many different models proposed to describe the composition and structure of the micelle (Fox and McSweeney, 1998b, Fox and McSweeney, 2003b, Qi, 2007). One well known model is the sub-micelle model proposed by Morr in 1967 (Fox and McSweeney, 1998b, Fox and McSweeney, 2003b, Walstra and Jenness, 1984, Walstra, 1999) and another model known as the open model developed by Carl Holt in 1992 (Holt, 1992, Holt, 1998). In the sub-micelle model, Morr proposed that casein micelle consists of several sub-micelles linked together by calcium phosphate (Fox and McSweeney, 1998b, Figure 2-2a). For individual sub-micelle, κ-casein content various from one another. However, there are certain rules: the κ-casein-deficient sub-micelles are located in the interior of the micelles with the κ-casein-rich sub-micelles concentrated at the surface. For α_{s1}-caseins, α_{s2}-caseins and β-caseins, they are wrapped in the centre of the sub-micelles due to their hydrophobic nature with relatively few exposed on the surface. These sub-micelles are held together by calcium phosphate (Walstra, 1990). The hydrophilic terminal of κ-casein protrudes from the surface, forming a ‘hairy’ layer, which plays a role in stabilizing casein micelles in the aqua system, preventing micelles from aggregating with one another. In 1992, Holt modified the sub-micelle model

by proposing that the casein micelle is a tangled web of flexible casein molecules forming a gel-like structure (Fox and McSweeney, 1998b, Holt, 1992, Figure 2-2b). Calcium phosphate serves an integral role in holding the caseins together forming sub-clusters while the κ-casein is predominantly located on the surface of the micelles, extending their hydrophilic terminal regions into the aqua phase to form a 'hairy' layer.

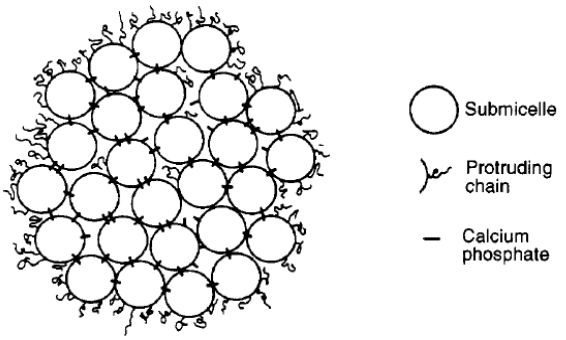

Sub-micelle model of casein micelle (adapted from P. Fox and P. MacSweeney, 1998)

Model of the casein micelle (adapted from Holt, 1992)

Figure 2-2 Proposed casein micelle models (Fox and McSweeney, 1998b, Holt, 1992)

There are still disagreements in the current literature on how to model the structure of the casein micelle but what is generally accepted is the stability of casein micelle. They are very stable even at high temperatures, coagulating only after heating up to 140 ^{o}C for 15-20 minutes at the natural pH of milk (Fox and McSweeney., 1998b, Walstra, 1990). This is primarily due to steric repulsion caused by the hairs of κ-casein. However, the hairs of κ-casein can change their configuration and lead to formation of lasting contact of the micelles (Walstra, 1990, Walstra and Jenness, 1984). Casein micelles are also quite stable under high pressure, high compactness, and high concentration of calcium. All these features of casein micelle are very important for dairy manufacturing as they enable the nutrients to remain intact under such conditions.

In summary, casein micelle plays a vital role in providing nutrition to the newborn, contributing to the amino acids content as well as calcium and inorganic phosphate composition of milk.

2.1.1.2. Whey protein

Major applications of whey protein include uses in dietetic and energetic products, or in infant formulas (Thomas et al., 2004). Whey protein is a water soluble globular protein which has high levels of secondary, tertiary and in most cases, quaternary structures (Fox,

2001, P śeck ý, 1997). Whey protein can be classified into four main types: β-lactoglobulin (β-Lg), α-lactalbumin (α-La), blood serum albumin (BSA) and immunoglobulins (Ig).

Generally, whey protein is very easily denatured upon heating, and the denaturation of whey protein is irreversible (Fox and McSweeney, 1998b). Upon heating to a high enough temperature and duration, whey protein starts to unfold, exposing the hydrophobic amino acid residues that are usually hidden deep within the protein. These hydrophobic residues will associate with the hydrophilic environment, such as κ-casein on the micelle surface, forming aggregates (Fox and McSweeney, 2003b, Donato and Guyomarc'h, 2009, Anema and Li, 2003, Corredig and Dalgleish, 1999, Singh, 2004). It has been identified that there is a direct interaction between whey protein (β-Lg) and casein micelles *via* the κ-casein on the micelle (Corredig and Dalgleish, 1999). This association with casein mainly involves β-Lg but may also involves α-La (Corredig and Dalgleish, 1999).

β-Lg/κ-casein complexes can be found in both micelles and the serum (Donato and Guyomarc'h, 2009), where the distribution between these two locations are dependent on various environmental factors. One such factor is the pH, upon application of heat, if the pH is less than pH 6.7, whey protein adhere to the casein micelle surface, whereas heating at higher pH values (e.g. 7.0) results in the dissociation of denatured whey protein/κ-casein complexes from the micelles (Figure 2-3) (Lucey et al., 1998, Corredig and Dalgleish, 1999).

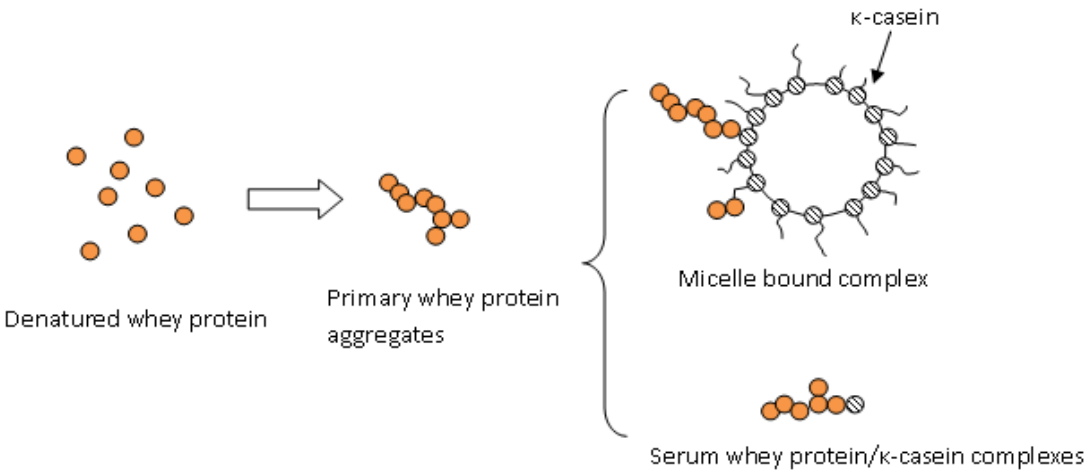

Figure 2-3 Schematic of heat-induced whey protein/κ-casein complexes in heated milk

The association of whey protein and casein micelle increases the size of the micelle, consequently induces loss of protein solubility (Anema and Li, 2003, Fox and

McSweeney, 1998b). Anema and Li reported that the changes in casein micelle size poorly correlated with the total levels of denatured whey proteins, but rather correlated well with the level of denatured whey proteins that were associated with the casein micelles (Anema and Li, 2003). They also found that the rate of denaturation of whey proteins was faster than the rate of association of the denatured whey protein with casein micelles (Anema and Li, 2003).

It has been reported that during the manufacturing process, most of the whey protein denaturation and association with casein micelle occurred in the preheating process, whereas the evaporation and drying process have little influence (Oldfield et al., 2005). However, during storage of milk protein concentrate, it is found that most of the insoluble materials are mainly casein rather than whey protein, and there are no evidence to suggest that the β-Lg/κ-casein complexes are involved in the formation of insoluble materials (Havea, 2006, Anema et al., 2006).

2.1.2. Lactose

Lactose is a major component of dairy products with whole milk powder containing 30% lactose and skim milk powder containing 50% lactose (Thomas et al., 2004). Structurally, protein, fat and air are dispersed in a continuous phase of amorphous solid lactose. Therefore, the amount of lactose in milk has a major impact on the properties of resultant milk powder as the concentration of lactose in milk powder will affect the microstructure of the powder (P śeck ý, 1997). From the nutritional point of view, lactose is the principal carbohydrate and an important energy source in milk, which promotes absorption of calcium, magnesium and manganese (Nasirpour et al., 2006). Chemically, lactose is a disaccharide consisting of galactose and glucose. There are two isomers of lactose: α-lactose and β-lactose. The structure of α-lactose and β-lactose are as shown in Figure 2-4.

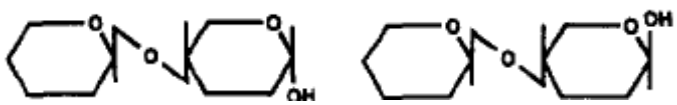

Figure 2-4 α-lactose and β-lactose structure (Fox and McSweeney, 1998a)

There are significant differences between α- and β-lactose, namely (Fox and McSweeney, 1998b):

- Solubility

- Crystal shape and size
- Hygroscopicity of crystal form
- Specific rotation
- Taste

The form of lactose existing in the milk system can significantly influence the solubility. There is a lactose equilibrium that exists in solution caused by the conversion between these two forms. When either isomer is dissolved in water, the two isoforms interchange between each other until equilibrium is established. The equilibrium constant β/α is 1.68 at 20˚C (Fox and McSweeney, 1998a, Kelly et al., 2003), temperature-dependent and is not affected by pH (Kelly et al., 2003).

Physically, lactose exists as an amorphous glass at temperatures below its glass transition temperature (Tg = 101 ℃) (Thomas et al., 2004). In the production of milk powder, water evaporation during spray drying is fast enough such that the lactose does not fully crystallize, but instead remains in the powder form as amorphous lactose. The amorphous lactose is very hygroscopic and absorbs water readily at moderate or high relative humidity (Kelly et al., 2003). When amorphous lactose absorbs sufficient water during storage, molecular plasticization of the lactose occurs and decreases the Tg. When Tg goes below the storage temperature, physical damages to the dairy powders occur, such as lactose crystallization, increased stickiness, and increased degree of caking (Jouppila et al., 1997, Jouppila and Roos, 1994b, Jouppila and Roos, 1994a, Thomas et al., 2004).

The crystallization of lactose has a very important impact on milk powder dissolution properties. Studies have shown that crystallization of lactose induces the migration of internal fat onto the particle surface (McKenna, 1997, Thomas et al., 2004). The hydrophobic nature of the free fat on surface makes it difficult for water to penetrate the particle and as a result, decreases the wettability of milk powder (Aguilar and Ziegler, 1994). On the other hand, the crystallization of lactose induces caking of milk powder, reduces the porosity of the particle surface, reducing the surface area and consequently reducing wettability. Even if the powder is stored at relatively low temperatures, the wettability of milk powder still decreases with increasing storage duration.

2.1.3. Lipids

Milk lipids serve as a source and storage of energy, therefore the fat content of milk will largely reflect the energy requirement of the specific species (Fox and McSweeney, 1998a). Fat also provides essential fatty acid and fat soluble vitamins, such as A, D and E (German and Dillard, 2006). Furthermore, fat is responsible for the flavour and rheological properties of milk powder (Huppertz and Kelly, 2006). Therefore, for many years, milk products' economical value is mainly or based completely on the fat content of the milk (Fox and McSweeney, 1998a).

Due to the apolar nature of lipid, there is a large surface tension between lipid and water. Hence, milk lipids usually exist in the form of globules, which is surrounded by a layer known as milk lipid globule membrane (MLGM) and are dispersed within the aqueous phase of milk. This membrane serves to prevent the fat globules from flocculation and coalescence, and protects the fat against enzymatic actions (Walstra and Jenness, 1984, Kaylegian, 1995). The lipid globules size ranges from 1 to 10 μm (average 3-4 μm) with very large surface areas (Burgess, 2001, German and Dillard, 2006). The MLGM consists of protein, phospholipids, and glycerides (Jensen, 2002, Burgess, 2001, Fox and McSweeney, 1992) and plays a very significant functional role for milk lipids by serving as a emulsion stabilizer, preventing globules from coalescing thus preventing lipids from lipolysis and oxidation reactions (Burgess, 2001, Jensen, 2002). Within the MLGM, 97-98% of the lipids is made up of triglycerides of different randomly arranged fatty acids (Burgess, 2001). The composition of milk lipids is as shown in Table 2-1 with the phospholipids making up less than 1% of the total lipid content. Nonetheless, phospholipids play a particularly important role in the MLGM because of their mixed hydrophilic and hydrophobic nature.

Milk contains a considerable amount of fat-soluble vitamins (Fox and McSweeney, 1998a). The chemical and physical properties of lipids mainly depend on the chemical class, each lipid class consisting of many different kinds of molecules with varying component of fatty acid residues. This fatty acid pattern is an important factor in determining lipid properties, such as melting range, chemical reactivity and nutritional value (Kaylegian, 1995).

Table 2-1 Composition of lipids and total phospholipids in Bovine milk (weight % of total lipids) (Fox and McSweeney, 1998a)

Lipid class	Total lipid weight %
Triacylglycerols	97.5
Diacylglycerols	0.36
Monoacylglycerols	0.027
Cholestery esters	Trace
Cholesterol	0.31
Free fatty acids	0.027
Phospholipids	0.6

Another type of lipid is known as "free fat", which occurs when the lipids are insufficiently enclosed by the membrane, or the membrane are damaged due to contact with air bubbles, agitation or coalescence (Fox and McSweeney, 1992, Huppertz and Kelly, 2006, Kaylegian, 1995, Thomas et al., 2004). Studies have shown that lipids residing on the surface of powders are mainly free fat, forming different types of physical patterns, for example pools or irregular patches or a thick fatty layer (Kim et al., 2002, Kim et al., 2003, Nijdam and Langrish, 2006). Under this surface layer of lipids comes the protein-covered fat globule and protein (Kim et al., 2003). Kim *et al*. proposed'binary' diffusivity ratio between each component with reference to lactose which could explain the high surface coverage of free fat on the spray dried dairy powders during drying (Kim et al., 2003). Nijdam and Langrish showed that a small change in the average fat content at low fat concentration resulted in a large change in the surface fat coverage (Nijdam and Langrish, 2006). In addition, Nijdam and Langrish also found that the milk particle size decreases with increasing fat content, which could be due to changes in the surface tension during the atomization process (Nijdam and Langrish, 2006). Gaiani *et al*. reported a strong correlation between the powder wettability and the migration of lipids on the powder surface during storage (Gaiani et al., 2007a). Marabi *et al*. investigated the correlation between the fat content and the dissolution enthalpy (Marabi et al., 2008) and found that dairy powder exhibited exothermic dissolution behaviour possibly due to the amorphous state of main components. However, the exothermic response decreases with increasing fat content which consequently decreases the dissolution rate (Marabi et al., 2008).

Another important physical property of milk lipids is the melting temperature range. The melting temperature range of milk lipids is relatively wide, ranging from -40 ℃ to +40

℃, giving rise to milk fat having different phases (solid and liquid) coexisting at a particular temperature (over the wide range of temperatures) during processing and use (Kaylegian, 1995, Burgess, 2001). As mentioned earlier in section 2.1.2, the amorphous lactose crystallization may cause fat content to expel onto the powder surface. During storage or processing, some surface free fat might melt and flow over the surface of the particle, contributing to caking as the temperature is reduced. The effect of melting fat on caking is directly related to the proportion of crystallized fat and inversely related to the final cooling temperature (Foster et al., 2005, Nijdam and Langrish, 2006). Therefore, amorphous lactose is the primary cause of caking with free fat compounding the effect.

2.1.4. Salts

Milk salts are low molecular weight substances present in milk as ions, excluding apolar lipids and proteins. Salt content in milk remains relatively constant at about 0.7-0.8% and the main constituents of milk salts are as presented in Table 2-2 (Fox and McSweeney, 1998a, Walstra and Jenness, 1984).

Table 2-2 Main Constituents of Milk Salts

Cationic	mmol/kg	Anionic	mmol/kg
Sodium(23)[1]	17-28	Chloride(35.5)	22-34
Potassium(39.1)	31-43	Carbonate[2](60)	~2
Calcium(40.1)	26-32	Sulphate (96.1)	~1
Magnesium (24.3)	4-6	Phosphate[3] (95)	19-23
Amines	~1.5	Citrate[4] (189)	7-11
		Organic acids[5]	~2
		Phosphoric esters[6]	2-4

Note: [1]: Within parentheses is the atomic or residue weight

[2]: Including CO_2

[3]: Inorganic only

[4]: About 1% of this is isocitrate

[5]: Other than citric acid

[6]: Some also contain a basic group

Among these cations, calcium and magnesium are the most important. Milk salts are present in various forms, some as a completely dissolved phase, whereas those with higher concentrations exist partly as a soluble form and partly as an insoluble colloidal form associated with casein micelles (Fox, 2008). Casein micelles contain un-dissolved calcium phosphate, as well as some magnesium, citrate and traces of other elements (Fox, 2008, Fox and McSweeney, 1997).

2.2. Physical and functional properties of milk powder

The physical and functional properties of dairy powders are determined by its components and composition as discussed in the previous section. The composition of the primary components of the powders clearly affects the resulting powder's properties, either exerting the influence independently or in conjunction with other components. Furthermore, the effects of raw substrate quality and composition, as well as operational manufacturing conditions should not be disregarded. As such, the following section will describe key properties of the resulting milk powders and the effect changes in conditions and raw substrate properties have on the resultant powder properties.

2.2.1. Density

For milk powder, there are two types of densities to evaluate the quality of the final product, namely the **bulk density** and the **particle density** (Westergaard, 1994). The bulk density is widely used in industry due to its relation to the shipment, package and storage. High bulk density can reduce the shipping volume, reducing packing material and storage capacity. The bulk density is expressed as the weight per volume unit of a powder and in practice is expressed in g/cm^3, kg/m^3 and g/100mL and it is affected by the number and intensity of tapping to compact the powders. The bulk density is a complex property involving many other factors such as those listed:

- Solid density and occluded air
- Particle size distribution and particle shape
- Agglomeration degree

With regards to the amount of occluded air in the powders, it has been noted that low-heat products always have higher occluded air contents than high-heat products (P ś eck ý,

1997). This is due to the foaming ability of high protein content which is reduced by high heat treatment (P šeck ý, 1997).

In terms of particle size distribution, the more homogenous the milk powder particle size is, the more 'ideal' the milk powder is considered to be. However homogeneity is undesirable for bulk density (Westergaard, 1994) as uniform particle size will result in low bulk density caused by the relative large space between particles (where smaller size particles will be able to occupy in a inhomogeneous powder mixture). Hence, a wide particle size distribution is desirable for bulk density so that small particles can fill in the space between medium and large particles, consequently improving the bulk density.

Particle density includes both the solid density and occluded air density. The solid density is a result of the raw material composition, whereas the occluded air content is mainly influenced by the processing condition. From the difference between bulk density and particle density, the amount of interstitial air can be calculated as follows (Westergaard, 1994) in Equation 2-1:

$$Via = \frac{100}{\rho_{bulk}} - \frac{100}{\rho_{particle}}$$

Equation 2-1

where V_{ia} - volume of interstitial air in mL/100g powder

ρ_{bulk} - bulk density in g/mL

$\rho_{particle}$ - particle density in g/mL

2.2.2. Moisture Content

All milk powder contains certain degree of residual moisture. The moisture content in the milk powder will affect its shelf life, deteriorate its functionality and cause bacteriological problem. These issues are brought about potentially by protein denaturation, lactose crystallizing and Maillard reaction (Maillard reaction is a browning reaction caused by external heat where the powder may even become brown and lumpy). Therefore, the final moisture content of the milk powder is very important. The numerous kinds of powdered products have specification defining the maximum permissible level (Westergaard, 1994, P šeck ý, 1997). In the current manufacturing process, a second drying stage (fluidized bed)

is employed to further reduce the moisture content of the particles, as well as for coating, product cooling and particle selection (Chen and Patel, 2008).

2.2.3. Flowability

As many dairy powders are cohesive in nature, the flowability of powders becomes an important attribute for determining the ease of handling, processing and for final application (Fitzpatrick et al., 2007). The flowability of dairy powder is a complex phenomenon. In terms of microstructure, flowability depends on the inter- and intra-particle forces defined as the resistance of particle to flow (Kelly et al., 2003). In terms of macrostructure, it depends on the particle size and shape, surface structure, particle density, bulk density, moisture content and fat content (Kim et al., 2005). The flowability of milk powder can be categorized in the following descending order of flowability: 1) agglomerated SMP, 2) SMP, 3) agglomerated WMP, 4) WMP (Kelly et al., 2003). Kim *et al.* found that the surface composition of particle, especially that of the free fat content on the particle, strongly influences powder flowability (Kim et al., 2005). It has also been reported that a significant increase in cohesion occurs at the smaller size range of between 20-40 μm (Fitzpatrick et al., 2007). Furthermore, Fitzpatrick and co-worker reported that powder with higher amorphous lactose content form lumps more easily and causes caking. This is caused by the hygroscopic nature of amorphous lactose which absorb moisture easily when it comes into contact with air (Fitzpatrick et al., 2007).

2.2.4. Heat stability

Heat stability is an issue that is present in any process in which the substrate is subjected to heating. One of the key consequences of heat instability is precipitation by coagulation which is primarily caused by proteins which includes casein and lacto-albumin. Precipitation can consequently bring about variations in resulting powder's properties or functionality with a wider range of precipitation sizes. It is hard to determine the degree of heat instability of more directly level of precipitation as they occur even during characterization or analytic investigations whereby the powder has to be subjected to heating. Generally, there are four main factors affecting the heat stability of milk powder (P ś eck ý, 1997):

- The basic properties of raw milk
- The manufacturing process

- The physical structure of the resulting powder
- The conditions of the test method

It has been noted that pre-heat treatment of milk can enhance the heat stability of milk powder (Kelly et al., 2003).

2.2.5. Reconstitution Properties

Reconstitution or dissolution of food powder generally consists of four steps or phases:

- Wetting of powder particles
- Sinking
- Dispersing, and finally
- Particles completely dissolving into solution.

The dissolution process generally takes place in the sequence as indicated above. However, different phases often overlap as shown in Figure 2-5 (Chen, 1992), such that observing each phase independently of each other would be a challenge (Schubert, 1993). These identified phases lead to the four important reconstitution properties of food powder; namely wettability, sinkability, dispersibility, and solubility.

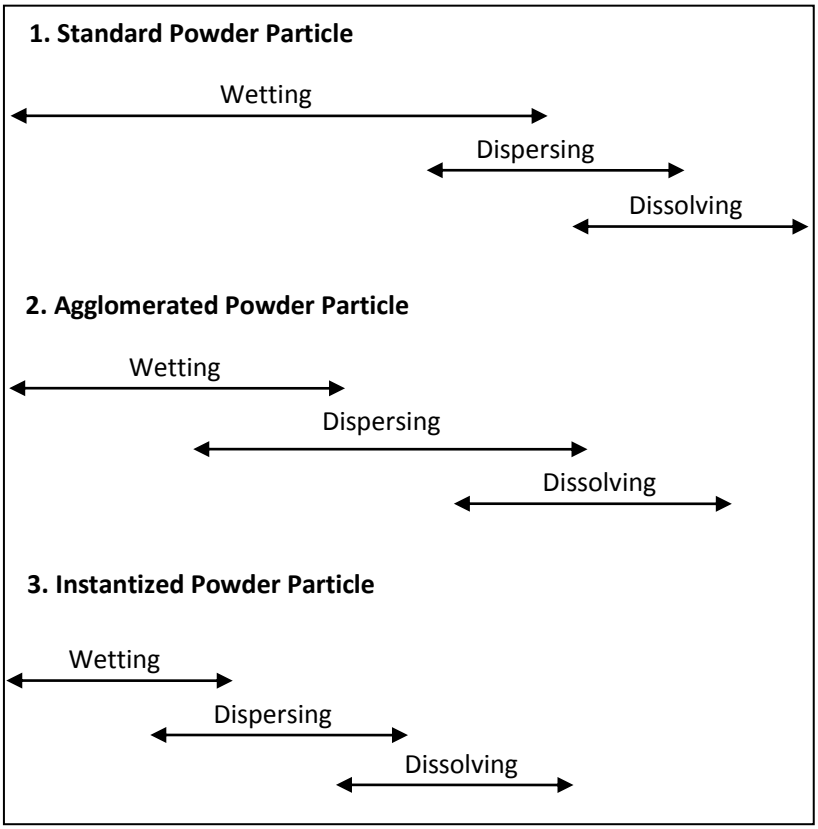

Figure 2-5 Schematic of dissolution timeline for different powder types showing overlaps between different phases with time

2.2.5.1. Wettability

Wettability is the ability of powder particles to overcome the surface tension between powder and water. A powder particle that fails to wet sufficiently will lead to the formation of a substance called scum (Kelly et al., 2003). Scums will gradually adhere together, forming a distinct layer on the walls of containers. Numerous efforts have been done to model the kinetics of dairy powder wetting using capillary effect (Asthana, 2000, Borowko, 1984, Good, 1973, Laskowski, 1999, Lavi and Marmur, 2006, Lee et al., 2006a, Newman, 1968, Nicholas and Peteves, 1994, O'Brien et al., 1968). Most of these existing studies were derived from the Washburn Equation (Asthana, 2000, Washburn, 1921) as shown in Equation 2-2. The Washburn Equation is usually applied to measure the dynamics of cylindrical capillary flow, ignoring the effect of gravity (Washburn, 1921)

$$\frac{dl}{dt} = \frac{r}{\eta}\frac{\gamma}{4l}\cos\theta$$

Equation 2-2

where (dl/dt) is the velocity of the liquid penetrating into the capillary, r is the capillary radius, γ is the surface tension of the liquid, η is the viscosity of the liquid, l is the water penetrating distance, and θ is the contact angle.

From Equation 2-2, it can be concluded that good wettability is favoured under the following conditions (Freudig et al., 1999, Hogekamp and Schubert, 2003) :

- Large pores due to the presence of large particles;
- High porosity, as long as a critical porosity (the value of which varies for different powders) is not exceeded; and
- Small contact angle.

However, the Washburn Equation may not be suitable to describe the kinetic wetting phenomenon of dairy powder. As the powder starts to get wetted, the surface tension γ continuously changes as several components of the milk powder such as lactose, whey protein and salts dissolve. Consequently, the porosity radii, r increases as lactose, which forms the matrix in milk powder, dissolves. The dissolution of lactose and protein also implies that the viscosity, η of the solution also increases. Furthermore, the contact angle θ changes continuously during the wetting procedure. The variations in the parameters of the Washburn Equation (γ, r, θ and η) due to the reactions between powder and solution

(i.e. dissolution), make it challenging to model the capillary effect for dairy powder dissolution.

Besides the effects of physical properties, the chemical composition of milk powder also influences the wettability, which depends on the free fat content and lactose crystallization. Free fat on particle surface reduces wettability due to its hydrophobicity, making it difficult for water to penetrate into the powder. Lactose in milk powder exists in an amorphous form when it is stored below 101^{o}C, which is the glass transition temperature of lactose (Thomas et al., 2004), but gradually crystallizes if the temperature (i.e. during storage) increases. The crystallization of lactose is also the main cause of caking in milk powder, reducing wettability. Even storing the powder at a relatively low temperature does not prevent the wettability of milk powder from decreasing with increasing storage time. This is caused by slow diffusion of the small molecules in milk powder and water (which are considered to be of small molecular weight and relatively high mobility) into the glassy matrix, decreasing the viscosity of the system even at temperatures below the glass transition temperature of milk powder (92^{o}C) (Hogekamp and Schubert, 2003). Therefore, either the increase in storage temperature and/or increasing in the storage time would eventually have a similar effects on milk powder caking, and consequently on the wettability. In addition, biochemical reactions such as non-enzymatic browning can occur below the glass transition temperature (Thomas et al., 2004).

In general, wetting is considered to be the rate-controlling step of the reconstitution process (Kim et al., 2002), with the surface composition strongly affecting wettability (Gaiani et al., 2006). As such, a high lactose content coupled with a low protein level on the particle surface will result in good wettability; while the presence of fat on the surface reduces wettability (Kim et al., 2002).

2.2.5.2. Sinkability

After the powder has been wetted, the gaseous phase surrounding each particle is gradually replaced by an aqueous phase as the particles began to sink. At this stage, the powder particles initiate the solubilisation process (Kelly et al., 2003). The sinkability of the powder particles is defined as the falling of powder particles below the surface of an aqueous phase or liquid (Thomas et al., 2004), and is primarily dependent on the density of the particles. A higher particle density combined with a lower quantity of occluded air

(air content enclosed within powder particle) results in a faster sinking rate (Caric and Milanovic, 2002). Previous studies showed that powder particles with size ≥ 100 μm and density ≈ 1.5 g/cm^3 should be able to sink into a solvent (Hogekamp and Schubert, 2003, Schubert, 1993).

In addition to the physical structure of a single particle, macromolecular events also influence sinkability. An example is the agglomeration of milk powder, which increases sinkability due to the resulting higher aggregate density, particularly for skim milk powder. Lactose crystallisation, which is dependent on the moisture content, also induces agglomeration. This is partly the reason why whole milk powder has relatively poor sinkability. Its high fat content implies that the particle surface is relatively hydrophobic, reduces the moisture content and consequently decreases the extent of lactose crystallisation and sinkability (Aguilar and Ziegler, 1994, Nijdam and Langrish, 2006).

Other macromolecular events such as swelling can significantly inhibit particle sinking (Freudig et al., 1999). In the initial stage of powder reconstitution, the density of particles decreases since the components with larger molecular weights, such as lactose and minerals, tend to dissolve faster. Their dissolution will increase solution density, such that the density difference between particle and solution is gradually reduced, inhibiting further sinking. This phenomenon often induces particles to rise after the initial sinking stage. In both the industrial and laboratory measurements, the powder is usually considered to be wetted from the point that they start to sink into the solution. Based on these considerations, the terms “sinkability” and “wettability” are often interchangeable.

2.2.5.3. Dispersibility

Once the agglomerated particles are wetted and have sunk, they would start to disperse uniformly into the aqua medium as individual particles, while agglomerates gradually breaks up and eventually cease to exist. The dispersibility of food powder is mainly dependent on the ability of casein to disperse in solution. The rate of dispersion determines whether the dairy powders in question can be categorized as ‘instant’, where they need good dispersibility, wettability, and optimal agglomeration (Westergaard, 1994).

It has been shown that dispersibility increases with particle size, and decreases with the percentage of fine particles (below 90 μm)(Vojdani, 1996). Poor agglomeration due to a

small mean particle size, or having a significant amount of fine particles with size smaller than 125 μm, could result in visibly large lumps and slurry settling at the bottom of the container (P ŕeck ý, 1997). Highly porous particles and/or high density particles appear to be the necessary criteria for good dispersibility (Goalard et al., 2006).

2.2.5.4. Solubility

In most cases, food powder must be able to provide good solubility to be useful and functional (Morr et al., 1985). Solubility is the final step of powder dissolution and is considered as the key determinant of the overall reconstitution quality. As such, solubility is often used to represent the complete phenomenon of milk powder reconstitution, comprising soluble components such as lactose, un-denatured whey protein, and salts, as well as dispersible components like casein (Thomas et al., 2004). Generally, the dissolution rate is favoured by the presence of small hydrophilic molecules on the surface (Lillford and Fryer, 1998). Similarly, the solubility of protein is dependent on the ability of soluble, polar residues interacting with water *via* hydrogen bonding, while the hydrophobic part of the protein folds to avoid contact with water (Schein, 1990). Increasing storage time and temperature could reduce the solubility of milk powder, due to the formation of a network of cross-linked proteins at the particle surface (Anema et al., 2006). This cross-linked network could act as a barrier for water to penetrate, thus inhibiting the rehydration of the powder particles (Anema et al., 2006). The solubility of milk powder is likewise affected by the pH and temperature of the solution (Chen and Ozkan, 2007).

In the dairy industry, the most widely used indicator of solubility is the solubility index. The solubility index (SI) (also expressed as insolubility index ISI) is the conventional indicator to determine the solubility of milk powders, although it has also been used on whey protein powder, dried butter milk, milk-based baby food, and other products where the milk fat has been replaced by another type of fat. SI is measured by dispersing a certain amount of protein powder or milk powder in water under well-defined conditions, followed by the recovery of sediment after centrifugation, and measuring its volume in terms of millilitres. The measured value is an inverse of the actual solubility, and this index is used to grade milk powders, as it reflects the extent of denaturation of proteins in milk powders during drying or heat treatments (Vojdani, 1996). Denaturation usually

results in cross-linking or aggregation of protein molecules which then become insoluble. Other indicators available to quantify the solubility of proteins are Protein Dispersibility Index (PDI), Water Dispersible Protein (WDP) (sometimes interchangeable with PDI) (Vojdani, 1996), and Nitrogen Solubility Index (NSI) that determines the amount of dispersed nitrogen under the conditions of a standardized test (AOCS, 1987).

2.3. Standard methods to measure powder dissolution in industry

The standard method used in the industry to analyse the wettability of milk powders is relatively straightforward (as shown in Figure 2-6a) (Niro, 2005b, Varnam and Surherland, 1994). It involves weighing a certain mass of powder and pouring this mass into a funnel which is positioned on top of a beaker containing 100 mL of deionised water. The temperature of water is adjusted according to the powder to be tested (20 ± 0.2 °C for skim milk powder, and 40 ± 0.5 °C for whole milk powder). A pestle is placed inside the funnel to block the lower opening. The recording time starts when the pestle is lifted to allow the powder to drop onto the water surface. The time taken until all the powder is visually wetted is then recorded.

Dispersibility is estimated based on the International Dairy Federation (IDF) standard (as shown in Figure 2-6b) (Varnam and Surherland, 1994) . In this procedure, skim milk or whole milk powder is poured onto the surface of water at 25°C and stirred well after which the mixture is poured through a 250-micron sieve. The dispersibility is defined by the amount of dispersed particles, estimated from the total amount of solid that is present in the filtrate. This is expressed in terms of percentage of dispersed solids against the total amount of solids. Another method to measure dispersibility is to mix the powder with water at room temperature, stirred until there are no visible lumps at the bottom of the glass. The dispersibility is defined by the time taken to disperse the milk powder, measured using a stopwatch. Subsequently, Niro developed another tool to measure the slow dispersibility of agglomerated dairy products (Niro, 2005a). In this procedure, skim milk (26 ± 0.1 g) or whole milk powder (34 ± 0.1 g) is weighed out accordingly and poured into a beaker containing 250 ml of deionised water at a specific temperature according to the powder type. The mixture is stirred with 30 complete circular movements for 20 seconds and then left to stand for 2 minutes. After another 5 circular movement in 3

seconds, the mixture is poured through a Bűchner funnel. The filter paper is immediately compared with a standard scale (0-5) where the lowest grade refers to no particles found on the filter paper.

On the other hand, milk powder solubility measurement is usually carried out by mixing milk powder with water at high speed for 90 seconds at room temperature (as shown in Figure 2-6c). The mixture is then left to stand for 15 minutes, after which a portion is centrifuged to remove the supernatant. The recovered sediment is further mixed with water and centrifuged once again for 5 minutes. The amount of leftover solids after the second centrifugation is then quantified to give the insolubility index (Varnam and Surherland, 1994, Niro, September 2006).

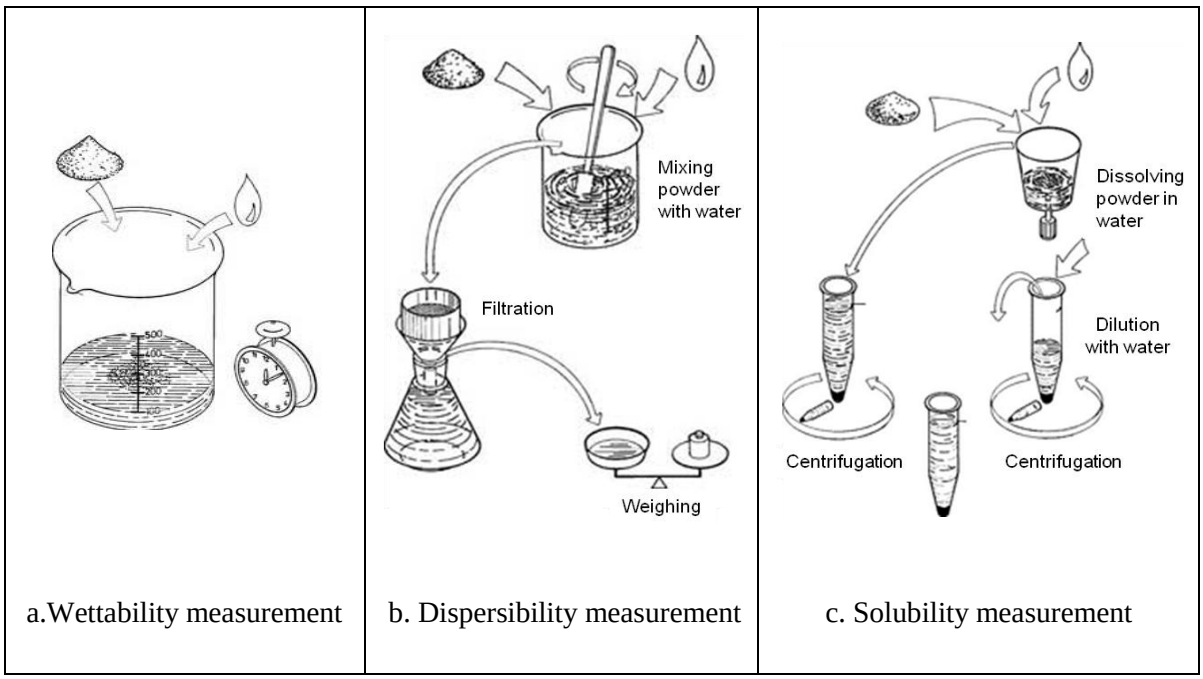

a.Wettability measurement | b. Dispersibility measurement | c. Solubility measurement

Figure 2-6 IDF Method to measure wettability, dispersibility and solubility of dairy powder (Varnam and Surherland, 1994)

Although the standard analytical methods used in the dairy industry are very simple and quick to implement, they tend to be qualitative with poor reproducibility. A typical example is shown in Table 2-3. Wettability of skim milk powder (SMP), whole milk powder (WMP) and milk protein concentrate (MPC) were measured according to the IDF method, No. A 5 b (Niro, 2005b). The powders were divided into different groups according to their particle size (>244 μm, 100~224 μm and <100 μm). The wettability test was conducted and wetting time recorded. From Table 2-3 it can be seen that this method failed to recognize the wettability of powder with relative high hydrophobicity such as

MPC. According to the standard, reproducibility is determined by having a percentage error of less than 20% which is a reflection of the reproducibility of the method. However, for WMP (D>244 μm), the percentage error is 63.5% and the standard deviation increases significantly with wetting time. As such, it can be suggested that the reproducibility of this method is considerably poor and very empirical.

It was also observed that this method is not suitable for MPC because all the result samples for MPC returned un-wetted. From visual observation, after pouring the MPC onto the water surface, the powder in immediate contact with water started to form a floating layer of powdered suspension, wetting, swelling and insulating the bulk of the dry powder on top of it. This insulating film of wetted powder thus prevented further wetting of more powders and did not sink, regardless of the time duration applied.

Table 2-3 Wettability of Different Powders with Different Particle Size Fractions

	SMP (sec)	% Error	WMP (sec)	% Error	MPC(sec)	% Error
>224 μm	6.27±0.67	10.6	76.48±48.55	63.5	Unwetted*	N.A.
100~224 μm	31.86±5.83	18.3	77.07±30.96	40.2	Unwetted*	N.A.
<100 μm	Unwetted*	N.A.	Unwetted*	N.A.	Unwetted*	N.A.

*** the wetting time more than 5 minutes is assumed as unwetted ,**

 # Percentage Error = [(Standard Deviation / Mean) x 100%]

The results from different methods are often not comparable due to a lack of standardisation in techniques. With the proliferation of various functional powders other than the common dairy products, there is an increasing need to develop quantitative methods that can predict their properties for specific end-usages and to fulfil the demands of customers. In addition to providing a profile of the powders for specific applications, these methods could give scientific insights into potential ways to improve the powder's quality.

2.4. Measurement techniques in the laboratories

2.4.1. Wettability

As mentioned earlier, particle wetting is usually considered to be the rate-controlling step (Schubert, 1993, Kim et al., 2002) and many attempts have been made to characterize this behaviour. In 1960s, Bullock and Winder established a method to measure the sinkability of whole milk powder, the parameter of which is now commonly known as wettability (Bullock and Winder, 1960). Their experimental setup, as shown in Figure 2-7, consists of a funnel-shaped extension on top of a customized vessel with a flask placed beneath the outlet of the vessel. The vessel was originally filled with 500 mL of distilled water at 25 $^{\circ}$C with its outlet clamped. 500 g testing dried milk powder was placed in a thimble. To start the experiment, the dried milk was quickly sprinkled using the thimble over the surface of the water in the vessel. The time when the sample first struck the water surface was recorded. After a predetermined time interval (usually between 20 seconds to 3 minutes, depending on the type of powder being tested), the pinch clamp was released and the portion of milk powder which had sunk into the water was drawn off quickly into the flask, thereby partitioning out the layer of sample that had not sunk. In this way, the wettability (sinkability) of the milk powder could be determined by Equation 2-3 (Bullock and Winder, 1960). A notable aspect of this setup was that the time interval employed in each test has to be indicated and recorded for the test results to be comparable and reproducible.

$$\text{Sinkability } \% = \frac{\text{weight of solids in 5mL aliquot} \times 50 \times 100}{\text{weight of original sample} \times 5}$$

Equation 2-3

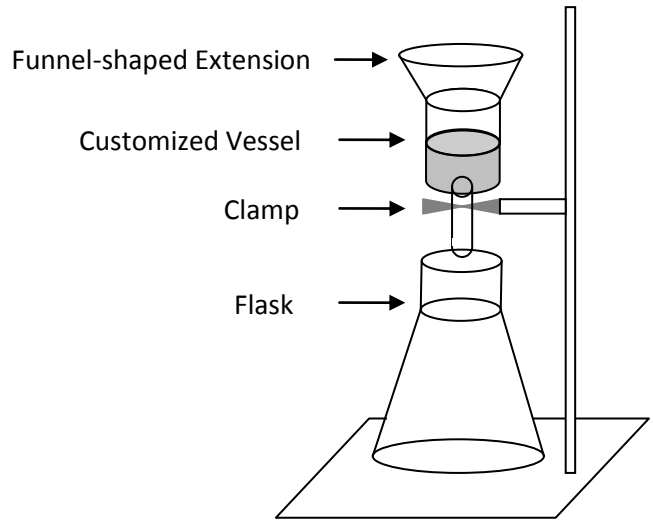

Figure 2-7 The customized device to measure the sinkability of whole milk powder

Another study focused on the effect of particle size of instant coca beverage powders on the wetting behaviour (Hla and Hogekamp, 1999) (Figure 2-8). Here the wetting time was measured by using a container to hold the testing liquid, with the powder sample placed 2-3 mm above the container on a slide, which was connected to a spring. When the slide was unlocked, the spring quickly pulled the slide sideways, so that the entire powder sample was poured on the top of solution simultaneously. The wetting time was then defined as the time necessary for all of the powder to get wetted and fell below the surface of the liquid, measured using a stopwatch (Hla and Hogekamp, 1999). The effects of different testing liquids on wetting time were tested using water and milk with various fat contents. In general, recording the wetting time is a common way to measure the wettability of food powder.

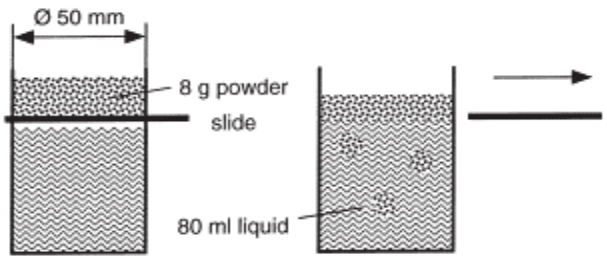

Figure 2-8 Schematic view of the wetting time testing device (Hla and Hogekamp, 1999)

To further understand the kinetics of wettability, a method was developed to measure the dynamic wetting property of food powders (Freudig et al., 1999). This method quantified the maximum powder feed rate per surface area at the point where a visible layer of powder starts to form on the water surface. The sample powder was supplied *via* a pipe to

distribute the particle over the liquid surface, as it was slowly mixed by agitation in the vessel. The powder feed-rate was gradually increased until a layer formation was visually observed. Another method was developed to minimize the movement of liquid surface (Freudig et al., 1999). In this setup (Figure 2-9), a flow channel was built with a powder feeder. In the channel, the powder was transported away from the feed point by the flow, which mimicked the situation on the liquid surface for an un-baffled stirred vessel. Different feed rates and flow rates were applied. This method was useful to characterize most of the wetting properties, such as the conventional wetting time, and the dynamic wettability under a specified feed rate. Different powder would have different wetting behaviour, with some requiring a shorter wetting time due to good wettability, while others take a longer duration. By adjusting the flow rate and the powder feed rate, the method can potentially be used to quantify the wetting properties of a variety of powder products in a reproducible manner, if the exact flow velocity distribution on the surface is known, and the determination of the point where the powder starts to sink can be estimated accurately. Hence, this approach can be improved by using more sophisticated imaging tools to determine the sink point, and modifying the channel dimension to reduce the effects that the wall applied on velocity distribution.

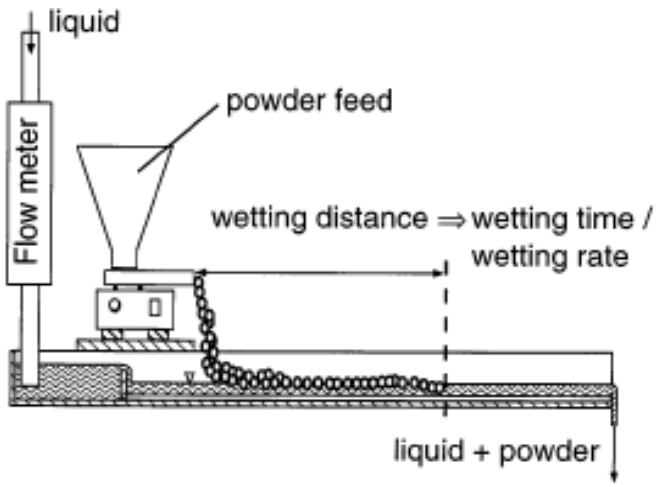

Figure 2-9 Flow channel to measure the dynamic wettability (Freudig et al., 1999)

In another study, Gaiani *et al*. measured the wettability of casein powder by employing a turbidity sensor, Analite NEP 160 (Gaiani et al., 2005). In this setup, the turbidity sensor was positioned just below the liquid surface through the vessel wall to minimize disturbances during stirring. Data were collected automatically at specified time intervals. The sensor measures the changes in turbidity associated with the rehydration of casein

powder. The sensor utilised light in the near-infrared region of 860 nm, while an electronic receptor detected changes by receiving the reflected beams from particles in suspension at 180°. The same method has been employed in the study of dairy powder rehydration (Gaiani et al., 2007b). In this study, a static light scattering technique was used to verify the turbidity values at different stages of rehydration, with relatively good correlations. The turbidity sensor allowed continuous monitoring of the rehydration properties of dairy powders, including wetting time, swelling time and the total time of rehydration.

2.4.2. Dispersibility

There are several techniques for measuring the dispersibility, including the measurement of dispersion kinetics using an optical fibre sensor to collect the light back-scattered by the particles in suspension as shown in Figure 2-10 (Galet et al., 2004). The changes in particle volume concentration could be monitored based on the received signals. The sensor was made up of a centrally positioned light-emitting optical fibre, while the back-scattered light was collected by a six-fibre crown. The measurement principle was based on the fluctuations in volume concentrations of particle in the suspension, which reflected the quality of the dispersion. This technique has also been used to determine the dissolution kinetics of alginate powders (Larsen et al., 2003), as well as the influence of granule size on the dispersion kinetics of cocoa powder (Vu et al., 2003).

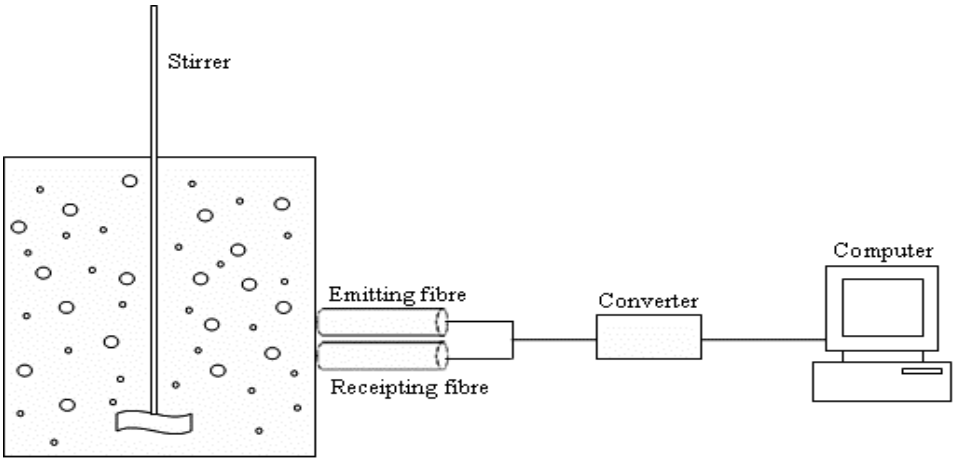

Figure 2-10 Using optical fibre sensor to measure dispersibility (Galet et al., 2004)

Particle sizing instrument based on the principle of forward light scattering is another common tool to measure powder dispersibility in either air or a suitable liquid, by monitoring the changes in the particle size distributions of powders with time. A typical study using such instrument (Malvern Particle Sizer) was carried out by Chen and Lloyd

(Chen and Lloyd, 1994). Several groups of dried milk powder samples with different size fractions (0~180 μm and 180~360 μm) were added to the sample cell at specific water temperature and stirring speed. The results show that the mean diameters of these two size fractions eventually reach a size of 25 μm within 90 seconds. In this experiment, a very dilute milk solution was used (0.1 g total solids/L) to meet the light obscuration limit of the instrument. In practice, the milk powder suspension would contain a higher proportion of fine particles that may lead to less dispersibility.

Recently Goalard *et al*. investigated the dispersion behaviour of powders using two different techniques (Goalard et al., 2006). The first technique employed an optical fibre sensor (Galet et al., 2004), while the second technique used an Insitec EPCS (Ensemble Particle Concentration & Size Particle Analyser) as an in-line laser diffraction instrument to monitor the changes in particle-size distribution during dispersion. This setup enabled real-time continuous measurement of the particle-size distribution, as well as the light obscuration linked to the concentration of the dispersed suspension.

2.4.3. Solubility

2.4.3.1. General methods

Previous studies on food powder solubility have brought about a considerable number of methods based on different criteria. However, the vast discrepancy in data, even for those methods using the same standard, renders it impossible to compare the results from different tests. An earlier attempt was done to develop a rapid and standardized solubility procedure for measuring protein solubility, and to identify and remove the causes of variability in tests carried out by different laboratories (Morr et al., 1985). The proposed method was based on the nitrogen solubility index procedure (AOCS, 1982). The reference food proteins included whey protein concentrate, sodium caseinate, soy protein insolate, and egg white protein. In this procedure, dry protein was weighed and mixed with sodium chloride (NaCl). The solution was stirred and centrifuged, after which the resulting supernatant was filtered out. The protein content of the filtrate was subsequently determined using the micro-Kjeldahl and biuret methods. The results based on biuret method were inconsistent and showed greater standard deviations among repeated experimental results and laboratory mean data as compared to those of micro-Kjeldahl. Hence, it was concluded that the micro-Kjeldahl procedure was more reliable method for

routine protein solubility evaluation. This study provided a basis for further standardizing of food protein solubility procedure, as can be seen from the number of subsequent studies using this method (Szpendowski et al., 1997, Nacka et al., 1998, Goubet et al., 1999, Moughal et al., 2000).

A recent example of solubility-measuring technique is that of Lee *et al*, which measured the solubility of whey protein processed under high hydrostatic pressure (Lee et al., 2006b). The method was similar to that used by Morr *et al*. (1985), while the solubility was determined using the biuret procedure. The difference was that the whey protein (in phosphate buffer or salt solutions) was pre-treated under high hydrostatic pressure before centrifugation. The study showed that under high hydrostatic pressure, the pre-treatment of whey protein resulted in an increase in surface hydrophobicity. Another study demonstrated that the protein solubility of MPC powders was affected by protein interactions (Havea, 2006). In his study, the solubility of the MPC was determined through centrifugation technique separating the MPC into two fractions: the soluble protein in the supernatant, and the insoluble protein in the sediment. It was noted that under certain experimental conditions, soluble materials which includes aggregated proteins could be falsely classified as 'insoluble'. One such condition may be that of using different centrifugation speed. As such, the study concluded that the term 'solubility' should be considered as relative, and could only be applied under certain experimental conditions (Havea, 2006).

Lamiot *et al*. measured the hydration of whey powders using different methods, namely the Baumann's method, the absorption capacity test, the paste-water retention method, and the filtration/centrifugation test (Lamiot et al., 1998). The Baumann's method involved dispersing a fine layer of powder onto a cellulose membrane filter (porosity 0.1 μm) placed in a Baumann capillary apparatus (Wallingford and Labuza, 1983). Spontaneous water uptake was recorded until equilibrium or up till the maximum absorption of water was reached.

The absorption capacity test was conducted by placing a known amount of powder into a glass cylinder of 2 cm diameter; one-end of which was closed with a fitted glass lid. The open-end of the cylinder was then placed in contact with water for a fixed period. The weight of the cylinder before and after the water contact was recorded along with the

weight of the dry powder layer in the cylinder. The extent of hydration, which strongly correlated to the hydration time, was calculated according to Equation 2-4:

$$\text{Hydration} = \frac{\text{Weight of cylinder after - Weight of cylinder before}}{\text{Weight of powder in cylinder - Weight of upper dry powder}}$$

Equation 2-4

The paste-water retention method was adapted from Quinn and Paton (1979) (Lamiot et al., 1998). In this method, powder was weighed into a centrifuge tube and water was added in small increments while stirring the mixture until a paste was formed. The paste was then centrifuged and the supernatant weighted. The water absorbed by the powder was considered as the approximate value of hydration. Based on this approximate value of hydration, the same routine was repeated. A series of tubes was tested with the same quantity of powder being added but with a different amount of water each time. By comparing these results, the comparative boundary of the hydration value could be narrowed down to determine the actual hydration value.

The filtration/centrifugation test used an aliquot of 0.5 g of a powder dispersed in water. The aliquot was placed in a micro-partition system with membrane filters. Centrifugation was then done at two different rates but with the same centrifugation duration. From the results, hydration was calculated as water retention by finding the difference in weight of the aliquot before and after centrifugation.

Comparison of these four methods suggests that the filtration/centrifugation test tends to give the highest hydration capacity, while the paste-water retention method gave the lowest estimate. In testing the whey protein concentrates from electro-dialyzed whey powders, the Baumann method and paste-water retention method were suitable to distinguish their hydration capacities, as the results from these two methods were well-correlated to the protein and lactose content of the powders. As such, it can be argued that a mixture of methods is likely to be necessary for a reliable characterization of powder hydration.

Another method applied to characterize milk powder reconstitution is the ultrasound spectroscopy (Meyer et al., 2006). In this experiment, a visual inspection was conducted to evaluate the final product quality; following which an ultrasound spectroscopy was employed to measure the reconstitution ability of instant milk powder. Upon comparison

of these two results, it was found that the ultrasonic attenuation coefficient correlated well with the visual inspection test, whereas ultrasonic velocity was found to be relatively uncorrelated. Therefore, the concept of using ultrasonic attenuation to measure food powder solubility might be a feasible idea, primarily because the ultrasound attenuation is based on the density difference between the continuous phase and the dispersed particles. Ultrasonic spectroscopy was also employed in the study of molecular relaxation and aggregation of whey protein molecules in aqueous solutions (Bryant and McClements, 1999).

2.4.3.2. Solubility kinetic measurements

In recent years, the kinetics of food powder dissolution have attracted great attention, since rapid and complete dissolution of food powder is of great practical significance to commercial manufacturing and food processing industry. If the dissolution time is too short, the resulting products might not be homogenous. On the other hand, if the dissolution time is too long, the efficiency of the process will be very poor. Therefore, a better understanding of the behaviour of food powder kinetics dissolution will enable manufacturers to adopt improved methods of production and higher quality control.

The technique that is widely used in both industrial and laboratory to quantify the particle solubility is static light scattering (SLS). A recent example is that by Mimouni *et al*. who used SLS to monitor the rehydration process of milk protein concentrate powder as well as proposed a dissolution mechanism for this process (Mimouni et al., 2009). They measured the size distribution and volume concentration of the un-dissolved particle and quantified the dissolution kinetics. Their model consisted of two overlapping processes during MPC powder rehydration, namely the de-agglomeration of big particles and the dissolution of primary particles, and concluded that the rate-limiting step was the primary particle dissolution.

Another way to monitor the kinetic of powder dissolution was using ultrasonic pulses (Saggin and Coupland, 2002). When an ultrasound (high frequency sound) wave passed through a material, it resulted in a series of compressions and rarefactions in the waves. Low-intensity ultrasonic waves generated by low-energy sources have been found to cause no permanent alteration to the physical and chemical properties of the sample, which is advantageous for scientific research. Furthermore, low-intensity ultrasonic waves were sensitive to changes in the physical structure and composition of the sample, and this

difference in structure and composition could be detected by measuring the mechanical oscillations produced as the wave propagated through the material.

Another useful measuring technique used in the laboratory is the Nuclear Magnetic Resonance (NMR). NMR transverse relaxation has been introduced for evaluating the state of water in dairy product on the basis of changes in mobility when water binds with other components in the solution (Belloque and Ramos, 1999). The transverse relaxation time (T_2) has been found to be affected by the interaction of water with macromolecules (Granizo et al., 2007). The NMR signal, detected during the relaxing of nuclear spins back to their equilibrium state, decreases with time. This phenomenon is caused by two types of relaxation: longitudinal relaxation, characterized by the T_1 time, and transverse relaxation, which is characterized by the T_2 time. Each nucleus within a single molecule has a characteristic T_1 and T_2 time, depending on their individual molecular mobility. Being a non-invasive tool, NMR is potentially applicable for many food or non-food products (Figure 2-11). Davenel *et al.* demonstrated that the milk's reconstitution ability could be quantified by NMR transverse relaxation rate (Davenel et al., 2002). The method gave an indication of the water absorption rate of powder particles and dissolution of the particles, thus showing the kinetics of powder dissolution. However it could not be used to estimate the solubility index, or indicate clearly whether the milk powder had been fully and completely dispersed in solution. In other word, it is not possible to use NMR alone to distinguish the solubility of food powder; hence other complementary techniques are required to provide for example, a quantitative value of solubility index alongside the NMR result. A relatively similar study was carried out by Schuck *et al.*, which used NMR to investigate the rehydration of casein powders (Schuck et al., 2002).

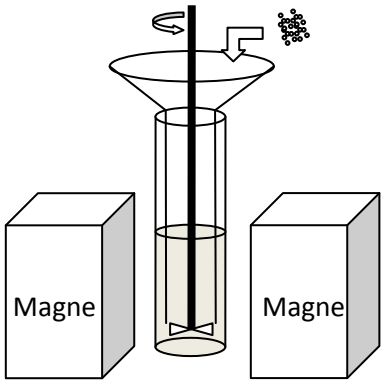

Figure 2-11 Experiment setup for monitoring the reconstitution process of powders by NMR

Recently, Granizo *et al*. demonstrated that NMR transverse (T_2) relaxation can be used to monitor changes in solubility over time, however, no exact quantitative value of the solubility was presented (Granizo et al., 2007). In this experiment, the T_2 values from different protein powders with different solubility were compared, results show that T_2 was independent of mixing time regardless of the solubility of the powder. This outcome demonstrated that the absolute T_2 value on its own was not a useful indicator for ingredient solubility (Schuck et al., 2002). However, the changes in solubility over time could still be quantified by employing a simple one or two term model of T_2 relaxation (Granizo et al., 2007). In food processing applications, where the emphasis is on quick and simple technique for monitoring, rather than high precision tools, the NMR technique may be sufficient based on its ease of application and speed (Granizo et al., 2007).

In studying the kinetics of dissolution, Kravtchenko *et al*. stressed the importance of the geometry of the apparatus, especially when testing polymer powders which may become a sticky gel before dissolving (Kravtchenko et al., 1999). Some powders, such as hydrocolloids, tend to exhibit an increase in viscosity while dissolving, resulting in an increased torque on the stirrer, and subsequently leading to deposits sticking to the stirrer. The increased viscosity would thus result in poor reproducibility of the dissolution measurement. Therefore, in this experiment, the torque on the stirrer was proportional to the viscosity of the solution (monitored by a viscometer), and proportional to the dissolved polymer concentration.

Another tool applied include a combined pH electrode and a reference electrode to monitor the kinetic dissolution of calcium hydroxyapatite powder (Gramain et al., 1989, Thomann et al., 1990) The probes detected the proton and calcium activities in the solution, based on the ionic activity. However, this method may not be suitable for dairy powders, which generally only contain trace amounts of salt.

Another example of technique used to measure the dynamic solubility is called the Focused Beam Reflectance Measurement (FBRM). FBRM provide the *in situ* monitoring of particle size and the change in particle counts, and is often used to monitor the particle size distribution and kinetics of particles in suspension (Hu et al., 2008, Kougoulos et al., 2005b, Kovalsky and Bushell, 2005, Yu and Erickson, 2008, Heath et al., 2002, Barrett and Glennon, 1999). It has been widely using in many fields, such as crystallization (Kempkes et al., 2008, Doki et al., 2004, Kougoulos et al., 2005a, Hermanto et al., 2010,

O'Sullivan et al., 2003), granulation (Närvänen et al., 2009, Närvänen et al., 2008, Hu et al., 2008, Tok et al., 2008), flocculation (Blanco et al., 2002, Owen et al., 2002, Swift et al., 2004, Yoon and Deng, 2004, Farrow et al., 2000), dissolution (Sun et al., 2009, Tajarobi et al., 2009), to name a few. The FBRM probe, in conjunction with a Particle Vision and Measurement (PVM) probe can be positioned inside a mixing vessel for *in situ* measurement to provide a visual validation (Jia et al., 2008, Wang et al., 2006, Schöll et al., 2006, O'Sullivan et al., 2003). The hardware configuration of this device primarily consists of a laser probe, and a stirrer to keep the sample well mixed as depicted in Figure 2-12. Inside the probe, a 780 nm laser beam is directed through a lens rotating at a speed of 4500 r.p.m. (Heath et al., 2002). The laser beam is focused onto a point near the sapphire window of the probe. The size of the focused beam is approximately 0.7 μm × 2 μm (Heath et al., 2002). When the rotating beam comes across an entity in the measuring solution, part of it is reflected back and picked up by the detector (Figure 2-13). As the tangential velocity of the beam is known, the detector can measure the duration of the reflected light proportional to the width of the particle. In this case, the measured distance across the particle is known as the chord length as calculated using Equation 2-5. Typically, thousands of chord lengths are measured per second, with the numbers of counts dependent on the concentration of solids present in the suspension (Barrett and Glennon, 1999). However, the results from FBRM can be related to both particle diameter and shape (Barrett and Glennon, 1999). If the particles are nearly spherical particles, the measured chord lengths are closer to the particle diameters.

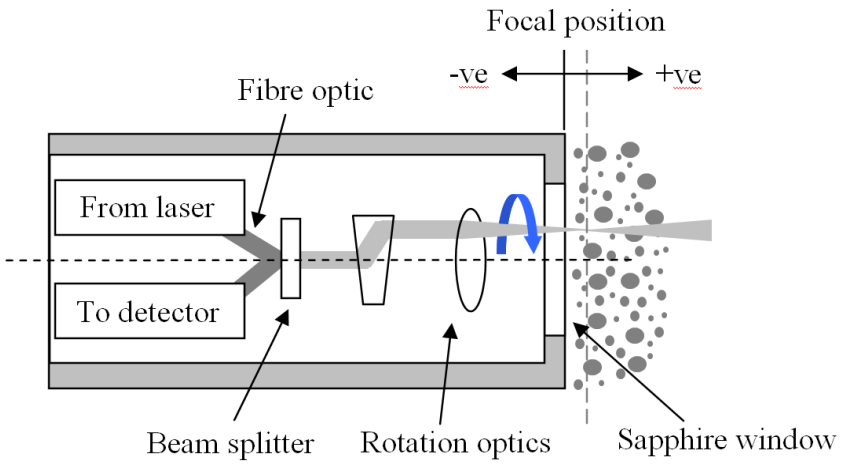

Figure 2-12 Schematic of the FBRM probe

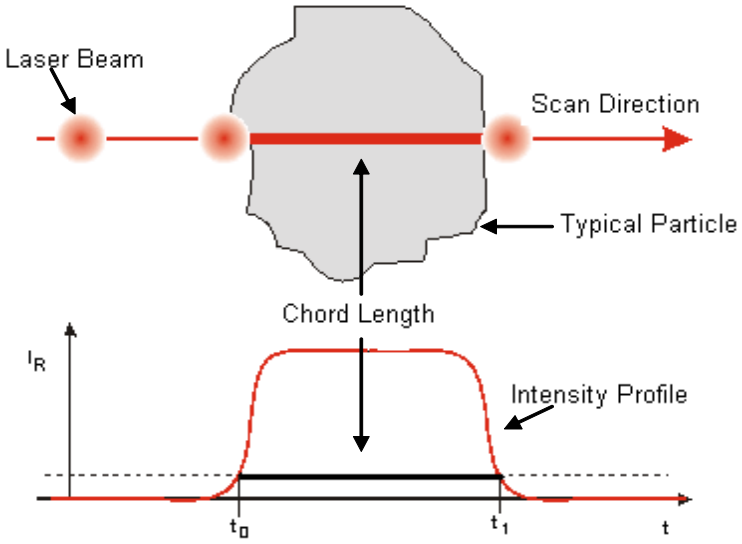

Figure 2-13 Schematic of a chord length (Hartman, 2007)

$$\text{Chord length} = \text{Beam velocity} \times \text{Measuring duration}$$

Equation 2-5

In the case of characterizing particle dissolution, as the powders start to dissolve, they break up into smaller sized agglomerates, subsequently into primary particles, and eventually releasing their materials into solution. This dynamic change in size over the whole sample will be reflected by the decrease in the average chord length across the whole population of the powder. Therefore, by monitoring the change in average chord length of the sample with time using FBRM, the solubility profile can be quantitatively represented and reported. In comparison to other light scattering techniques to measure particle size (i.e. Malvern Mastersizer), FBRM can be used directly in situ without the need of further dilution of samples.

Some of the measurement techniques which have been highlighted in this review are summarized in Table 2-4.

Table 2-4 Summary of measurements of food powder reconstitution properties

		Method	Reference	Equipment	Test Material	Feature
Wettability		Separation method	Bullock & Winder, 1960	Customized vessel	WMP	Time interval is recorder.
		Slide method	Hla & Hogekamp, 1999	Beaker, slide and spring	Cocoa powder	Conventional method. Applicable for a majority of food powders.
		Flow channel	Freudig *et al.*, 1999	Flow channel	SMP	Potentially useful with further modification.
		Measuring turbidity	Gaiani *et al.*, 2005	Turbidity sensor	Casein powder	Enable continuous monitoring
Dispersibility		Forward light scattering	Chen & Lloyd, 1994	Malvern Particle Sizer	Instantized WPM	Monitoring changes in particles size distribution to estimate dispersion rate.
		Backward light scattering	Galet *et al.*, 2004	Optical fiber sensor	Cocoa powder	Monitoring dispersion based on the volume fluctuation of particles in suspension
		In-line laser diffraction	Goalard *et al.*, 2006	Insitec EPCS	Talc granule	Real time continuous measurement of the particle-size distribution
Solubility	**Static Method**	Nitrogen solubility index procedure	Morr *et al.*, 1985	Centrifuge	Protein powders	Provide a basis for further standardizing of protein solubility measurement procedure
		Baumann's method	Lamiot *et al.*, 1998	Baumann capillary apparatus	Whey protein powder	Useful for routine analysis as it is well correlated to the physical characteristics of powders.
		Absorption Capacity Test		Cylinder with defined geometry		Relatively simple set-up and measurement
		Paste-water retention method		Centrifuge		This method is suitable to distinguish the hydration capacities.
		Filtration/centrifugation test		Micro-partition system equipped with membrane filters, centrifuge		Provided relatively high hydration capacity, but not clearly related to composition or physical characteristics of powders.
		Ultrasound attenuation	Meyer *et al.*, 2006	Ultrasound spectroscopy	Instant milk powder	Based on the density difference between water and dispersed particles. Show good correlation with the visual inspection test.
	Dynamic Method	Ultrasound pulse	Saggin & Coupland, 2002	Ultrasonic device	Sucrose and lactose	On-line measurement
		NMR transverse relaxation	Belloque & Ramos, 1999 Davenel *et al.*, 2002 Schuck *et al.*, 2002 Granizo *et al.*, 2007	NMR spectrometer	NPCS[a], WPC[b], CCP[c] Casein powder	Monitor changes in solubility over time. Unable to give an exact quantitative value of the solubility

a: Native phosphocaseinate suspension **b: Whey protein concentrate** **c: Cow casein powders**

2.5. Summary and remarks

Spray drying in food industry is considered the most effective and economic ways of producing food powders and it is possible to produce powder with tailored composition, physicochemical characteristics, quality and food safety (Chen and Patel, 2008, Kelly, 2006). With the increasing capacity of spray drier, a major challenge has emerged involving how the processing parameters will affect the resulting powder microbiology, as well as the functionalities. At the moment, spray drying operations are mostly conducted based on a trial and error approach where the operating conditions are adjusted according to product quality, without an in-depth understanding of the processes involved (Singh and Creamer, 1991, Kelly, 2006, Schuck, 2008, Chen and Patel, 2008, Baldwin, 2010, Gaiani et al., 2010, Oldfield et al., 2005). This approach inevitably causes inefficient operations and also leads to formation of undesirable agglomeration during production and loss of functionality. In light of that, it is clear that there is a need for better understanding of the biochemical properties of milk before and during spray drying, and how these conditions influence the functional and chemical properties of resultant powder products. This knowledge will enable manufacturers to optimize operations of dairy plants in terms of energy and monetary cost as well as final product quality (Schuck, 2008).

From the literature surveyed thus far, the following points have been summarised:

i. Milk is a very complex system. It consists of basic components including water, protein, lipid, lactose and traces of salts. The composition provides information regarding the physical state, structure and engineering properties (Aguilera, 2005). Different compositions play different roles on the resulting powder functionalities. Therefore, an understanding of the relationship between processing conditions on the resulting composition differences (micro-scale level), as well as on the functional behaviours (macro-scale level) is necessary for both quality control and for new product development.

ii. Current industrial standards for characterizing powder dissolution properties were primarily developed based on traditional powders such as skim milk powder and whole milk powder. However, for non-traditional powders such as whey protein, milk protein concentrates, and fortified powders, these standards were unable to effectively characterise and quantify the dissolution properties. There are lack of reproducible

and cohesive methods and specific benchmarks of comparison to measure food powder reconstitution for different powder types. As such, it is necessary to look into a more effective, reliable, and reproducible method to characterize the functionality of different powder types.

iii. A number of laboratory-based methods currently available have the potential to quantify food powder reconstitution properties, such as powder wettability and protein solubility. A brief review providing an overview of the range of emerging and existing methods had been conducted to aid in the development of standardised method(s) of measurement to effectively test the properties of a specific product.

2.6. Investigation and assessment of characterization techniques

It is clear that there is a need for robust technique(s) to characterise powder dissolution for different types of powders with varying functional and physical properties. Thus an initial investigation of selected measurements techniques was carried out.

Chemical characterization techniques recently applied to dairy powder characterization included Fourier Transform Infrared (FTIR) (Paradkar and Irudayaraj, 2002, Mendenhall and Brown, 1991, Kher et al., 2007) and X-ray Photoelectron Spectroscopy (XPS) (Gaiani et al., 2010, Millqvist-Fureby et al., 2001, Kim et al., 2005, Gaiani et al., 2006, Kim et al., 2009). These techniques were found to be very useful in term of particle surface composition characterization. Another potential technique investigated was gel electrophoresis to identify and quantify the proteins in dairy powder. This method was useful to analyse protein denaturation and will be discussed in more details in Chapter 5.

In general, physical characterization techniques were better established with techniques including moisture content measurement, particle size measurement (static light scattering *via* Malvern Mastersizer), particle morphology characterization (Scanning Electron Microscopy, Transmission Electron Microscopy, & light microscope), particle density measurement, and others being actively applied to dairy powders. SEM and TEM have been found to be useful for visual interpretations, which provide assistance in microstructure property analysis. Malvern Mastersizer measures the average particle size but has a limited working range of concentrations and thus the need for sample dilution.

Nonetheless, as a generally accepted measurement technique, it can be applied for particle size analysis. In this project, SEM, TEM, moisture content measurements and Malvern Mastersizer were employed as complementary methods for characterisation of physical properties.

Functional characterisation techniques were less well established for powder particle characterisation. There have been many techniques applied for dairy powder characterisation, however they are mostly qualitative or are specific for only a limited number of powder types. Another limitation was that the results from these various techniques are not comparable. As such, selected techniques were assessed for their suitability to characterise powders dissolution behaviour including techniques to measure wettability (flow channel), dispersibility (Turbiscan) and solubility (FBRM). The following sections outline the investigations of the methods assessed in this work.

To further evaluate the wettability of different powders, an experimental setup comprising an in-house flow channel designed with modifications from Freudig's study was constructed. This setup extended the observation from two dimensions (top down view) to three dimensions by adding a camera for the side view of particles dispersing under the water surface, to monitor the wettability and dispersibility of the powders (Appendix 1). An optical analyser Turbiscan MA 2000 was also used to further evaluate dispersibility (Appendix 2).

To evaluate the solubility of different powders, Focused Beam Reflectance Measurement (FBRM) was evaluated. The key features were the ability to monitor the changes in particle size with time in situ, and the wide concentration range with no sample dilution required. The suitability of FBRM technique to characterize the solubility of different dairy powders types was discussed in details in Appendix 3.

In summary, both the flow channel system and Turbiscan were able to qualitatively distinguish the different powder types, but lack the robust reproducibility and quantitative measurement capabilities. On the other hand, FBRM was found to be suitable to characterise the dissolution kinetics for different powder types.

2.7. References

AGUILAR, C. A. & ZIEGLER, G. R. 1994. Physical and Microscopic Characterization of Dry Whole Milk with Altered Lactose Content. 2. Effect of Lactose Crystallization.

AGUILERA, J. M. 2005. Why Food Microstructure? Journal of Food Engineering, 67, 3-11.

ANEMA, S. G. & LI, Y. 2003. Association of Denatured Whey Proteins with Casein Micelles in Heated Reconstituted Skim Milk and its Effect on Casein Micelle Size. Journal of Dairy Research, 70, 73-83.

ANEMA, S. G., PINDER, D. N., HUNTER, R. J. & HEMAR, Y. 2006. Effects of Storage Temperature on the Solubility of Milk Protein Concentrate (MPC85). Food Hydrocolloids, 20, 386-393.

AOCS 1987. Official Methods and Recommended Practices of the American Oil Chemists' Society. In: SOCIETY, A. O. C. (ed.) 3nd Edition ed.: Champaign.

ASTHANA, R. 2000. Dissolutive Capillary Penetration with Expanding Pores and Transient Contact Angles. Journal of Colloid and Interface Science, 231, 398-400.

BALDWIN, A. J. 2010. Insolubility of Milk Powder Products – A Minireview. Dairy Sci. Technol., 90, 169-179.

BARRETT, P. & GLENNON, B. 1999. In-line FBRM monitoring of particle size in dilute agitated suspensions. Part. and Part. Syst. Charact., 16, 207-211.

BELLOQUE, J. & RAMOS, M. 1999. Application of NMR spectroscopy to mik and dairy products. Trends in Food Science & Technology, 10, 313-320.

BLANCO, A., FUENTE, E., NEGRO, C. & TIJERO, J. 2002. Flocculation Monitoring: Focused Beam Reflectance Measurement as a Measurement Tool. The Canadian Journal of Chemical Engineering, 80, 1-7.

BOROWKO, M. 1984. Liquid Adsorption Chromatography with Multicomponent Mobile Phase. Journal of Colloid and Interface Science, 102, 519-526.

BRYANT, C. M. & MCCLEMENTS, D. J. 1999. Ultrasonic spectroscopy study of relaxation and scattering in whey protein solutions. Journal of the Science of Food and Agriculture, 79, 1754-1760.

BULLOCK, D. H. & WINDER, W. C. 1960. Reconstitutability of Dried Whole Milk. I. The Effect on Sinkability of the Manner of Handling Freshly Dried Milk. J. Dairy Sci., 43, 301-316.

BURGESS, K. J. 2001. Milk Fats as Ingredients. International Journal of Dairy Technology, 54, 56-60.

CARIC, M. & MILANOVIC, S. 2002. Milk Powders | Physical and Functional Properties of Milk Powders. Encyclopedia of Dairy Sciences. Oxford: Elsevier.

CHEN, X. D. 1992. Whole Milk Powder Agglomeration—Principles and Practice. Milk Powder for the Future. Palmerston North, New Zealand: Dunmore Press.

CHEN, X. D. & LLOYD, R. J. 1994. Some aspects of measuring the size and rate of dispersion of milk powder agglomerates using the Malvern Particle Sizer 2600c. Journal of Dairy Research, 61, 201-208.

CHEN, X. D. & OZKAN, N. 2007. Stickiness, Functionality, and Microstructure of Food Powders. Drying Technology, 25, 969-979.

CHEN, X. D. & PATEL, K. C. 2008. Manufacturing Better Quality Food Powders from Spray Drying and Subsequent Treatments. Drying Technology: An International Journal, 26, 1313 - 1318.

CORREDIG, M. & DALGLEISH, D. G. 1999. The mechanisms of the heat-induced interaction of whey proteins with casein micelles in milk. International Dairy Journal, 9, 233-236.

DAVENEL, A., SCHUCK, P., MARIETTE, F. & BRULÉ, G. 2002. NMR Relaxometry as a Non-invasive Tool to Characterize Milk Powders. Le Lait, 82, 465-473.

DOKI, N., SEKI, H., TAKANO, K., ASATANI, H., YOKOTA, M. & KUBOTA, N. 2004. Process Control of Seeded Batch Cooling Crystallization of the Metastable α-Form Glycine Using an In-Situ ATR-FTIR Spectrometer and an In-Situ FBRM Particle Counter. Crystal Growth & Design, 4, 949-953.

DONATO, L. & GUYOMARC'H, F. 2009. Formation and properties of the whey protein/κ-casein complexes in heated skim milk - A review. Dairy Sci. Technol., 89, 3-29.

FARROW, J. B., FAWELL, P. D., JOHNSTON, R. R. M., NGUYEN, T. B., RUDMAN, M., SIMIC, K. & SWIFT, J. D. 2000. Recent developments in techniques and methodologies for improving thickener performance. Chemical Engineering Journal, 80, 149-155.

FITZPATRICK, J. J., BARRY, K., CERQUEIRA, P. S. M., IQBAL, T., O'NEILL, J. & ROOS, Y. H. 2007. Effect of composition and storage conditions on the flowability of dairy powders. International Dairy Journal, 17, 383-392.

FOSTER, K. D., BRONLUND, J. E. & PATERSON, A. H. J. 2005. The contribution of milk fat towards the caking of dairy powders. International Dairy Journal, 15, 85-91.

FOX, P. F. 2001. Milk proteins as food ingredients. International Journal of Dairy Technology, 54, 41-55.

FOX, P. F. 2008. Milk: an overview. In: ABBY, T., MIKE, B. & HARJINDER, S. (eds.) Milk Proteins. San Diego: Academic Press.

FOX, P. F. & MCSWEENEY, P. L. H. 1992. Lipids, London ; New York, Elsevier Applied Science.

FOX, P. F. & MCSWEENEY, P. L. H. 1997. Lactose, Water, Salts and Vitamins, New York, Kluwer Academic/Plenum Publishers.

FOX, P. F. & MCSWEENEY, P. L. H. 1998a. Dairy Chemistry and Biochemistry. Springer - Verlag.

FOX, P. F. & MCSWEENEY, P. L. H. 1998b. Dairy Chemistry and Biochemistry. Springer - Verlag.

FOX, P. F. & MCSWEENEY, P. L. H. 2003a. Protein. Advanced dairy chemistry New York ; London Kluwer Academic/Plenum.

FOX, P. F. & MCSWEENEY, P. L. H. 2003b. Proteins, Part A, New York, Kluwer Academic/Plenum Publishers.

FREUDIG, B., HOGEKAMP, S. & SCHUBERT, H. 1999. Dispersion of powders in liquids in a stirred vessel. Chemical Engineering and Processing, 38, 525-532.

GAIANI, C., BANON, S., SCHER, J., SCHUCK, P. & HARDY, J. 2005. Use of a Turbidity Sensor to Characterize Micellar Casein Powder Rehydration: Influence of Some Technological Effects. Journal of Dairy Science, 88, 2700-2706.

GAIANI, C., EHRHARDT, J. J., SCHER, J., HARDY, J., DESOBRY, S. & BANON, S. 2006. Surface composition of dairy powders observed by X-ray photoelectron spectroscopy and effects on their rehydration properties. Colloids and Surfaces B: Biointerfaces, 49, 71-78.

GAIANI, C., MORAND, M., SANCHEZ, C., TEHRANY, E. A., JACQUOT, M., SCHUCK, P., JEANTET, R. & SCHER, J. 2010. How surface composition of high milk proteins powders is influenced by spray-drying temperature. Colloids and Surfaces B: Biointerfaces, 75, 377-384.

GAIANI, C., SCHER, J., EHRHARDT, J. J., LINDER, M., SCHUCK, P., DESOBRY, S. & BANON, S. 2007a. Relationships between Dairy Powder Surface Composition and Wetting Properties during Storage: Importance of Residual Lipids. Journal of Agricultural and Food Chemistry, 55, 6561-6567.

GAIANI, C., SCHUCK, P., SCHER, J., DESOBRY, S. & BANON, S. 2007b. Dairy Powder Rehydration: Influence of Protein State, Incorporation Mode, and Agglomeration. Journal of Dairy Science, 90, 570-581.

GALET, L., VU, T. O., OULAHNA, D. & FAGES, J. 2004. The Wetting Behaviour and Dispersion Rate of Cocoa Powder in Water. Food and Bioproducts Processing, 82, 298-303.

GERMAN, J. B. & DILLARD, C. J. 2006. Composition, Structure and Absorption of Milk Lipids: A Source of Energy, Fat-Soluble Nutrients and Bioactive Molecules. Critical Reviews in Food Science and Nutrition, 46, 57 - 92.

GOALARD, C., SAMIMI, A., GALET, L., DODDS, J. A. & GHADIRI, M. 2006. Characterization of the Dispersion Behavior of Powders in Liquids. Particle & Particle Systems Characterization, 23, 154-158.

GOOD, R. J. 1973. The rate of penetration of a fluid into a porous body initially devoid of adsorbed material. J. Colloid Interface Sci. ; Vol/Issue: 42:3, Pages: 473-477.

GOUBET, R., CHOBERT, J. M. & HAERTLE, T. 1999. Functional properties of milk proteins glycated in mild conditions. Sci. Alim., 19, 423-438.

GRAMAIN, P. H., THOMANN, J. M., GUMPPER, M. & VOEGEL, J. C. 1989. Dissolution Kinetics of Human Enamel Powder : I. Stirring Effects and Surface Calcium Accumulation. Journal of Colloid and Interface Science, 128, 370-381.

GRANIZO, D. P., REUHS, B. L., STROSHINE, R. & MAUER, L. J. 2007. Evaluating the Solubility of Powdered Food Ingredients using Dynamic Nuclear Magnetic Resonance (NMR) Relaxometry. Lebensmittel-Wissenschaft & Technologie - Food Science and Technology, 40, 36-42.

HARTMAN, T. 2007. Part 3 Understanding the FBRM Measurement. Lasentec FBRM® vs. PVM®.

HAVEA, P. 2006. Protein interactions in milk protein concentrate powders. International Dairy Journal, 16, 415-422.

HEATH, A. R., FAWELL, P. D., BAHRI, P. A. & SWIFT, J. D. 2002. Estimating average particle size by focused beam reflectance measurement (FBRM). Part. and Part. Syst. Charact., 19, 84-95.

HERMANTO, M. W., CHOW, P. S. & TAN, R. B. H. 2010. Implementation of Focused Beam Reflectance Measurement (FBRM) in Antisolvent Crystallization to Achieve Consistent Product Quality. Crystal Growth & Design.

HLA, P. K. & HOGEKAMP, S. 1999. Wetting Behaviour of Instantized Coca Beverage Powders. International Journal of Food Science and Technology, 34, 335-342.

HOGEKAMP, S. & SCHUBERT, H. 2003. Rehydration of Food Powders. Food Science and Technology International, 9, 223-235.

HOLT, C. 1992. Structure and stability of bovine casein micelles. Advances in Protein Chemistry, 43, 63-151.

HOLT, C. 1998. Casein Micelle Substructure and Calcium Phosphate Interactions Studied by Sephacryl Column Chromatography. J. Dairy Sci., 81, 2994-3003.

HU, X., CUNNINGHAM, J. C. & WINSTEAD, D. 2008. Study growth kinetics in fluidized bed granulation with at-line FBRM. Int. J. Pharm., 347, 54-61.

HUPPERTZ, T. & KELLY, A. L. 2006. Physical Chemistry of Milk Fat Globules. In: FOX, P. F. & MCSWEENEY, P. L. H. (eds.) Advanced Dairy Chemistry Volume 2 Lipids. Springer US.

JENSEN, R. G. 2002. The Composition of Bovine Milk Lipids: January 1995 to December 2000. J. Dairy Sci., 85, 295-350.

JIA, C.-Y., YIN, Q.-X., ZHANG, M.-J., WANG, J.-K. & SHEN, Z.-H. 2008. Polymorphic Transformation of Pravastatin Sodium Monitored Using Combined Online FBRM and PVM. Organic Process Research & Development, 12, 1223-1228.

JOUPPILA, K., KANSIKAS, J. & ROOS, Y. H. 1997. Glass Transition, Water Plasticization, and Lactose Crystallization in Skim Milk Powder. J. Dairy Sci., 80, 3152-3160.

JOUPPILA, K. & ROOS, Y. H. 1994a. Glass Transitions and Crystallization in Milk Powders. J. Dairy Sci., 77, 2907-2915.

JOUPPILA, K. & ROOS, Y. H. 1994b. Water Sorption and Time-Dependent Phenomena of Milk Powders. J. Dairy Sci., 77, 1798-1808.

KAYLEGIAN, K. E. 1995. Functional Characteristics and Nontraditional Applications of Milk Lipid Components in Food and Nonfood Systems. J. Dairy Sci., 78, 2524-2540.

KELLY, A. L., O'CONNELL, J. E. & FOX, P. F. 2003. Manufacture and Properties of Milk Powders. In: P.F. FOX & P.L.H. MCSWEENEY (eds.) Advanced Dairy Chemistry. 3rd ed. Cork, Ireland: Kluwer Academics / Plenum Publishers.

KELLY, P. M. 2006. Innovation in milk powder technology. International Journal of Dairy Technology, 59, 70-75.

KEMPKES, M., EGGERS, J. & MAZZOTTI, M. 2008. Measurement of particle size and shape by FBRM and in situ microscopy. Chem. Eng. Science, 63, 4656-4675.

KHER, A., UDABAGE, P., MCKINNON, I., MCNAUGHTON, D. & AUGUSTIN, M. A. 2007. FTIR investigation of spray-dried milk protein concentrate powders. Vibrational Spectroscopy, 44, 375-381.

KIM, E. H. J., CHEN, X. D. & PEARCE, D. 2002. Surface Characterization of Four Industrial Spray-Dried Dairy Powders in relation to Chemical Composition, Structure and Wetting Property. Colloids and Surfaces B: Biointerfaces, 26, 197-212.

KIM, E. H. J., CHEN, X. D. & PEARCE, D. 2003. On the Mechanisms of Surface Formation and the Surface Compositions of Industrial Milk Powders. Drying Technology, 21, 265 - 278.

KIM, E. H. J., CHEN, X. D. & PEARCE, D. 2005. Effect of surface composition on the flowability of industrial spray-dried dairy powders. Colloids and Surfaces B: Biointerfaces, 46, 182-187.

KIM, E. H. J., CHEN, X. D. & PEARCE, D. 2009. Surface composition of industrial spray-dried milk powders. 1. Development of surface composition during manufacture. Journal of Food Engineering, 94, 163-168.

KOUGOULOS, E., JONES, A. G., JENNINGS, K. H. & WOOD-KACZMAR, M. W. 2005a. Use of focused beam reflectance measurement (FBRM) and process video imaging (PVI) in a modified mixed suspension mixed product removal (MSMPR) cooling crystallizer. Journal of Crystal Growth, 273, 529-534.

KOUGOULOS, E., JONES, A. G. & WOOD-KACZMAR, M. W. 2005b. Modelling particle disruption of an organic fine chemical compound using Lasentec focussed beam reflectance monitoring (FBRM) in agitated suspensions. Powder Technol., 155, 153-158.

KOVALSKY, P. & BUSHELL, G. 2005. In situ measurement of fractal dimension using focussed beam reflectance measurement. Chem. Eng. J., 111, 181-188.

KRAVTCHENKO, T. P., RENOIR, J., PARKER, A. & BRIGAND, G. 1999. A Novel Method for Determining the Dissolution Kinetics of Hydrocolloid Powders. Food Hydrocolloids, 13, 219-225.

LAMIOT, E., POULIOT, M., LEBEUF, Y. & PAQUIN, P. 1998. Hydration of Whey Powders as Determined by Different Methods. Journal of Food Science, 63, 789-792.

LARSEN, C. K., GA SERØD, O. & SMIDSRØD, O. 2003. A novel method for measuring hydration and dissolution kinetics of alginate powders. Carbohydrate Polymers, 51, 125-134.

LASKOWSKI, J. S. 1999. Comments on "Adsorption of Dextrin at Mineral/Water Interface" by G. Bhaskar Raju, Allan Holmgren, and Willis Forsling. Journal of Colloid and Interface Science, 211, 178.

LAVI, B. & MARMUR, A. 2006. The capillary race: Optimal surface tensions for fastest penetration. Colloids and Surfaces A: Physicochemical and Engineering Aspects, 282-283, 263-271.

LEE, K. T., FARID, M. & NGUANG, S. K. 2006a. The mathematical modelling of the rehydration characteristics of fruits. Journal of Food Engineering, 72, 16-23.

LEE, W., CLARK, S. & SWANSON, B. G. 2006b. Functional properties of high hydrostatic pressure-treated whey protein. Journal of Food Processing and Preservation, 30, 488-501.

LILLFORD, P. J. & FRYER, P. J. 1998. Food particles and the problems of hydration. Institution of Chemical Engineers, 76, 797-802.

LUCEY, J. A., TAMEHANA, M., SINGH, H. & MUNRO, P. A. 1998. Effect of interactions between denatured whey proteins and casein micelles on the formation and rheological properties of acid skim milk gels. Journal of Dairy Research, 65, 555-567.

MARABI, A., RAEMY, A., BAUWENS, I., BURBIDGE, A., WALLACH, R. & SAGUY, I. S. 2008. Effect of fat content on the dissolution enthalpy and kinetics of a model food powder. Journal of Food Engineering, 85, 518-527.

MCKENNA, A. B. 1997. Examination of whole milk powder by confocal laser scanning microscopy. Journal of Dairy Research, 64, 423-432.

MENDENHALL, I. V. & BROWN, R. J. 1991. Fourier Transform Infrared Determination of Whey Powder in Nonfat Dry Milk. Journal of Dairy Science, 74, 2896-2900.

MEYER, S., RAJENDRAM, V. S. & POVEY, M. J. W. 2006. CHARACTERIZATION OF RECONSTITUTED MILK POWDER BY ULTRASOUND SPECTROSCOPY. Journal of food quality, 29, 405-418.

MILLQVIST-FUREBY, A., ELOFSSON, U. & BERGENSTÅHL, B. 2001. Surface composition of spray-dried milk protein-stabilised emulsions in relation to pre-heat treatment of proteins. Colloids and Surfaces B: Biointerfaces, 21, 47-58.

MIMOUNI, A., DEETH, H. C., WHITTAKER, A. K., GIDLEY, M. J. & BHANDARI, B. R. 2009. Rehydration process of milk protein concentrate powder monitored by static light scattering. Food Hydrocolloids, 23, 1958-1965.

MORR, C. V. 1985. Functionality of Heated Milk Proteins in Dairy and Related Foods. J. Dairy Sci., 68, 2773-2781.

MORR, C. V., GERMAN, B., KINSELLA, J. E., REGENSTEIN, J. M., BUREN, J. P. V., KILARA, A., LEWIS, B. A. & MANGINO, M. E. 1985. A Collaborative Study to Develop a Standardized Food Protein Solubility Procedure. Journal of Food Science, 50, 1715-1719.

MOUGHAL, K. I., MUNRO, P. A. & SINGH, H. 2000. Suspension stability and size distribution of particles in reconstituted, commercial calcium caseinates. International Dairy Journal, 10, 683-690.

NACKA, F., CHOBERT, J. M., BUROVA, T., LEONIL, J. & HEAERTLE, T. 1998. Induction of new physicochemical and functional properties by the glycosylation of whey proteins. Journal of Protein Chemistry, 17, 495-503.

NÄRVÄNEN, T., LIPSANEN, T., ANTIKAINEN, O., RÄIKKÖNEN, H., HEINÄMÄKI, J. & YLIRUUSI, J. 2009. Gaining fluid bed process understanding by in-line particle size analysis. Journal of Pharmaceutical Sciences, 98, 1110-1117.

NÄRVÄNEN, T., SEPPÄLÄ, K., ANTIKAINEN, O. & YLIRUUSI, J. 2008. A New Rapid On-Line Imaging Method to Determine Particle Size Distribution of Granules. AAPS PharmSciTech, 9, 282-287.

NASIRPOUR, A., SCHER, J. & DESOBRY, S. 2006. Baby Foods: Formulations and Interactions (A Review) Taylor & Francis, 46, 665-681.

NEWMAN, S. 1968. Kinetics of wetting of surfaces by polymers; capillary flow. Journal of Colloid and Interface Science, 26, 209-213.

NICHOLAS, M. G. & PETEVES, S. D. 1994. Reactive joining : chemical effects on the formation and properties of brazed and diffusion bonded interfaces. Scripta metallurgica et materialia (Scr. metall. mater.) 31, 1091-1096.

NIJDAM, J. J. & LANGRISH, T. A. G. 2006. The effect of surface composition on the functional properties of milk powders. Journal of Food Engineering, 77, 919-925.

NIRO. 2005a. Niro Method No. A 7 a: Slowly Dispersible Particles in Agglomerated Milk Powder [Online]. Available: http://www.niro.com/ndk_website/NIRO/cmsdoc.nsf/WebDoc/ndkw74jjl3 [Accessed 12th September, 2007].

NIRO. 2005b. Niro Method, A 5 a : Wettability (http://www.niro.com/ndk_website/niro/cmsdoc.nsf/WebDoc/ndkw6u9bbd) , Last Access: 5th May, 2010. [Online]. Niro A/S. Available:

http://www.niro.com/ndk_website/NIRO/cmsdoc.nsf/WebDoc/ndkw6u9bbd [Accessed 5th May, 2010].

NIRO. September 2006. Niro Method No. A 3 a: Insolubility Index, A 3 a [Online]. Available: http://www.niro.com/ndk_website/NIRO/cmsdoc.nsf/WebDoc/ndkw74jjk8 [Accessed 12th September, 2007].

O'BRIEN, W. J., CRAIG, R. G. & PEYTON, F. A. 1968. Capillary penetration between dissimilar solids. Journal of Colloid and Interface Science, 26, 500-508.

O'SULLIVAN, B., BARRETT, P., HSIAO, G., CARR, A. & GLENNON, B. 2003. In Situ Monitoring of Polymorphic Transitions. Organic Process Research & Development, 7, 977-982.

OLDFIELD, D. J., TAYLOR, M. W. & SINGH, H. 2005. Effect of preheating and other process parameters on whey protein reactions during skim milk powder manufacture. International Dairy Journal, 15, 501-511.

OWEN, A. T., FAWELL, P. D., SWIFT, J. D. & FARROW, J. B. 2002. The impact of polyacrylamide flocculant solution age on flocculation performance. International Journal of Mineral Processing, 67, 123-144.

PARADKAR, M. M. & IRUDAYARAJ, J. 2002. Determination of cholesterol in dairy products using infrared techniques: 1. FTIR spectroscopy. International Journal of Dairy Technology, 55, 127-132.

P ŠECKÝ, J. 1997. Handbook of Milk Powder Manufacture, Copenhagen, Denmark, Niro A/S.

QI, P. X. 2007. Studies of casein micelle structure: the past and the present. Lait, 87, 363-383.

SAGGIN, R. & COUPLAND, J. N. 2002. Ultrasonic Monitoring of Powder Dissolution. Journal of Food Science, 67, 1473-1477.

SCHEIN, C. H. 1990. Solubility as a Function of Protein Structure and Solvent Components. Nature Biotechnology 8, 308-317.

SCHÖLL, J., BONALUMI, D., VICUM, L., MAZZOTTI, M. & MÜLLER, M. 2006. In Situ Monitoring and Modeling of the Solvent-Mediated Polymorphic Transformation of l-Glutamic Acid. Crystal Growth & Design, 6, 881-891.

SCHUBERT, H. 1993. Instantization of powdered food products. International Chemical Engineering, 33, 28-45.

SCHUCK, P. 2008. Effects of drying on milk proteins. In: ABBY, T., MIKE, B. & HARJINDER, S. (eds.) Milk Proteins. San Diego: Academic Press.

SCHUCK, P., DAVENEL, A., MARIETTE, F., BRIARD, V., MEJEAN, S. & PIOT, M. 2002. Rehydration of casein powders: effects of added mineral salts and salt addition methods on water transfer. International Dairy Journal, 12, 51-57.

SINGH, H. 2004. Heat stability of milk. International Journal of Dairy Technology, 57, 111-119.

SINGH, H. & CREAMER, L. K. 1991. Denaturation, aggregation and heat stability of milk protein during the manufacture of skim milk powder. Journal of Dairy Research, 58, 269-283.

SUN, Y., SONG, X., WANG, J., LUO, Y. & YU, J. 2009. On-line monitoring of lithium carbonate dissolution. Crystal Research and Technology, 44, 1223-1229.

SWIFT, J. D., SIMIC, K., JOHNSTON, R. R. M., FAWELL, P. D. & FARROW, J. B. 2004. A study of the polymer flocculation reaction in a linear pipe with a focused beam reflectance measurement probe. International Journal of Mineral Processing, 73, 103-118.

SZPENDOWSKI, J., SMIETANA, Z. & SWIGON, J. 1997. Selected physicochemical and functional properties of caseinates Pol. J. Food Nutr. Sci, 6, 79-87.

TAJAROBI, F., ABRAHMSÉN-ALAMI, S., CARLSSON, A. S. & LARSSON, A. 2009. Simultaneous probing of swelling, erosion and dissolution by NMR-microimaging--Effect of solubility of additives on HPMC matrix tablets. European Journal of Pharmaceutical Sciences, 37, 89-97.

THOMANN, J. M., VOEGEL, J. C. & GRAMAIN, P. 1990. Kinetics of Dissolution of Calcium Hydroxyapatite Powder. III: pH and Sample Conditioning Effects. Calcified Tissue International 46, 121-129.

THOMAS, M., SCHER, J., DESOBRY-BANON, S. & DESOBRY, S. 2004. Milk Powders Ageing: Effect on Physical and Functional Properties. Critical Reviews in Food Science and Nutrition, 44, 297-322.

TOK, A., GOH, X., NG, W. & TAN, R. 2008. Monitoring Granulation Rate Processes Using Three PAT Tools in a Pilot-Scale Fluidized Bed. AAPS PharmSciTech, 9, 1083-1091.

VARNAM, A. H. & SURHERLAND, J. P. 1994. Milk Powder Technology: Evaporation and Spray Drying, Copenhagen, Denmark, NIRO A/S.

VOJDANI, F. 1996. Solubility. In: HALL, G. M. (ed.) Methods of Testing Protein Functionality. London: Blackie Academic & Professional.

VU, T. O., GALET, L., FAGES, J. & OULAHNA, D. 2003. Improving the dispersion kinetics of a cocoa powder by size enlargement. Powder Technology, 130, 400-406.

WALLINGFORD, L. & LABUZA, T. P. 1983. Evaluation of the Water Binding Properties of Food Hydrocolloids by Physical/Chemical Methods and in a Low Fat Meat Emulsion. Journal of Food Science, 48, 1-5.

WALSTRA, P. 1990. On the Stability of Casein Micelles. Journal Dairy Science, 73, 1965-1979.

WALSTRA, P. 1999. Casein sub-micelles: do they exist? International Dairy Journal, 9, 189-192.

WALSTRA, P. & JENNESS, R. 1984. Dairy Chemistry and Physics, New York, Chichester, Brisbane, Toronto, Singapore, A Wiley-Interscience Publication.

WANG, Z., WANG, J. & DANG, L. 2006. Nucleation, Growth, and Solvated Behavior of Erythromycin as Monitored in Situ by Using FBRM and PVM. Organic Process Research & Development, 10, 450-456.

WASHBURN, E. W. 1921. The Dynamics of Capillary Flow. Physical Review, 17, 273.

WESTERGAARD, V. 1994. Milk Powder Technology: Evaporation and spray drying, Copenhagen, Denmark, NIRO A/S.

YOON, S.-Y. & DENG, Y. 2004. Flocculation and reflocculation of clay suspension by different polymer systems under turbulent conditions. Journal of Colloid and Interface Science, 278, 139-145.

YU, W. & ERICKSON, K. 2008. Chord length characterization using focused beam reflectance measurement probe - methodologies and pitfalls. Powder Technol., 185, 24-30.

Monash University

Declaration for Thesis Chapter Three

In the case of Chapter 3, the nature and extent of my contribution to the work was the following:

Name	% contribution	Nature of contribution
Yuan Fang	85%	Initiation, Key ideas, Experimental works, Development, Data analysis, Writing up
Dr. Cordelia Selomulya	10%	Initiation, Key ideas, Development, Review
Prof. Xiao Dong Chen	5%	Initiation, Development, Review

Declaration by co-authors

The undersigned hereby certify that:

(1) they meet the criteria for authorship in that they have participated in the conception, execution, or interpretation, of at least that part of the publication in their field of expertise;
(2) they take public responsibility for their part of the publication, except for the responsible author who accepts overall responsibility for the publication;
(3) there are no other authors of the publication according to these criteria;
(4) potential conflicts of interest have been disclosed to (a) granting bodies, (b) the editor or publisher of journals or other publications, and (c) the head of the responsible academic unit; and
(5) the original data are stored at the following location(s) and will be held for at least five years from the date indicated below:

Location(s)	**Department of Chemical Engineering, Monash University** **Clayton campus, Australia**

Signature		
Signature		
Signature		

Chapter 3

Characterization of Milk Protein Concentrate Powder Powder (MPC) Solubility Using Focused Beam Reflectance Measurement (FBRM)

3.1. Introduction

Milk protein concentrate (MPC) is a new generation of dairy product, which contains 40-90% protein in total solid (Havea, 2006, Kher et al., 2007). The protein content of MPC powder is usually specified as part of its name, for example MPC 80 and MPC 85 would consist of 80% and 85% protein contents, respectively (Havea, 2006, Carr et al., 2007). They are produced by subjecting the skim milk through ultra- and dia-filtration prior to drying in order to remove lactose and minerals (Havea, 2006, Castro-Morel and Harper, 2002). MPC has a wide range of applications as ingredients in the food and beverage industry for cheese and yoghurt manufacturing, confectionery, and coffee. In the manufacturing of cheese, the protein content of milk can be increased by adding MPC powder which improves the efficiency and consistency of the resulting cheese product (Carr et al., 2007). However, their uses are somewhat restricted due to the varying solubility of the different MPC powders (Castro-Morel and Harper, 2002), especially under cold water (Carr et al., 2007).

An experiment was carried out to investigate the difference in dissolution behaviour between MPC and skim milk powder (SMP). **Error! Reference source not found.** shows an image of a MPC particle on a glass slide when a drop of distilled water is dropped onto it at room temperature. The MPC did not dissolve but instead increased in particle size from 300 µm initially to 600 µm at the end of 3 hours. In contrast, for the same experiment conducted on SMP, the moment the droplet of water was dropped onto the powder particle, it started to disperse and dissolve, and forming a homogeneous solution within 10 seconds, as shown in **Error! Reference source not found.**. The experiment demonstrated the poor dissolution property of MPC powder. This challenging issue has brought about various studies to quantify the functional properties of MPC powders (Gaiani et al., 2005, Havea, 2006, Anema et al., 2006).

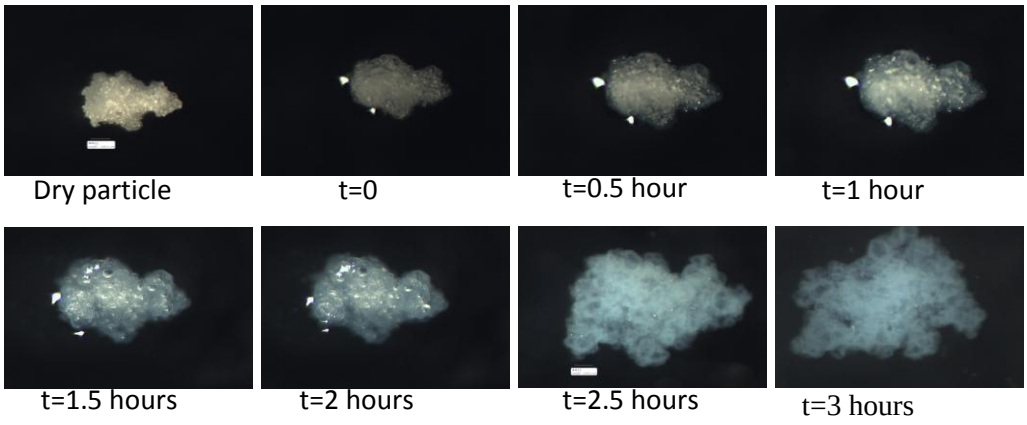

Figure 3-1 A single MPC powder rehydration (3 hours duration)

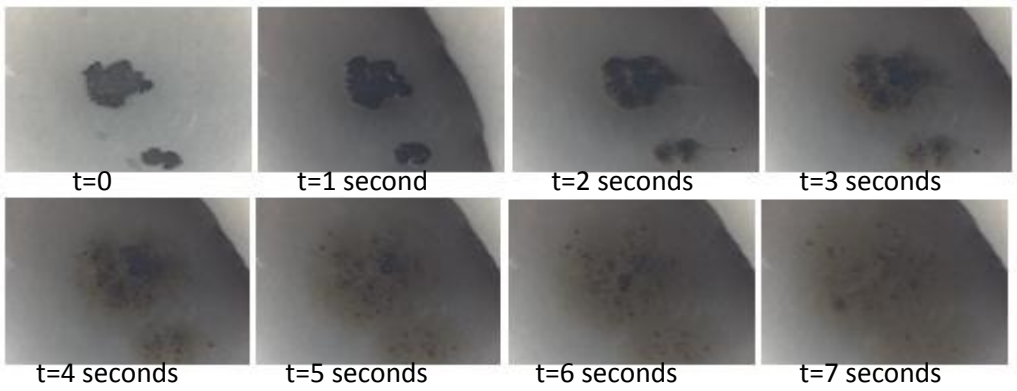

Figure 3-2 A single skim milk particle dissolution (10 second)

The functionality of MPC varies according to their different composition, heating history, and storage duration, with MPC solubility reported to decrease with storage time and storage temperature (Anema et al., 2006, Mistry and Hassan, 1991). A possible explanation for this particular phenomenon is that the proteins on the surface of MPC powder form cross-linked networks with neighbouring proteins (on adjacent powder)

during storage. This cross-linked network could act as a barrier for water to penetrate, thus inhibiting the rehydration of MPC particles (Anema et al., 2006). However, it is noted that the increasing number of cross-links adversely affects the solubility of the powder only after a certain threshold limit of the cross-link (Anema et al., 2006). Previous studies also have indicated no clear correlation between protein content and the functionality of MPC (Castro-Morel and Harper, 2002).

In recent years, more studies have been conducted to characterize the MPC dissolution properties. One such study determined the solubility of MPC using a centrifugation technique, by separating the MPC into two fractions: the soluble protein in the supernatant and the insoluble protein in the sediment (Havea, 2006). In this study, aggregated proteins may be classified as 'soluble' (in the supernatant) or 'insoluble' (in the sediment) depending on the experimental conditions such as different centrifugation speed. As such, it was concluded that the term 'solubility' should only be considered as a relative measure, and was specific for a fixed set of experimental conditions (Havea, 2006). In another study, a turbidity sensor was employed to measure the rehydration property of protein-rich dairy powders (Gaiani et al., 2009). With the assistance of other techniques (such as static light scattering microscopy), turbidity was used as a measure to differentiate the different powder rehydration phases in building a rehydration profile, from wetting and swelling phase, to the dispersion phase, and finally a homogeneous fluid liquid phase. In some of the studies, the dissolution properties of dairy powders were characterized using Malvern Mastersizer (Malvern Instruments Ltd., Malvern, UK) (Gaiani et al., 2007, Kwak et al., 2009, Gaiani et al., 2006, Chen and Lloyd, 1994, Gaiani et al., 2005). However, this method requires sample preparation such as dilution and is restricted to very dilute concentration of MPC powders (less than 0.1%). During the analysis process, the measuring solution is pumped from the stirring tank to the sample cell in which the laser light is transmitted through a Fourier lens (Kwak et al., 2009).

Here, the technique of Focused Beam Reflectance Measurement (FBRM) was employed to characterize the solubility of MPC powders. FBRM technique provides *in situ* monitoring of particle size and the change in particle counts (Heath et al., 2002, Hu et al., 2008, Yu and Erickson, 2008, Kougoulos et al., 2005, Kempkes et al., 2008, Kovalsky and Bushell, 2005), in a relatively robust manner without the need for off-line sampling. This unique property enables FBRM to be widely applied in both industrial and laboratory

processes, such as crystallization (Kempkes et al., 2008), and fluidized bed granulation (Hu et al., 2008) etc.

In the dairy industry, powder dissolution is considered as the key determinant of the overall reconstitution quality. The aim of this study was to investigate the suitability of FBRM as a tool to characterize MPC solubility, so that a protocol for quantifying dissolution of MPC can be proposed and the dissolution profile of MPC established. In comparison to other light scattering techniques to measure particle size (i.e. Malvern Mastersizer), FBRM can be used directly *in situ* without the need of further dilution of samples. The method for monitoring the change in MPC chord length with time using FBRM was outlined in the Section 3.2.2. The suitability of using FBRM as a tool to quantify solubility was first assessed by comparing the results with those obtained from standard insolubility tests. The effects of different parameters such as stirring rate and initial powder concentration were also investigated to minimise inconsistency due to testing conditions. The particle size population counts were investigated which can provide further information regarding different particle dissolution mechanism.

Using the FBRM data, a dissolution-temperature profile is generated for each MPC powder. This study is the first step to establish a dynamic dissolution model for dissolution kinetics of MPC in particular. The future model is expected to provide greater insights into MPC powder dissolution behaviour under specific conditions.

3.2. Materials and Methods

3.2.1. Materials

Six types of industrial spray-dried MPC powders with different protein contents, heating and storage history were obtained from a local dairy factory. They were categorized as powders A, B, C, D, E and F respectively (Further details of these powders are not mentioned here due to confidentiality matters).

3.2.2. Experimental set up and procedure

Each experiment was carried out in a 600 mL vessel equipped with an overhead stirrer 4-blade impeller of 50 mm diameter (RW16, IKA WERKE, Germany), rotating at 800 r.p.m.. The testing temperature was pre-set and maintained at 20°C, 30°C, 40°C, 50°C, and 60°C using a water bath as shown in Figure 3-1.

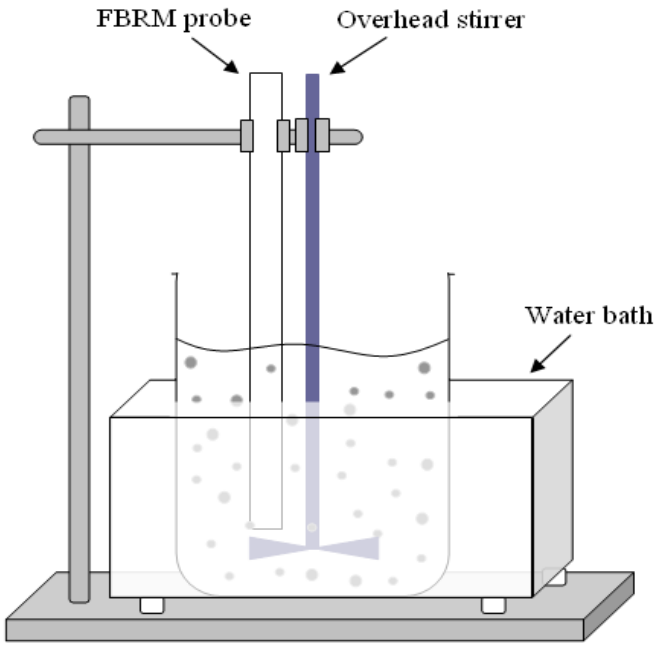

(a). Experimental setup

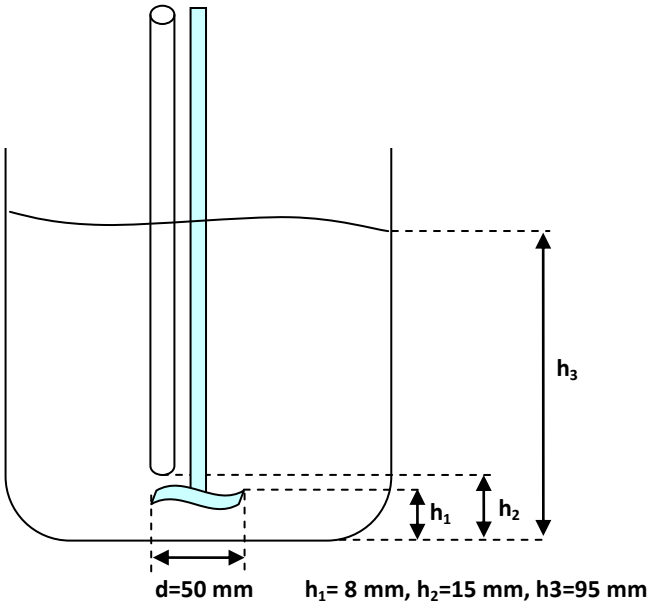

(b). Dimensions of vessel used for experiment

Figure 3-1 Schematic of the experimental setup

For each set of test, 7.50 ± 0.01 g MPC powder were measured and poured into the beaker with 500 mL distilled water, preheated up to the testing temperature before commencement of the experiment, to make up a 1.5 wt% solution. The stirrer was adjusted to a stirring rate of 800 r.p.m. The data from FBRM (Lasentec® D600L, Mettler Toledo) was collected using an iC FBRM™ software (Mettler Toledo) and the data collecting

interval was set at 10 seconds with the measuring duration of 30 minutes. After 30 minutes, the insolubility test was carried out according to Niro method A.3a (Niro, September 2006) with slight modification as follow. The resulting solution from FBRM was collected into 4 centrifuge tubes using a 50 mL syringe. Each tube was filled with about 50 mL of mixture sample. The weight of each centrifuge tube before and after filling with sample solution was recorded. The sample solution was then centrifuged for 5 minutes at 1000 r.p.m. (88 g) and the supernatant was discarded. The sediment remaining at the bottom of the tubes were extracted and dried overnight at 50 °C in the oven. The sediment amount after drying was recorded. The insolubility index (ISI) of the different MPC powders was calculated using Equation 3-1:

$$ISI = \frac{m_{tube+sed} - m_{tube}}{m_{tube+sol} - m_{tube}} \times 100\%$$

Equation 3-1

where m_{tube} is the weight of empty centrifuge tube, $m_{tube+sed}$ is the weight of tube with sediment after drying, $m_{tube+sol}$ is the weight of centrifuge tube with solution before centrifugation.

One needs to note that given long enough time, MPC would dissolve completely in most cases (Bhandari, Personal communication, 2009). Hence, the ISI actually characterize a dynamic behaviour. The consumers who use the powders are often interested in 'shorter' time behaviour.

3.2.3. Relative particle counts (RPC) and initial particle size

In this study, the particle counts (PC) of different powders were recorded. FBRM could provide data such as particle population information based on particle size ranges from between 1 to 1000 µm. The software by default divides the particle population into 5 groups; namely those with particle size less than 10µm, between 10-50 µm, 50-150 µm, 150-300 µm and 300-1000 µm, respectively. In this study, the general dissolution behaviour of the powders investigated with particle populations were classified into 3 categories: fine particles (1-10 µm), median sized particles (10-150 µm), and big/agglomerate particles (150-300 µm). It is noted that for the set of powders used in this study, no particle count within 300-1000 µm was detected in all the experiments.

The experimental procedure described in Section 3.2.2 was also carried out at 0 °C. The readout for the last 5 minutes from the FBRM were averaged and defined as the initial particle size in suspension of a particular powder (A-F). It is expected that the particle size will not vary at such a low temperature. This will be utilised as the baseline for the analysis of the dissolution kinetics for a particular powder at different testing conditions. As such, the PC at this early stage of dissolution (i.e. 0 °C, 1 minute from dissolution commencement) will be the reference PC for the subsequent dissolution analysis.

For the dissolution analysis of each type of powder, the relative particle counts (RPC) was calculated using Equation 3-2:

$$RPC_{i,\,tmp}(t) = \frac{PC_{i,\,tmp}(t)}{PC_{i,\,0\,^{\circ}C}(1\,min)}$$

Equation 3-2

where $RPC_{i,tmp}(t)$ is the relative particle counts of powder *i* at certain testing temperature *tmp* at time *t*, $PC_{i,tmp}(t)$ is the actual particle counts of powder *i* at certain testing temperature *tmp* at time *t*, and $PC_{i,0\ ^{\circ}C}\ (1\ minutes)$ is the particle counts for powder dissolved at 0 °C solution after 1 minute.

3.3. Results and Discussion

3.3.1. Reproducibility of the solubility measurement of MPC

The reproducibility of FBRM solubility measurement for MPC powders was investigated. The measurement was carried out using powder A (1.5 wt%) at 20 ℃, 800 r.p.m. stirring rate. Duplicates were obtained for each measurement to get the average chord length. As shown in Figure 3-2, the reproducibility of FBRM is very good with a percentage error of less than 5%.

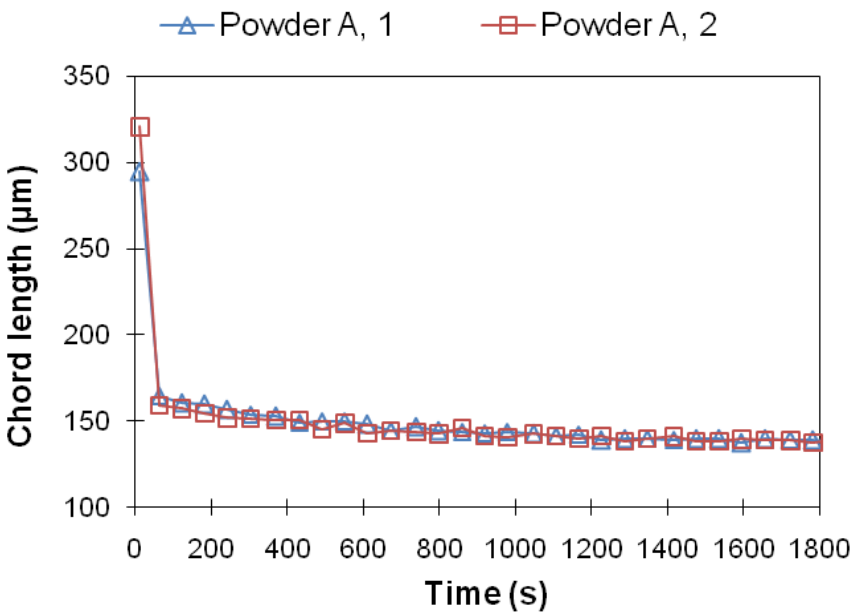

Figure 3-2 Chord length of powder A at 20 ℃ (repeat measurement)

3.3.2. The effect of external factors on FBRM's MPC chord length

These tests were conducted to eliminate the possibility that external factors, such as stirring rate and powder concentration, had any effect on the FBRM particle size results.

The FBRM results for powder A tested at 50 ℃ with different stirring rate are as shown in Figure 3-3. It can be observed that the chord length for high stirring rate is smaller (more soluble) than that for low stirring rate. It can therefore be concluded that stirring rate has substantial effect on measured particle size. To investigate the effect of powder concentration, powder A was tested at different concentrations (1.5 wt% and 0.75 wt%) and results are as shown in Figure 3-4. Negligible differences (<5%) can be observed at different initial solids concentrations indicating that the solid concentration has no observable effect on measured particle size.

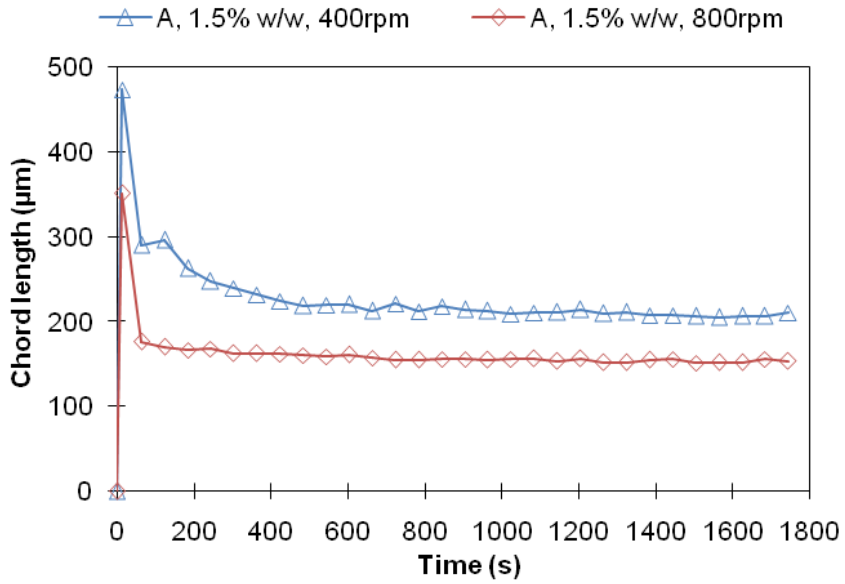

Figure 3-3 The effect of stirring speed on chord length of powder A at 50 ℃

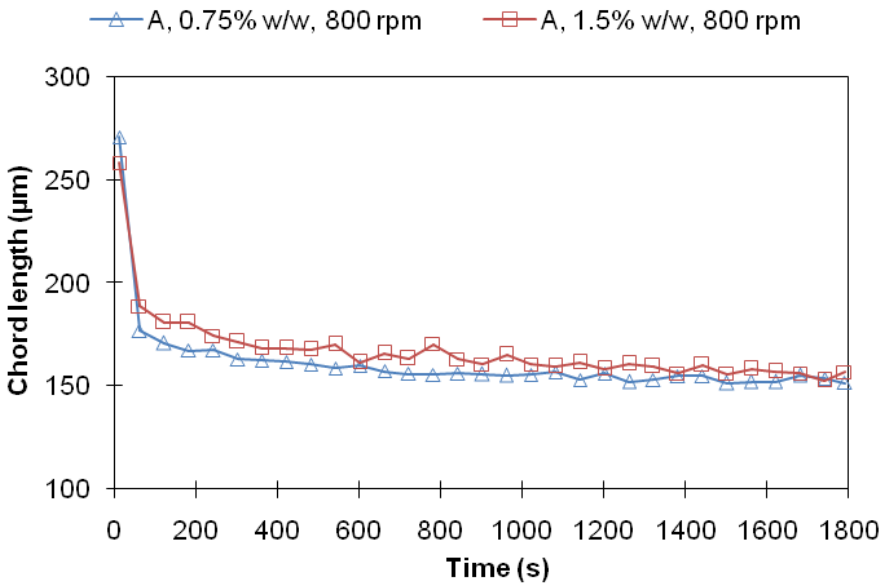

Figure 3-4 The effect of concentration on chord length of powder A at 50 ℃

3.3.3. Defining solubility for MPC

Figure 3-5 shows the changes of chord length as represented by chord length measured by FBRM against time for powders A-F. Each curve represents data plotted at a specific testing temperature.

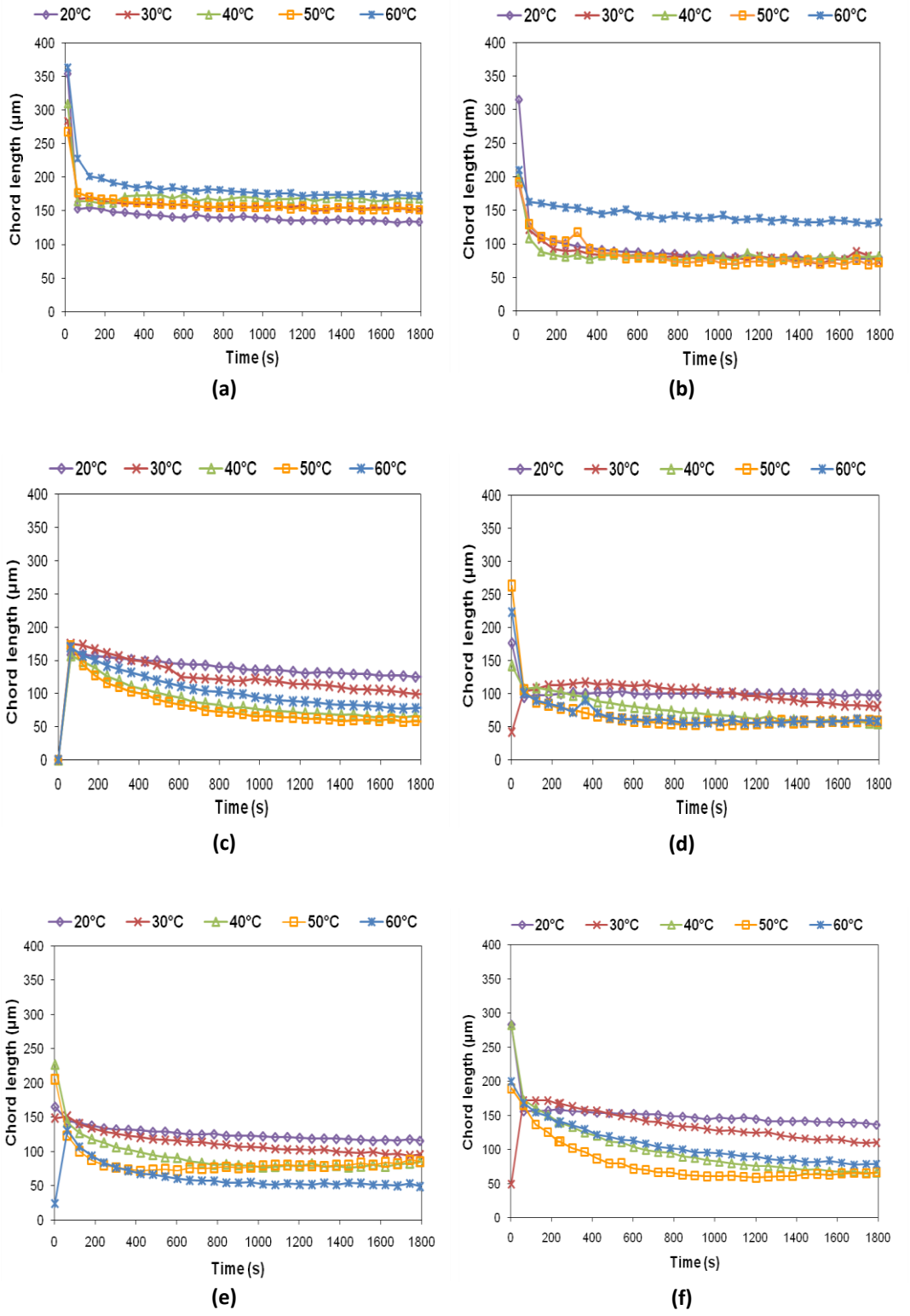

Figure 3-5 Results of powder A-F obtained from FBRM

(a. Powder A; b. Powder B; c. Powder C; d. Powder D; e. Powder E; f. Powder F)

As solubility is a relative measure which varies according to different testing conditions (Havea, 2006), it is necessary to define a physical quantity of measure for the solubility of MPC powders, considering the dynamic nature of this solubility as mentioned earlier. Using FBRM, the mean chord length of the particles in suspension was used to quantify powder solubility. During the dissolution process, agglomerated MPC particles would gradually break up into smaller particles (Fang et al., 2008, Mimouni et al., 2009) which were shown by the decrease in chord length from the FBRM readout. A smaller chord length measured would imply a lesser amount of un-dissolved particles in the suspension. If the suspension still contained un-dissolved particles, the standard insolubility test (Niro Method A.3a) should exhibit presence of sedimentation after centrifugation. Therefore, the chord length from FBRM should be directly related to the amount of sediment (insolubility test) for a particular powder, giving rise to the same relationship trend under different testing conditions as observed in Figure 3-6.

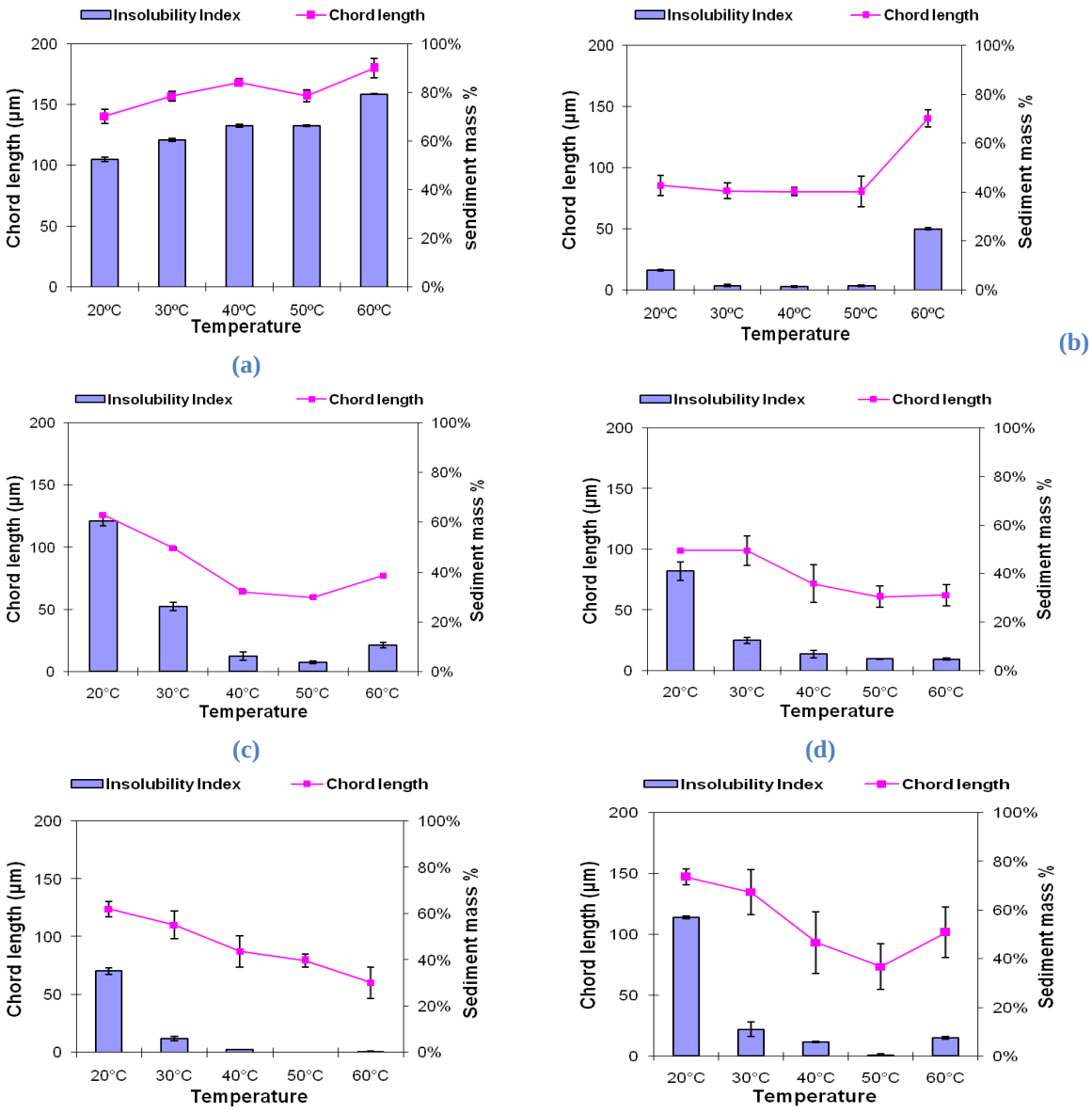

Figure 3-6 Powder A-F chord length / insolubility against temperature (a. Powder A; b. Powder B; c. Powder C; d. Powder D; e. Powder E; f. Powder F)

Firstly, the data from FBRM and the insolubility test were compared for each powder. This was done by averaging the chord length from FBRM (between 100 seconds and 1800 seconds, and will be explained in detail in the Section 3.3.4.) for each temperature. Results from both tests exhibit similar trends for the solubility of the powder at different temperatures, thus verifying that FBRM can be adopted as a technique to assess the solubility of MPC powders.

An assumption which is usually taken is that after centrifuging the sample, the particles remaining in the supernatant was considered to be dissolved. To quantify this 'threshold' level of chord length (below which the powders are considered dissolved), the following

experiment was conducted. After centrifugation of the sample, the supernatant was measured by FBRM for 5 minutes. The measurement was duplicated and the FBRM results for all powders are as shown in Figure 3-7. The results indicated that the chord length (of the supernatant) for all the measurements were approximately 100 µm regardless of the particle size of the initial solution. This is important information as any particle with particle size smaller than 100 µm will be considered to be 'dissolved' in this study for practical purposes.

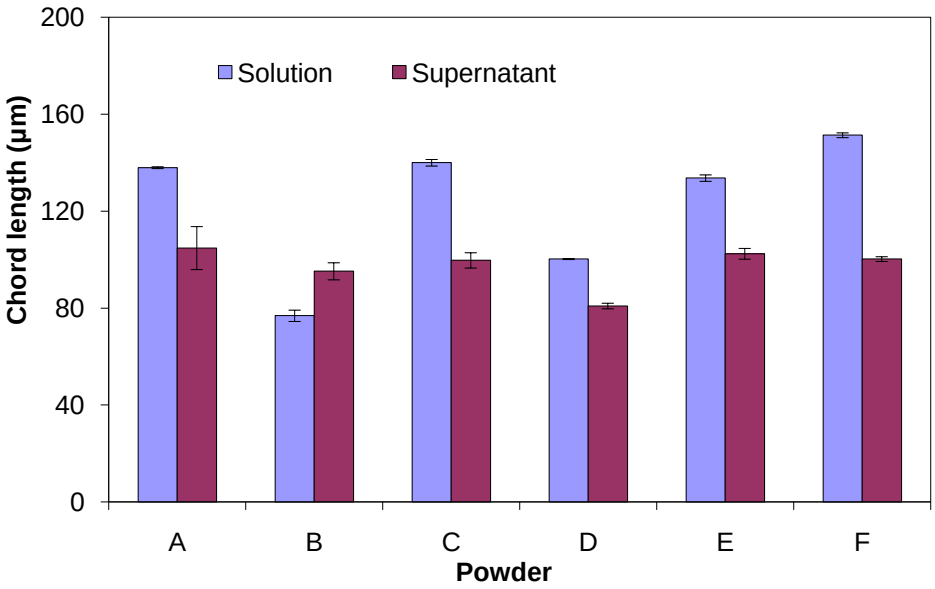

Figure 3-7 Chord length of the supernatant from different powders at 20°C

In the case of powder B, the chord length of the original solution was 75 µm before centrifugation but increased to 96 µm after centrifugation. A possible explanation is that the small particles might have come into contact and aggregated onto each other and form larger particles due to compaction during centrifugation. These larger particles (size greater than 96 µm) were removed along with the sediments while the smaller particles (<96 µm) remained in the solution. This resulted in an increasing chord length of the supernatant after centrifugation.

3.3.4. Establishing the dissolution profiles of MPC

From the FBRM data shown in Figure 3-5, it can be seen that at the beginning of each run, there was a sudden and sharp increase in chord length, after which it decreased and reached a plateau. A probable cause was that when the powder was poured onto the water surface, the powder first started to sink into the water causing the particle count to increase dramatically until all the powders had fully immersed. Thus, the FBRM reading showed large particle size with low particle counts initially, while the chord length increased

sharply from 0 to the measured particle size. In this case, in order to have a reproducible starting point for monitoring powder dissolution, the FBRM measured particle size at 0 °C was defined as the original size of the specific powder and used in Section 3.3.6 as the initial particle size for dissolution kinetic analysis.

From Figure 3-5, it can be observed that the dissolution behaviour of various powders were very different, due to the fact that the powders had been subjected to different production and storage conditions, in addition to the different protein contents. For powder A, the chord length increased with increasing testing temperatures, implying that the solubility of powder A was worse at increasing testing temperature. Powder A had the best solubility at 20 °C and was least soluble at 60 °C. For powder B, the chord length at 20-50 °C were similar, but then increased sharply at 60 °C, implying that powder B was more soluble between 20-50 °C and less soluble at 60 °C. For powders C, D and F, similar dissolution trends were observed, with all showing better solubility at 50 °C than at any other temperatures. For powder E, the chord length decreased with increasing temperature. This indicates that its solubility increased with temperature ranging from 20 ℃ to 60 °C. Generally, it was noted that the solubility decreased (indicated by increase in chord length) at higher temperature (>50 ^{o}C) for most of the powders. These results also indicate that the solubility of MPC powder was strongly affected by the testing condition (e.g. the temperature) which is in agreement with the findings of Mimouni *et al.* (Mimouni et al., 2009). This dependence on temperature could be due to the further denaturation and the greater extent of aggregation of protein at higher temperatures, causing an increase in particle size and hence poorer solubility. In addition, it can be seen from Figure 3-5 that for all powders at each testing temperature, the chord length exhibited the most dynamic changes in the first 200 seconds. This indicates that the majority of MPC powders dissolution activities occurred during this period.

These results highlight the usefulness of FBRM to characterize the dissolution behaviours of different MPC powders *in situ* and in a reproducible manner. For the application of FBRM on characterization of other dairy powder solubility (skim milk powder, whole milk powder, milk protein concentrate and whey protein concentrate), refer to Appendix 3.

3.3.5. Particle size population analysis

During the dissolution of a powder, two processes are known to occur simultaneously: the breaking up of agglomerates into primary particles, and the dissolution of primary

particles into solution (Mimouni et al., 2009). Intuitively, the solubility of a certain powder is directly related to how well the powder breaks down into its constituent components. It is therefore important to understand the dynamics of different particle size populations during the course of the dissolution process.

With different particle sizes, the three particle populations are expected to show different behaviour during dissolution. Therefore it is expected that the number of particle size between 150-300 μm (large particle population) should decrease with time whereas the number of particle size between 1-10 μm (fine particle population) may actually increase with time. The medium particle population size could vary, due to the influx and efflux of particles between the other two populations.

Comparison of the RPC for fine particles and large particles clearly shows different dissolution behaviours as demonstrated in Figure 3-8. Taking powder A as an example of a poorly soluble powder, the fine particle population counts for powder A increased only slightly from 0 to 1 in the first 200 seconds, and remained relatively constant thereafter for all testing temperatures. As for the large particle population counts, the RPC decreased from 1.2 to 1 at 60 ℃ with similar trends observed for other temperatures. This indicated that for powder A, both the fine and large particle population counts did not change significantly within the testing period, implying that the particles hardly break up from the agglomerates form into smaller particles (<10 μm). This could be due to possible pre-denaturation or drying (concentrate the small elements within each particle of MPC) during processing where elements contact tightly, making them extremely hard to break down. Therefore, powder A's dissolution rate is attributed to the limitation of the rate of de-agglomeration.

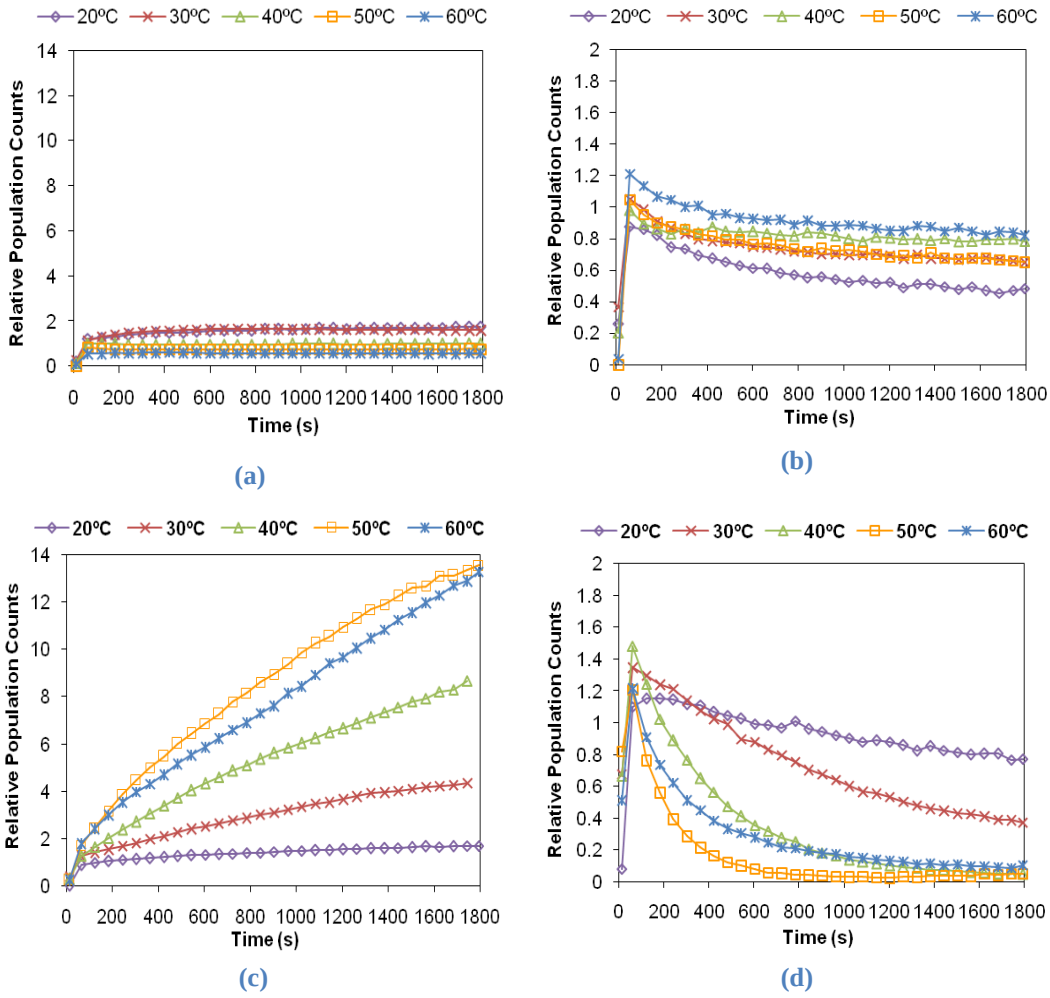

Figure 3-8 Particle population counts for fine/big particles of Powder A and Powder F

(a. Powder A fine particle counts; b. Powder A large particle counts; c. Powder F fine particle counts; d. Powder F large particle counts)

This difference in solubility and RPC results between the different size populations can be further emphasized by comparing with powder F, an example of a powder with good solubility. Figure 3-8 shows the RPC of fine and big particles for both powders A and F and it is clear significant differences were observed.

Dissolution of the powder can be clearly seen in the change of RPC with dissolution time as the fine particle population count increases significantly whereas the large particle population count decreases substantially (to 0 in some cases). The dissolution trends between different testing temperatures could be clearly observed for powder F. The RPC of powder F fine particles shows significant increase till the end of dissolution, with the rate of increase dependent on the testing temperature (from 1.7 at 20 °C to 13.6 at 50 °C, slightly decreasing to 13.3 at 60 °C, all recorded at 1800 seconds). As for the RPC of large particle population, the rate of decrease was also dependent on the temperature with

increasing rate from 20 °C to 50 °C, and then decreasing at 60 °C. This indicates that at higher dissolution temperature (i.e. 50 °C), powder F readily de-agglomerate into primary particles; consequently reduced the dissolution time.

The results were also verified by the images taken using SEM and light microscopy as shown in Figure 3-9 and Figure 3-10. From the SEM images, it is clear that the dry particles of powder A appear to be highly agglomerated whereas powder F dry particle appeared to be smoother and less agglomerated. From the light microscopy images, the particles of powder A still remained in agglomerated form even after dissolution at 20 °C, whereas the particles of powder F appeared as fine particles under the same condition.

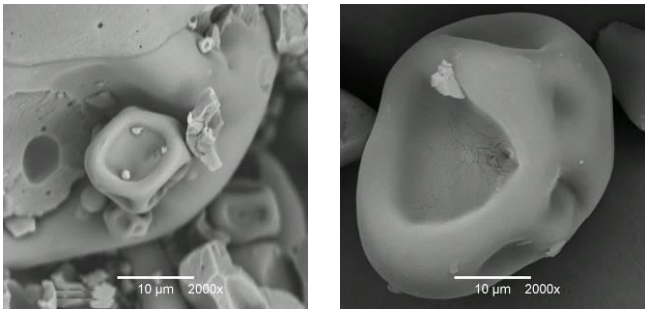

(a). Powder A (b). Powder F

Figure 3-9 SEM images of powder A and F

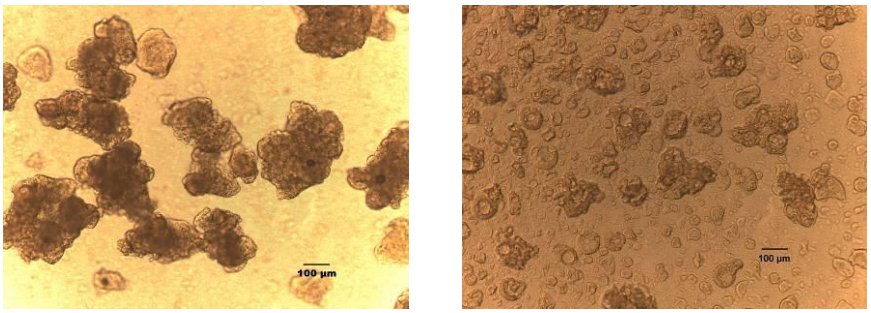

(a). Powder A after dissolution (20°C) (b). Powder F after dissolution (20°C)

Figure 3-10 Light microscopy images of Powder A and F dissolved at 20°C

Taken together, these results show that the population analysis with FBRM can be used to characterise the dissolution dynamics and solubility of different powder type. In this instance, it successfully monitored the dissolution dynamics of specific powders and also distinguished between powders with good and poor solubility.

Additional information can also be obtained from population analysis. As mentioned earlier, there were two phenomena observed during dissolution. One was the de-

agglomeration of big particles shown by the decrease in RPC for big particles. The other was the breaking down into primary particles shown by the increase in RPC of fine particles. However, at the early period of each test, it was noted that there was a significant rise in the RPC for the large particle population. The RPC values in this case was greater than 1 (i.e. powder A, increase from 0 to 1.2 by 1 minute at 60 °C) which meant a greater number of big particles as compared to the initial number. This was possibly caused by the collision of particles during stirring. This sudden increase was also observed in the RPC for the fine particle population (i.e. powder A, increase from 0 to 0.5 by 1 minute at 60 °C). Taken together, looking at the chord length plot which takes into account all the populations of particles, it can be deduced that both increases of big and fine particles at the early period of each experiments indicates the competition of the two processes, agglomeration and breaking up for the powder particles. On the one hand, collision due to stirring act to increase big particles by 'combining' smaller particles, while on the other hand, the breaking up process tries to increase the fine particle population by breaking up larger particles into smaller ones. These effects lasted only for a very short period of time until the particles start to disperse into the water. This effect was more prominent in the large particle population and subsequent changes in numbers of big particles will therefore significantly affect the chord length. As such, the collision of large particles can be considered the dominant process at the beginning of dissolution and reflected by the sharp increase in chord length at the start of each experiment.

3.3.6. Characterization of dissolution parameters with FBRM

Using the dissolution-temperature profile for various powders formulated by the FBRM analysis, a better understanding of the dynamic behaviour of these powders can be obtained. One way to achieve this is by data fitting the experimental data obtained to investigate any correlation between data parameters and process conditions. The changes in particle size from the original particle size to steady state under different temperatures were fitted with logarithmic plots that gave the best fit as shown in Figure 3-11. From the fit, the following parameters can be obtained:

The ***initial dissolution rate*** indicates how fast the chord length drops from the original particle size until it reaches equilibrium (i.e. the gradient/slope of the fitting curve). The greater the magnitude implies a faster dissolution rate of the powder. The ***lag time*** is defined as the duration from when the powder is first introduced until the chord length in

suspension reaches the original particle size (i.e. defined as the starting point to monitor powder dissolution).

The lag time gives an indication on how fast the powder is being wetted, the degree of compactness and agglomeration which will affect the amount of surface area the powder interacts with the water. The results from Section 3.3.5 also indicate the cause of lag time which is possibly due to the collision of particles. The duration required to break up colliding particles is depending on the property of particles (i.e. hydrophobicity). The shorter the lag time, the easier the agglomerates break up into smaller particles with greater surface area in contact with water surface, and thus a better solubility. This is conversely true for a longer lag time. As such these properties could provide an indirect relationship between the physical and functional properties.

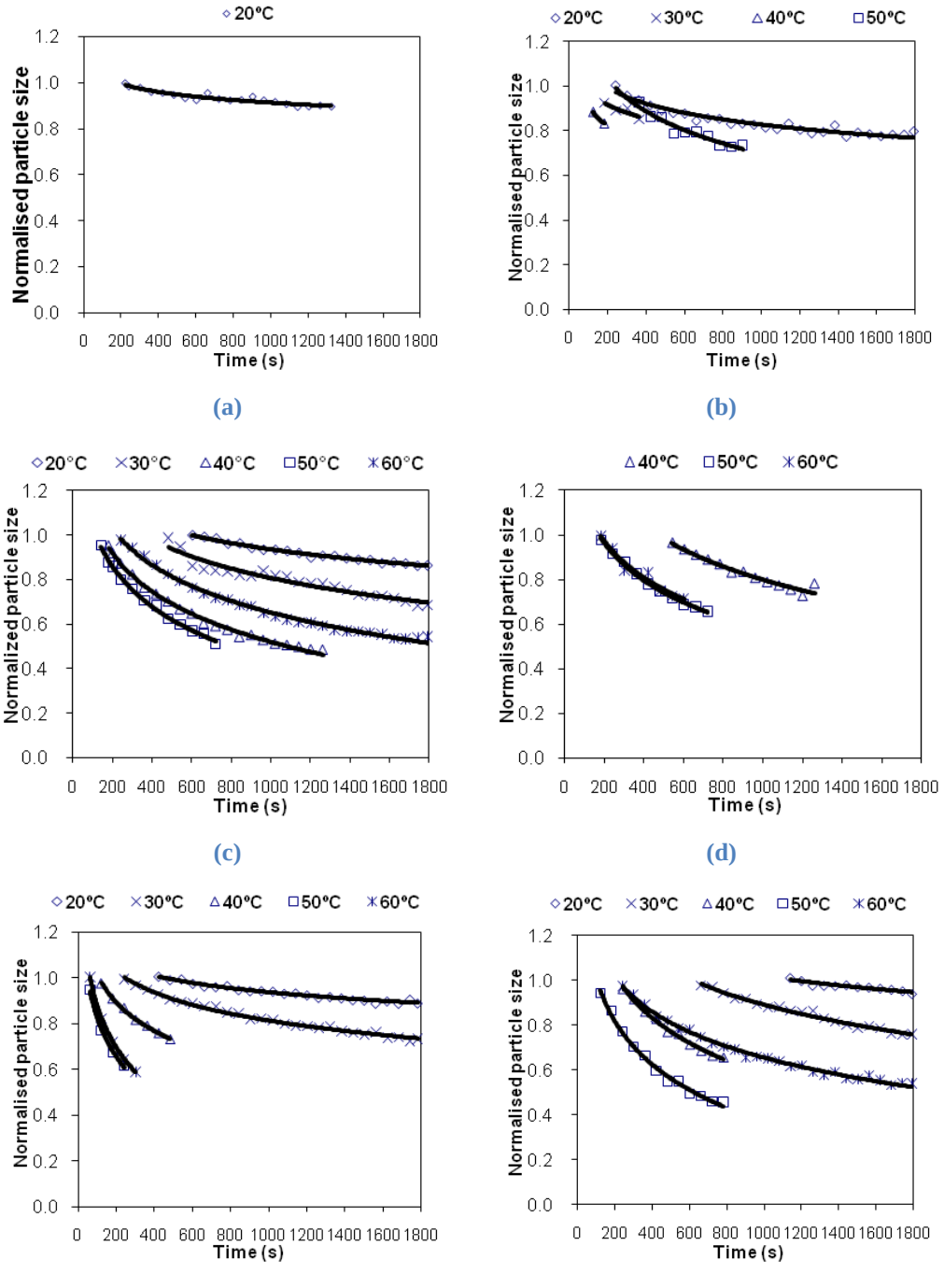

Figure 3-11 Normalized particle size of powder A-F

(a. Powder A; b. Powder B; c. Powder C; d. Powder D; e. Powder E; f. Powder F)

For a few of the powders (i.e. powder A, B and D), there are several temperature points missing. This is due to the fact that the particle size did not drop below initial particle size within the testing period.

The normalized slope-temperature profile curve and lag-time-temperature profile curve were plotted as shown in Figure 3-12. In general, the normalized insolubility test and FBRM results was able to reproduce the 'U' shaped dissolution profile trend over the

testing temperature with the minimum value shown to be at around 40 - 50 °C. This suggests that powder B-F have the best solubility at around 40 - 50 °C (powder B at 40 °C). However no slope-temperature profile and lag-time-temperature profile was available for powder A as only one set of the temperature-data profiles acquired was applied for this analysis. As for the normalized slope and lag-time profiles, the results generally correlate well with that of the insolubility and FBRM results. As expected, the 'U' shaped trend was once again observed for powder B-F over the testing temperature, which indicates the fastest dispersion and dissolution rate to be around 40-50 °C.

This highlights the potential of these various techniques in formulating standard models to characterize the properties of these various powders. In particular, the profiles generated from the initial rate and lag time data can potentially be applied to reduce the required testing time. As these two parameters are derived from the early stages of the dissolution process (which is when most of the dissolution events occur), the amount of time needed to acquire such data can be considerably reduced. The profiles generated can be used for quick analysis of a certain powder to determine the possible functionality of the powder without the need to conduct lengthy dissolution test. This could potentially save time, labour cost and equipment usage time.

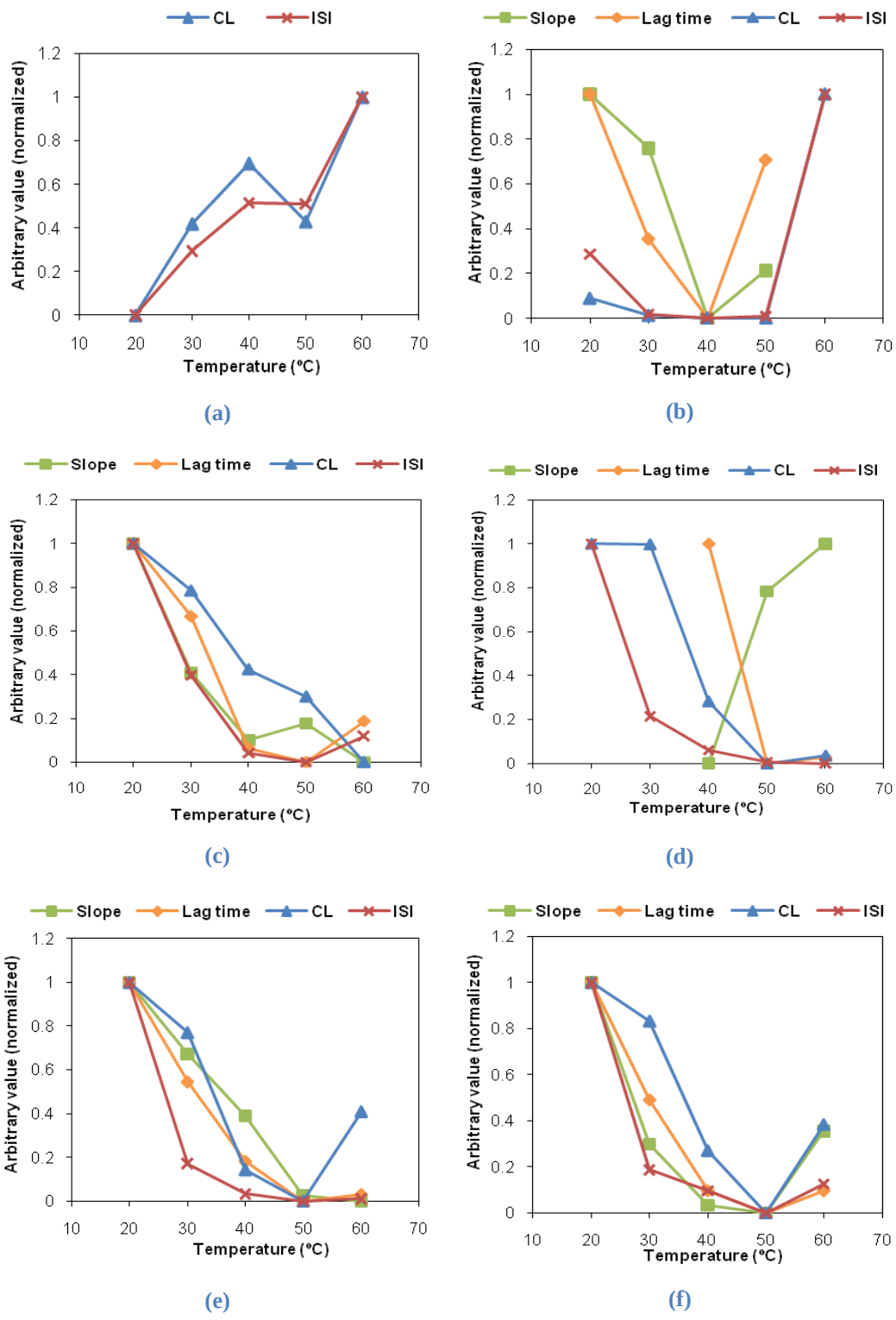

Figure 3-12 Normalised parameters of powder A-F (CL: chord length, ISI: insolubility index)

(a. Powder A; b. Powder B; c. Powder C; d. Powder D; e. Powder E; f. Powder F)

3.4. Conclusion

This study has demonstrated the applicability of FBRM to characterize the solubility of MPC powders. A systematic approach has been taken which offers a versatile and reproducible manner for quantifying the solubility of MPC powder under different conditions. One advantage of FBRM is that it can handle high solids content suspensions. This method can provide the capacity to quantitatively measure the dissolution behaviour for a specific powder under a set of specific conditions. The FBRM results have indicated that solubility of MPC powders is strongly affected by the testing water temperature. The most dramatic changes of chord length take place in the first 200 seconds of the dissolution test. An analysis based on particle population counts has also been proposed to characterise the dissolution behaviour of different MPC powders.

More significantly, this protocol can potentially be applied within the dairy industry to easily predict the solubility of a powder at any specific temperature from its dissolution-temperature profile. The relatively quick analysis for characterising dairy powders should be beneficial for quality control and for reducing cost of dairy milk production. The next step is to establish an index to define the level of solubility so as to quantify the extent of the solubility of specific MPC powders.

3.5. References

ANEMA, S. G., PINDER, D. N., HUNTER, R. J. & HEMAR, Y. 2006. Effects of storage temperature on the solubility of milk protein concentrate (MPC85). *Food Hydrocoll.,* 20**,** 386-393.

CARR, A., BHASKAR, G. & RAM, S. 2007. *Monovalent salt enhances solubility of milk protein concentrate*. EP1553843.

CASTRO-MOREL, M. D. & HARPER, W. J. 2002. Basic functionality of commercial milk protein concentrates. *Milchwissenschaft,* 57**,** 367-370.

CHEN, X. D. & LLOYD, R. J. 1994. Some aspects of measuring the size and rate of dispersion of milk powder agglomerates using the Malvern Particle Sizer 2600c. *J. Dairy Sci.,* 61**,** 201-208.

FANG, Y., SELOMULYA, C. & CHEN, X. D. 2008. On measurement of food powder reconstitution properties. *Dry. Technol.,* 26**,** 3 -14.

GAIANI, C., BANON, S., SCHER, J., SCHUCK, P. & HARDY, J. 2005. Use of a turbidity sensor to characterize micellar casein powder rehydration: influence of some technological effects. *J. Dairy Sci.,* 88**,** 2700-2706.

GAIANI, C., SCHER, J., SCHUCK, P., DESOBRY, S. & BANON, S. 2009. Use of a turbidity sensor to determine dairy powder rehydration properties. *Powder Technol.,* 190**,** 2-5.

GAIANI, C., SCHER, J., SCHUCK, P., HARDY, J., DESOBRY, S. & BANON, S. 2006. The dissolution behaviour of native phosphocaseinate as a function of concentration and temperature using a rheological approach. *Int. Dairy J.,* 16**,** 1427-1434.

GAIANI, C., SCHUCK, P., SCHER, J., DESOBRY, S. & BANON, S. 2007. Dairy powder rehydration: influence of protein state, incorporation mode, and agglomeration. *J. Dairy Sci.,* 90**,** 570-581.

HAVEA, P. 2006. Protein interactions in milk protein concentrate powders. *Int. Dairy J.,* 16**,** 415-422.

HEATH, A. R., FAWELL, P. D., BAHRI, P. A. & SWIFT, J. D. 2002. Estimating average particle size by focused beam reflectance measurement (FBRM). *Part. and Part. Syst. Charact.,* 19**,** 84-95.

HU, X., CUNNINGHAM, J. C. & WINSTEAD, D. 2008. Study growth kinetics in fluidized bed granulation with at-line FBRM. *Int. J. Pharm.,* 347**,** 54-61.

KEMPKES, M., EGGERS, J. & MAZZOTTI, M. 2008. Measurement of particle size and shape by FBRM and *in situ* microscopy. *Chem. Eng. Science,* 63**,** 4656-4675.

KHER, A., UDABAGE, P., MCKINNON, I., MCNAUGHTON, D. & AUGUSTIN, M. A. 2007. FTIR investigation of spray-dried milk protein concentrate powders. *Vib. Spectrosc.,* 44**,** 375-381.

KOUGOULOS, E., JONES, A. G. & WOOD-KACZMAR, M. W. 2005. Modelling particle disruption of an organic fine chemical compound using Lasentec focussed beam reflectance monitoring (FBRM) in agitated suspensions. *Powder Technol.,* 155**,** 153-158.

KOVALSKY, P. & BUSHELL, G. 2005. *In situ* measurement of fractal dimension using focussed beam reflectance measurement. *Chem. Eng. J.,* 111**,** 181-188.

KWAK, B.-M., LEE, J. E., AHN, J.-H. & JEON, T.-H. 2009. Laser diffraction particle sizing by wet dispersion method for spray-dried infant formula. *J. Food Eng.,* 92**,** 324-330.

MIMOUNI, A., DEETH, H. C., WHITTAKER, A. K., GIDLEY, M. J. & BHANDARI, B. R. 2009. Rehydration process of milk protein concentrate powder monitored by static light scattering. *Food Hydrocoll.,* 23**,** 1958-1965.

MISTRY, V. V. & HASSAN, H. N. 1991. Delactosed, high milk protein powder. 2. Physical and functional properties. *J. Dairy Sci.,* 74**,** 3716-3723.

NIRO. September 2006. *Niro Method No. A 3 a: Insolubility Index, A 3 a* [Online]. Available: http://www.niro.com/ndk_website/NIRO/cmsdoc.nsf/WebDoc/ndkw74jjk8 [Accessed 12th September, 2007].

YU, W. & ERICKSON, K. 2008. Chord length characterization using focused beam reflectance measurement probe - methodologies and pitfalls. *Powder Technol.,* 185**,** 24-30.

Monash University

Declaration for Thesis Chapter Four

In the case of Chapter 4, the nature and extent of my contribution to the work was the following:

Name	% contribution	Nature of contribution
Yuan Fang	85%	Initiation, Key ideas, Experimental works, Development, Data analysis, Writing up
Dr. Cordelia Selomulya	5%	Initiation, Results Interpretation, Review
Dr. Sandra Ainsworth	3%	Initiation, Sample preparation
Dr. Martin Palmer	2%	Review
Prof. Xiao Dong Chen	5%	Key ideas, Development

Declaration by co-authors

The undersigned hereby certify that:

(1) they meet the criteria for authorship in that they have participated in the conception, execution, or interpretation, of at least that part of the publication in their field of expertise;

(2) they take public responsibility for their part of the publication, except for the responsible author who accepts overall responsibility for the publication;

(3) there are no other authors of the publication according to these criteria;

(4) potential conflicts of interest have been disclosed to (a) granting bodies, (b) the editor or publisher of journals or other publications, and (c) the head of the responsible academic unit; and

(5) the original data are stored at the following location(s) and will be held for at least five years from the date indicated below:

Location(s)	**Department of Chemical Engineering, Monash University Clayton campus, Australia**

Signature		
Signature		
Signature		
Signature		
Signature		

Chapter 4

On Quantifying the Dissolution Behaviour of Milk Protein Concentrate Powder

4.1. Introduction

In the food industry, powder ingredients with rapid dissolution properties are desirable as poorly dissolved powders result in prolonged processing time, increased production costs and likely poorer quality. Milk protein concentrate (MPC) is a newly developed functional ingredient used to enrich the nutritional / physiochemical properties of dairy product on per kilogram basis. It has an important role in the production of beverages, cheese, confectionary, yoghurt, and other food products. However, MPC powders are poorly soluble due to its high protein content (40-90 wt% solid content), thus potentially restricting their applications. Consequently, understanding the MPC dissolution properties, especially the dissolution kinetics, is important in the development, formulation and quality control in MPC powder manufacturing. Sensitive and reproducible dissolution data from standardised testing conditions are necessary to be able to compare the variability in dissolution profiles for different MPC powders. Considerable studies have been devoted towards the understanding of dissolution kinetics of powders, primarily in the pharmaceutical industry where standardised apparatus and dissolution models are available (Costa and Sousa Lobo, 2001, Marabi et al., 2008a, Siepmann and Peppas, 2001, Viness and Reza, 1999).

Various techniques have been applied to investigate the dissolution kinetics of food powders, including calorimetry (Marabi et al., 2007, Marabi et al., 2008a, Marabi et al., 2008b), rheological measurements (Kravtchenko et al., 1999, Larsen et al., 2003), static light scattering (Mimouni et al., 2009), optical fibre sensor, ultrasonic reflectance (Saggin and Coupland, 2002), and nuclear magnetic resonance (NMR) (Belloque and Ramos, 1999, Davenel et al., 2002). Marabi *et al.* investigated the dissolution kinetics of sucrose particle using a single particle approach (Marabi et al., 2008a). Using appropriate algorithms to analyse microscope images, the equivalent shrinking sphere of a single particle was monitored so that a mathematical model based on the shrinking sphere could be used to describe the dissolution process. Static light scattering (SLS) is another common technique to characterize food powder solubility. Mimouni *et al.* used SLS to monitor the rehydration process of a MPC powder and proposed a dissolution mechanism for MPC powders (Mimouni et al., 2009).

In pharmaceutical research, several dissolution models have been proposed, for example Weibull model and Baker-Lonsdale model (Costa and Sousa Lobo, 2001, Viness and Reza, 1999). Noyes-Whitney model was the first model proposed to investigate dissolution kinetics using a differential equation relating the rate of solids (solute) dissolution to the concentration of dissolved solute in the solvent (Dokoumetzidis and Macheras, 2006, Viness and Reza, 1999). The Noyes-Whitney equation led to increased research interest in dissolution from the point of view of physical chemistry (Niebergall et al., 1963, Skrdla, 2007, Dokoumetzidis and Macheras, 2006). The Noyes-Whitney model states that the rate of dissolution is proportional to the difference between the instantaneous concentration C ($g \cdot m^{-3}$) at time t (s), and the solubility at equilibrium, C_S ($g \cdot m^{-3}$) (Carstensen and Dali, 1999, Dokoumetzidis and Macheras, 2006, Costa and Sousa Lobo, 2001).

$$\frac{dC}{dt} = k(C_S - C)$$

Equation 4-1

where k (s^{-1}) is proportionality constant, C_S ($g \cdot m^{-3}$) is the solubility of solute at equilibrium in the solution under a specific condition (e.g. dissolution temperature) and C ($g \cdot m^{-3}$) is the concentration of solute at time t.

In 1900, Brunner and co-workers found that the rate of dissolution could be related to the solid area accessible to solution, the rate of stirring, temperature, structure of the surface and the arrangement of the apparatus (Dokoumetzidis and Macheras, 2006). Therefore, they extended Equation 4-1 into:

$$\frac{dC}{dt} = k_1 S(C_S - C)$$

Equation 4-2

where S (m^2) is the surface area of solute, and k_1 ($s^{-1} \cdot m^{-2}$) is the new proportionality constant = k/S. Brunner and Nernst investigated the problem further to find specific relationships between the constants involved. Their work was based on Fick's second law and was developed into the Nernst-Brunner equation (Dokoumetzidis and Macheras, 2006):

$$\frac{dC}{dt} = \frac{DS}{Vh}(C_S - C) \qquad (k_1 = \frac{D}{Vh})$$

Equation 4-3

where D ($m^2 \cdot s^{-1}$) is the diffusion coefficient, h (m) is the thickness of the diffusion layer and V (m^3)is the volume of liquid solution. In 1931, Hixson and Crowell modified the Noyes-Whitney equation (Equation 4-2) by multiplying both terms of the equation by V (Costa and Sousa Lobo, 2001, Dokoumetzidis and Macheras, 2006):

$$\frac{dC}{dt}V = \frac{dW}{dt} = k_1 S(C_S - C)V = k_1 S(VC_S - W)$$

Equation 4-4

where W (g) is the mass of dissolved solute at time t. Assuming a constant surface area, integrating Equation 4-4 gives:

$$W = VC_S[1 - \exp(-kt)]$$

Equation 4-5

VC_S gives the dissolved mass at equilibrium which is the mass W_E (g), thus substituting W_E for VC_S gives:

$$W = W_E[1 - \exp(-kt)]$$

Equation 4-6

In this study, focused beam reflectance measurement (FBRM) was employed to measure the solubility of MPC powder. FBRM is a unique technique which can on-line monitor the particle size change without sample preparation or dilution. It can provide the information of particle size change with time, the particle size distribution with different time interval and the population counts in different size groups (Havea, 2006, Hu et al., 2008, Kempkes et al., 2008, Kougoulos et al., 2005, Kovalsky and Bushell, 2005). It has been widely used in different processes such as granulation (Hu et al., 2008), crystallization (Kempkes et al., 2008) and flocculation (Yoon and Deng, 2004) etc. Our previous work in Chapter 3 has demonstrated the capability of FBRM to characterise powder dissolution with good reproducibility, with the data well correlated with sedimentation test results (Fang et al., 2010).

In this work, the dissolution kinetics of MPC powders was modelled using FBRM data to establish the protocols for benchmarking parameters applicable to specific powders. Specifically, this study is aimed at establishing the dissolution profiles of MPC powder subjected to various dissolution and storage conditions by developing a mathematical model to investigate both the dynamic and final dissolution properties. The information obtained would be useful to improve the efficiency and consistency of powder testing methods in the dairy industry, particularly for non-traditional or new types of powders, where the current standard methods were not suitable.

4.2. Material and methods

4.2.1. Materials

Fresh MPC85 powder was provided by Dairy Innovation Australia Ltd. (Werribee, Victoria, Australia). This powder has 81.8% protein content and 6.17±0.44% measured moisture content. Immediately after manufacture, the fresh powder was stored at 10°C, 25°C, and 35°C respectively, for the duration of 2 weeks and 2 months. The combinations of storage and dissolution conditions are shown in Table 4-1.

Table 4-1 Testing matrix for the effects of testing temperature, storage duration and temperature

Storage Duration	Storage Temperatures	Dissolution Temperatures				
		20°C	30°C	40°C	50°C	60°C
Fresh	-	√	√	√	√	√
2 Weeks	10°C	√				
	25°C	√			√	
	35°C	√	√	√	√	√
2 Months	10°C	√			√	
	25°C	√			√	
	35°C	√		√	√	√

4.2.2. Methods

4.2.2.1. Characterisation

The moisture content measurement was carried out according to Niro method No. A 1 b (Niro, September 2006a). 3 g of MPC powder was dried in the oven at 102 ℃ for 3 hours. The weight difference before and after drying was recorded. The particle size of the dry powder was measured by laser diffraction using a Malvern Mastersizer 2000 (Malvern Instruments Ltd., Malvern, UK) with a Scirocco 2000 dry powder feeder. The refractive index for MPC was set at 1.57 (Ambrose Griffin and Griffin, 1985). Each measurement was carried out in triplicate and the mean particle size recorded, with deviation of less than 5% of the average size. The sizes of fresh and aged powders (e.g. after storage at 35 °C for 2 months) were measured for comparison. Morphology of fresh and aged powder samples were observed using a Scanning Electron Microscope (JEOL 840A) operated at 20 kV in a low vacuum mode and equipped with a backscatter detector. Sample coated with platinum (~4nm thickness) was placed on a double-sided carbon tape for analysis.

4.2.2.2. Dissolution studies

The experimental setup was based on our previous work in Chapter 3 (Fang et al., 2010). 500 mL of distilled water was heated up in a 600 mL beaker to a specific temperature using a water bath before commencing the measurement. Different temperatures from 20 ^{o}C to 60 ^{o}C were investigated. 7.50 ± 0.01 g of powder was added into the beaker to make up a 1.5 wt% solution. An overhead stirrer was used at 800 r.p.m. stirring rate. The data

from FBRM was collected using iC FBRM^{TM} program (Mettler Toledo), with the collecting interval set at 10 seconds for 30 minutes duration. After 30 minutes, the sedimentation test was conducted as per described in Chapter 3 (Fang et al., 2010) as a comparison with the particle size reading from FBRM. 4 centrifuge tubes were weighted and filled with 50mL solution from FBRM measurement. The tubes were weighted again and centrifuged for 5 minutes at 1000 r.p.m. (88 g). The supernatant was discarded and the sediment dried at 50 ℃ in the oven overnight. The weight of sediment after drying was recorded. The sediment amount was calculated using Equation 4-7:

$$\text{Sediment Amount} = \frac{m_{tube+sed} - m_{tube}}{(m_{tube+sol} - m_{tube}) \times 1.5\%} \times 100\%$$

Equation 4-7

where m_{tube} is the weight of empty centrifuge tube, $m_{tube+sed}$ is the weight of tube with sediment after drying, $m_{tube+sol}$ is the weight of centrifuge tube with solution before centrifugation.

FBRM provides particle counts (PC) for different size ranges from 1 to 1000 μm. In this study, the general dissolution behaviour of the powders was investigated with particle populations classified into 3 categories: fine (1-10 μm), median (10-150 μm), and large/agglomerate (150-300 μm) particles. It is expected that during dissolution, the fine particle group (1-10 μm) should increase with time while the large particle group (150-300 μm) decrease with time. The median particle group is complex due to influx and efflux of particle between the two adjacent populations (Fang et al., 2010). It is again noted for set of powders used in this study, no particle count within 300-1000 μm was detected.

The term ‘dissolution’ used in this study encompasses the phenomena known as dispersibility and solubility of powder reconstitution properties (Fang et al., 2008). This interpretation is similar to that used in industrial applications for dairy powders. Theoretically, the MPC particle size is expected to decrease along with the dissolution process as the particles de-agglomerate into primary particles, while releasing casein micelles into the solution. By measuring the decrease of MPC particle size with time during the dissolution process, it can be used as an indication of the solubility of MPC powders.

4.2.2.3. Dissolution kinetics

In developing the kinetic models, a modified dissolution mechanism based on that proposed by Mimouni *et al*. (Mimouni et al., 2009) was shown in Figure 4-1. A typical agglomerated particle consists of identical spherical particles produced by atomization in the spray-dryer. When the agglomerated particles come into contact with water, they start to de-agglomerate and release the individual particles with initial diameter d_0. The releasing of materials from these individual particles into the aqueous suspension may simultaneously take place as indicated in Figure 4-1. Each particle is subjected to 'erosion' uniformly from all directions so that d decreases evenly in all dimensions. When d decreases and approaches the diameter of the occluded air (a), the remaining solids would collapse or break down. At this point, the dissolution process is assumed to be complete. It is noted that, as a first order estimate, an idealised model system comprising uniform spherical shaped particles is assumed here to investigate the dissolution process. This is based on an isometric system whereby each particle is subjected to uniform 'erosion' forces in all directions.

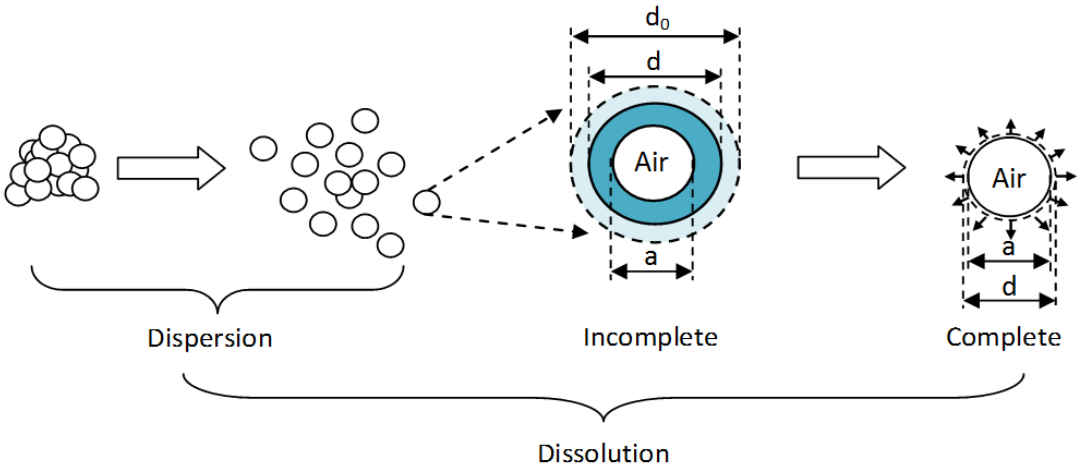

Figure 4-1 Proposed dissolution mechanism

The Noyes-Whitney model assumes the solution as the system of interest and describes the changes in solute concentration at the macro level. Here the property measured is the remaining undissolved particle size at the micro level. Thus the dissolved amount of solute W for each particle can be written as:

$$W = W_0 - W_t$$

Equation 4-8

$$W_E = W_0 - W_\infty$$

Equation 4-9

where W_E is the amount of dissolved solute in the solution at final stage of investigation, W_0 is the initial mass of the particle, W_∞ is the mass of remaining undissolved particle at the end of investigation and W_t is the undissolved particle at time t. Inserting Equation 4-8 and Equation 4-9 into Equation 4-6 gives:

$$W_0 - W_t = (W_0 - W_\infty)[1 - \exp(-kt)]$$

Equation 4-10

From Equation 4-10, there are two possible scenarios:

(1) The solute is dissolved completely ($W_\infty = 0$), implying that:

$$W_t = W_0 \exp(-kt)$$

Equation 4-11

(2) The solute is incompletely dissolved at steady state ($W_\infty < W_0$),

$$W_0 - Wt = (W_0 - W_\infty)[1 - \exp(-kt)]$$

Equation 4-12

Assuming that the solute consists of isometric particles (e.g. spheres), the particle volume, v is

$$v = \frac{1}{6}\pi \cdot d^3$$

Equation 4-13

where d is the diameter of the particle. For a population of N uniform particles, the mass term can be expressed in terms of particle size:

$$W = N\rho \cdot v = \frac{1}{6} N\pi\rho \cdot d^3$$

Equation 4-14

Inserting Equation 4-14 into Equation 4-11 and Equation 4-12gives

For complete dissolution:

$$d^3 = d_0^3 \cdot \exp(-kt)$$

Equation 4-15

For incomplete dissolution:

$$d^3 = (d_0^3 - d_\infty^3)\exp(-kt) + d_\infty^3$$

Equation 4-16

where d_0 is the initial particle size and d_∞ is the final particle size at the end of investigation ($d_\infty \leq d < d_0$).

4.3. Results and discussion

4.3.1. MPC dissolution profiles

The dissolution profiles of MPC powder stored under different durations and temperatures are represented by the changes in chord length as measured by FBRM with time at specific dissolution temperatures as shown in Figure 4-2. Profiles of fresh powders are used as baseline comparison under the respective testing conditions. In general under all the tested conditions, fresh powders exhibit the best solubility with the lowest chord length and it is noted that their solubility deteriorates with storage duration and temperature.

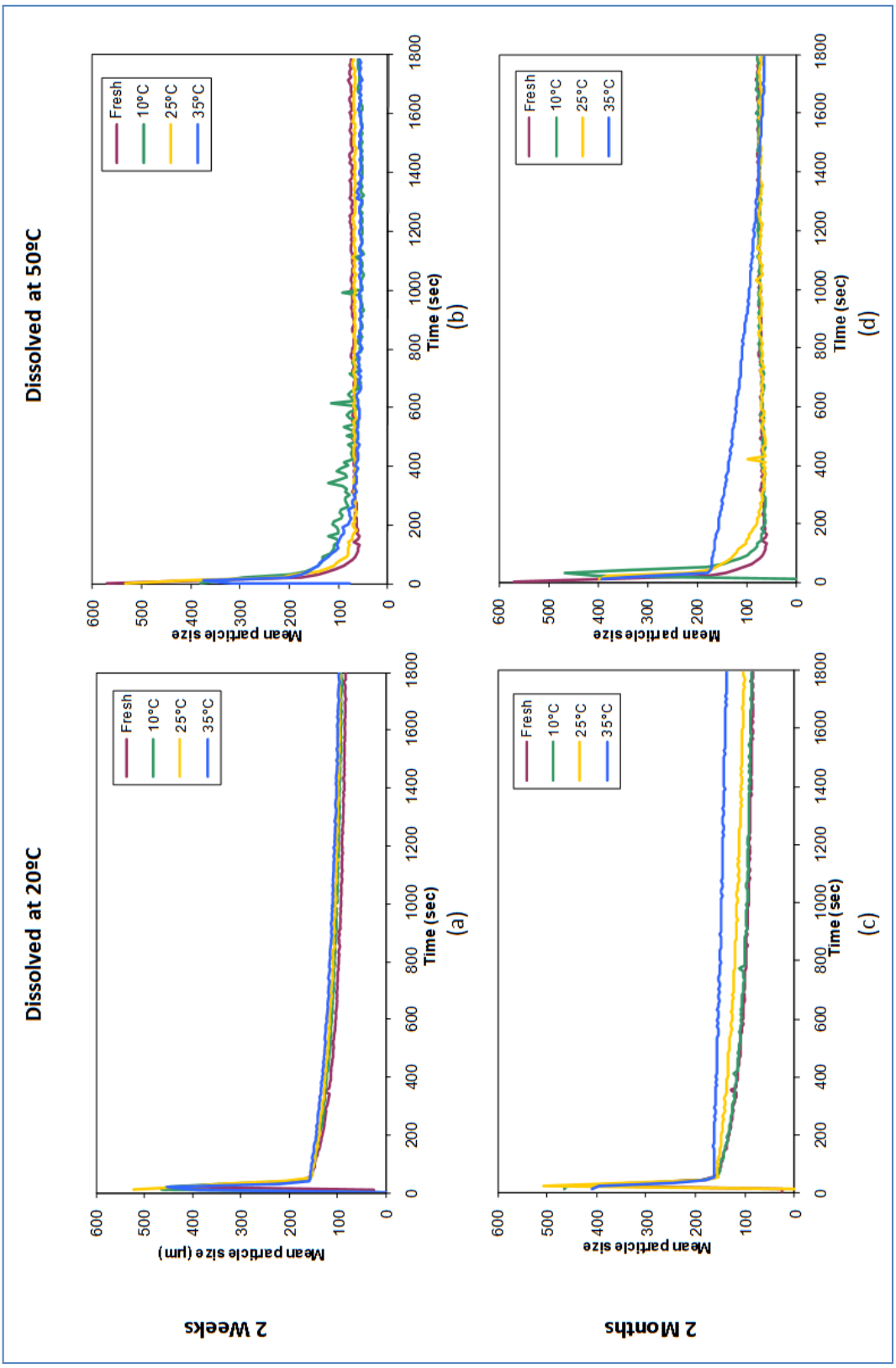

Figure 4-2 FBRM results of MPC powder size change with time under different storage duration and temperatures (tested at 20 and 50 ℃ respectively)

Figure 4-2 shows the dissolution profiles of powder tested at 20 ℃ and 50 ℃. Generally, powder dissolving at 20 ℃ (Figure 4-2a and Figure 4-2c) decreased slowly in chord length and does not reach plateau even up to 30 minutes. Comparatively at 50 ℃, the chord length decreased quickly to reach equilibrium within 200 seconds (Figure 4-2b and Figure 4-2d). These results are in agreement with findings from Chapter 3, where most powders showed the lowest chord length at 50 ℃ (Fang et al., 2010).

Looking at the effects of storage temperature, when the powder has been stored at 10 °C, the measured chord length after 30 mins was similar to that of the fresh powder. However, longer time was taken to reach the plateau for the chord length of powder stored at 35 °C, indicating that they became less soluble. It is noted that the effect of storage duration significantly magnifies the effect of storage temperature. For powders stored for 2 weeks, no substantial variation in dissolution profiles was found between the different storage temperatures (Figure 4-2a and Figure 4-2b). However, the difference could be clearly distinguished after 2 months with fresh powder and powder stored at 10 ^{o}C having the lowest average chord length in comparison to powder stored at 35 °C with larger particles still remaining in suspension (Figure 4-2c and Figure 4-2d). Therefore, these data confirm the adverse effects of storing powders at elevated temperatures and long durations.

From the analysis of the profiles, a few key features could be observed. Firstly, it should be noted that each dissolution curve appeared to initially increase sharply to reach a peak, followed by a significant decrease before gradually reaching plateau (Figure 4-2). Secondly, the height of the peak appeared to be ‘random’. This trend could be attributed to various macroscopic events like the manner of which the powder was introduced onto the water surface or how the agitation vortex dispersed the powder in water. The functionality of the testing powder such as wettability could also play a role in this phenomenon (Kravtchenko et al., 1999, Skrdla, 2007). A standardized starting point, D [v, 0.9] of dry powder, was used as the initial starting point for analysis (and later modelling) of the dissolution profiles (i.e. d_0). D [v, 0.9] refers to the particle size below which 90% (v/v) of the particles existed, and was chosen so that it covered the majority of the particles. The period of time before the size decreased to D [v, 0.9] was defined as the initial ‘induction period’ (Skrdla, 2007, Fang et al., 2010).

The profiles clearly demonstrate that the dynamic dissolution behaviour for an MPC powder could be distinguished with this method when subjected to different dissolution

and storage conditions. The information could be utilized to generate a better understanding of the optimum dissolution conditions for MPC powders. The next section covers the development and validation of a dissolution model to describe their dissolution kinetics.

4.3.2. Dissolution models

To validate the proposed models, Equation 4-15 and Equation 4-16 were applied to the dissolution data. The plot in Figure 4-3a indicated that the complete dissolution model (Equation 4-15) was not a suitable choice to describe the dissolution behaviour, as the fitting correlation was relatively poor (R^2=0.35264). This particular model may not be suitable possibly due to the fact that not all of the MPC particles had completely dissolved as evidenced from the presence of suspended solids remaining in the solution. This observation was also verified by corresponding light microscope images of samples taken from the suspension (Figure 4-4). The images showed that even after 4 hours of dissolution, some agglomerates were still present in the solution. Therefore, the complete dissolution assumption was not valid for MPC powders after 30 minutes of mixing.

On the contrary, the incomplete dissolution model (Equation 4-16) gave a much better fit (R^2=0.99944) with the data (Figure 4-3b), better describing the dissolution behaviour of MPC powder. This agreed with other findings in the literature (Kravtchenko et al., 1999, Larsen et al., 2003) where the mass/concentration of the solute was used as a measure of the dynamic dissolution behaviour, indirectly inferring as to whether the solute had or had not completely dissolved. Kravtchenko *et al*. investigated the dissolution kinetics of pectin using both dispersing and non-dispersing conditions (Kravtchenko et al., 1999). Their data showed undissolved particles in solution as the equilibrium level of mass dissolved was less than the initial mass. In this case, by measuring the size of the remaining particles, incomplete dissolution could be assumed as long as the remaining chord length could be detected. From Figure 4-5 it can be seen that there is good correlation between Equation 4-16 and MPC powder dissolution behaviours within this time range. The sensitivity of these two parameters to dissolution and storage conditions could be used to provide a guide on optimizing both conditions for a particular powder.

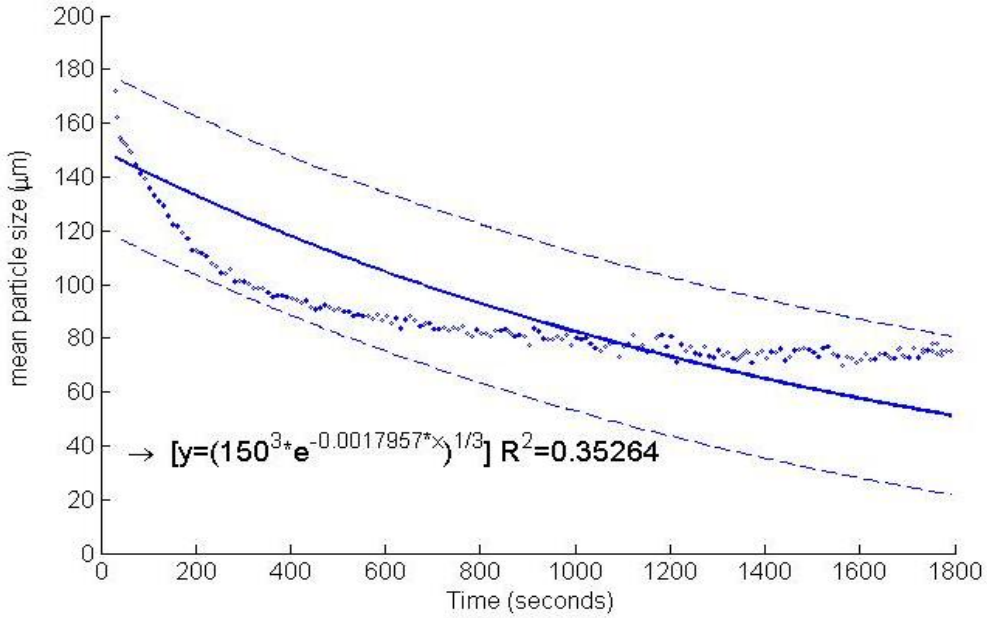

(a). Fitting of Equation 4-15

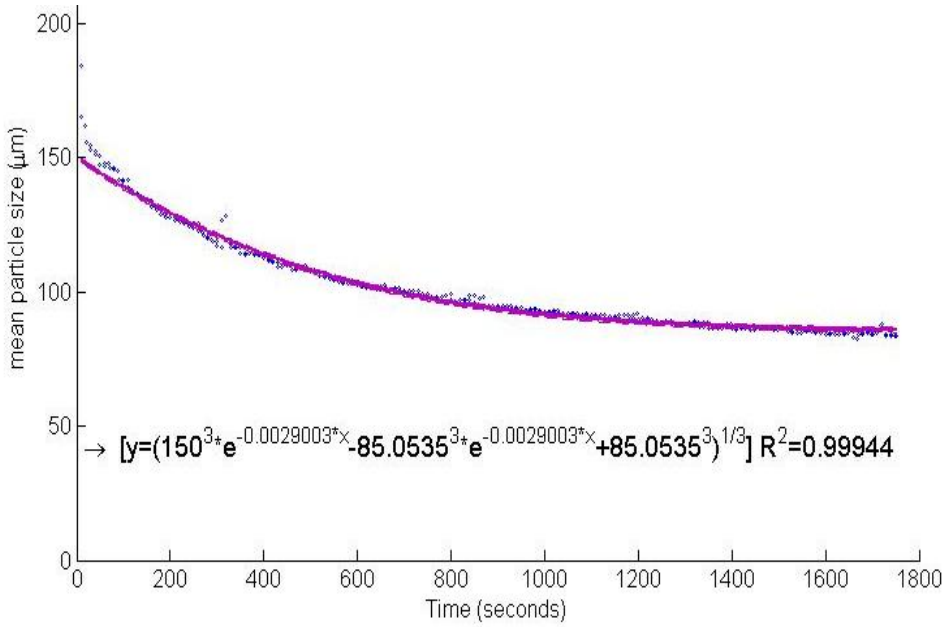

(b). Fitting of Equation 4-16

Figure 4-3 Equation 4-15 and Equation 4-16 fitted with experimental data

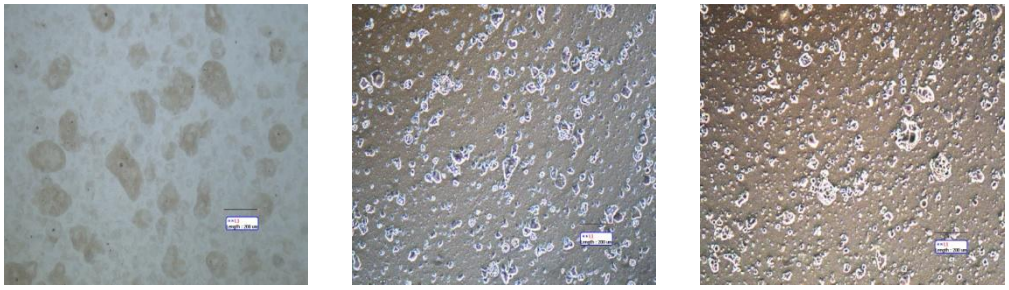

(a). 1 hour (b). 2 hours (c). 4 hours

Figure 4-4 Microscopy images of fresh MPC dissolved at 20 ℃ (reference bar: 200 µm)

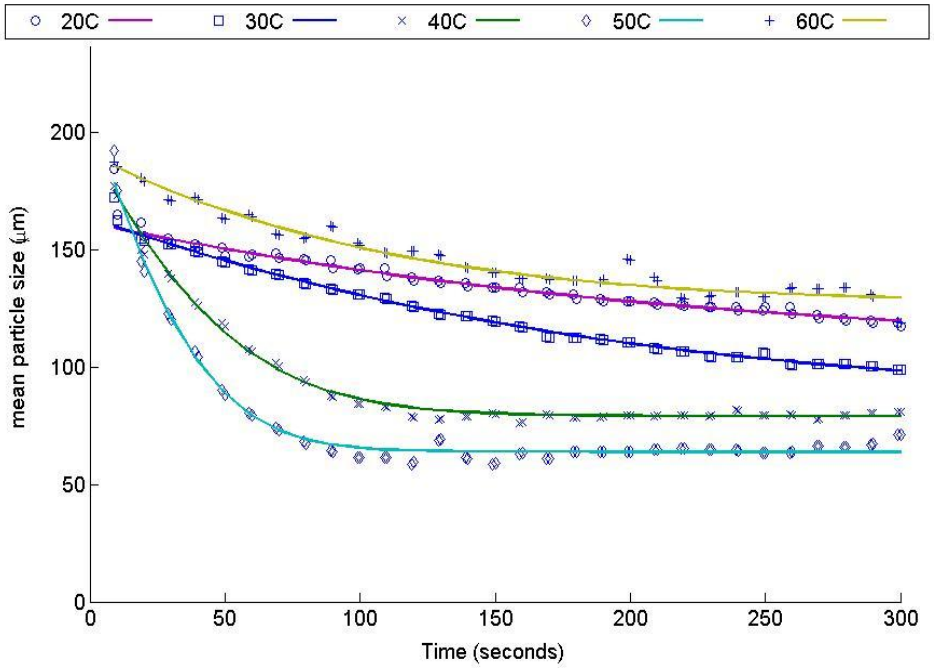

Figure 4-5 Fresh powder tested under different temperatures fitted with Equation 4-16 (○: tested at 20°C; □: tested at 30°C; ×: tested at 40°C; ◊: tested at 50°C; +: tested at 60°C)

4.3.3. Dissolution parameters

To further analyse the dissolution profiles, the incomplete dissolution model (Equation 4-16) was applied to the data. From the fitting results, two key parameters were obtained, namely the **dissolution rate constant** (k) and the **final particle size** (d_∞). The dissolution rate constant k described how fast a powder could dissolve initially under a specific dissolution condition, whereas the final particle size d_∞ is the size of the remaining particles in suspension which was related to sedimentation test results. In theory, all particles eventually would dissolve completely with time (personal communication with Professor Bhesh Bhandari). However in testing the properties of powders for practical applications, the powders are generally dissolved for 90 seconds and left for 15 minutes to stabilize before a sample is taken for centrifugation, where the insolubility is measured from the amount of sediment leftover (Niro, September 2006b). The dissolution rate constant is of interest to achieve the best solubility within a short period of time, as an important part of process optimization. Thus in this study, the first 300 seconds of dissolution period was modelled using Equation 4-16 to estimate the values of k and d_∞.

4.3.3.1. Dissolution rate constant

The dissolution rate constant, k can be taken to represent the dynamic dissolution behaviours of MPC powder under specific storage and dissolution conditions. Intuitively k

could be used to predict and provide a first estimate of the dissolution behaviour for a certain powder when the powder dispersion and dissolution were of interest.

For this particular MPC powder, *k* was generally highest at 50 °C as the optimum dissolution temperature, particularly for fresh powder (Figure 4-6). The variation of *k* was less evident when the powder had been stored for longer (e.g. 35 ℃ for 2 months). Thus the dissolution temperature had the most significant effects on fresh powder, but less so on the aged powders.

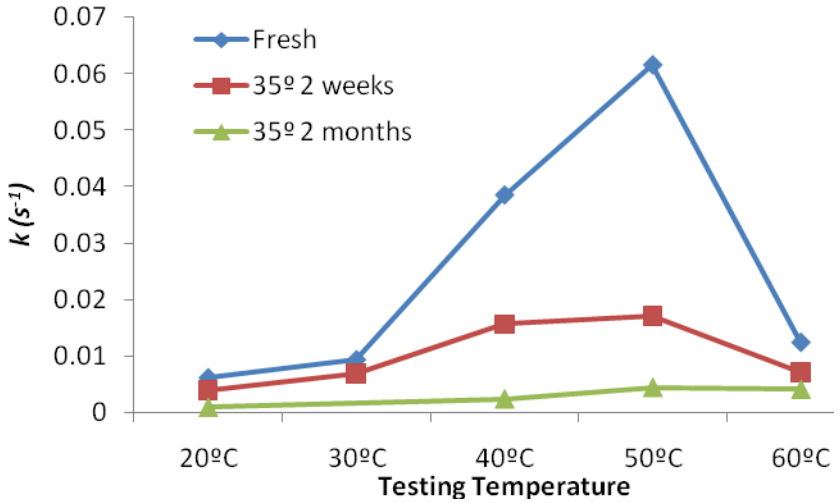

Figure 4-6 Testing temperature effect on *k*

(♦: fresh MPC; ■: MPC stored at 35 ºC for 2 weeks; ▲: MPC stored at 35 ºC for 2 months)

Figure 4-7 shows the effects of **storage temperature** and **storage duration**, where *k* decreases with increasing **storage temperature.** Again, *k* was highest for fresh powder and decreased with increasing storage temperature and extended storage duration. For all dissolution and storage temperatures, lowest dissolution rate constant was found for storage duration of 2 months, possibly due to the aging process, in agreement with the previous studies (Anema et al., 2006, Havea, 2006).

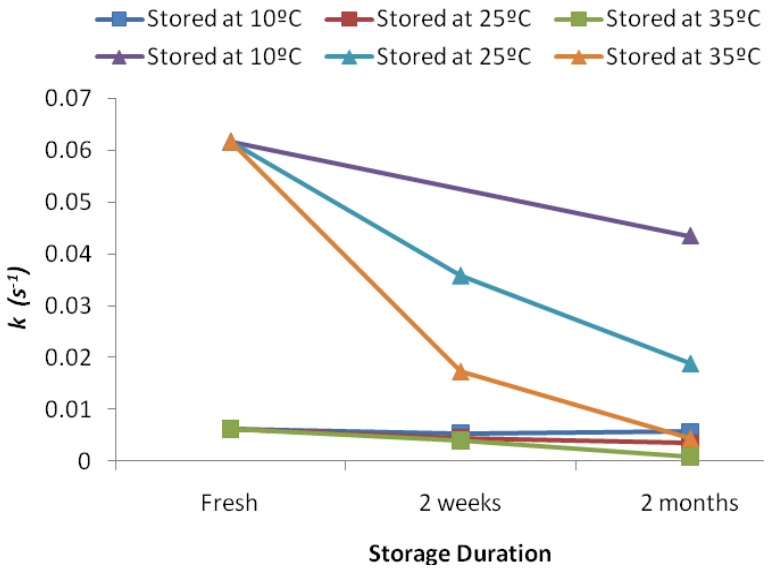

Figure 4-7 Storage temperature and duration effects on *k* (■: tested at 20 ºC; ▲: tested at 50 ºC)

The magnitude of decrease in k values (Δk) between different storage temperatures and durations are as shown in Figure 4-8. Δk is defined as the difference between k of the powder under a certain storage condition with respect to that of fresh powder. We can group $\Delta \boldsymbol{k}$ based on the dissolution temperatures of 20 ℃ and 50 ℃, where the effects of storage temperature and duration were more pronounced when the powder was tested at 50^{o}C. It is clear that a higher dissolution temperature magnifies the level of differences in k between the different storage temperatures and durations. These results imply that a higher dissolution temperature can better distinguish between fresh and aged powder. Functionality testing can take advantage of this feature for more robust estimations.

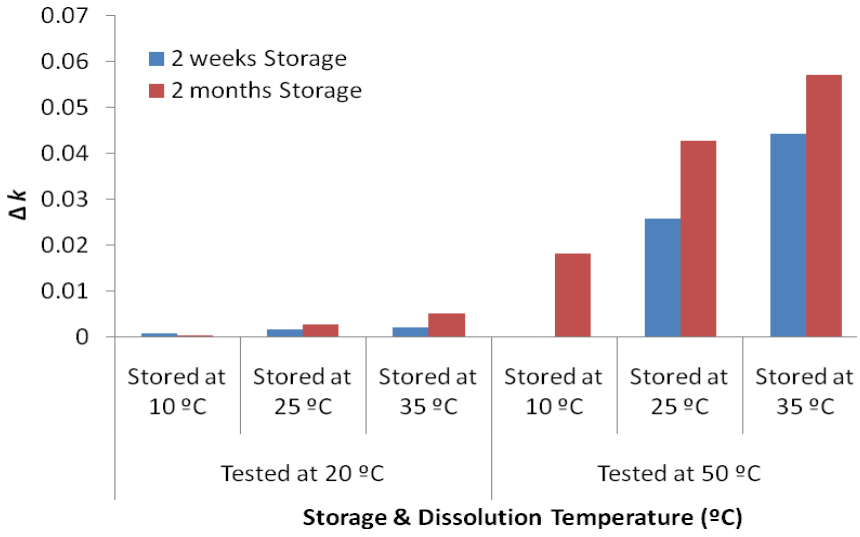

Figure 4-8 Δk for different dissolution and storage condition

4.3.3.2. Final particle size in suspension

As mentioned before, during the dissolution process, the MPC particles de-agglomerate and release the primary particles into solution, and the primary particles release the casein micelles into the aqua phase as demonstrated in Figure 4-1. As such, the measured particle size is expected to decrease with time. In this study, the first 300 seconds of the dissolution period was analysed with the smaller particle size d_{∞} at the end of the analysis period of 300 seconds defined as the 'final' particle size. In this way, the smaller this 'final' particle size, the more soluble the powders are under the specific dissolution condition.

Figure 4-9 shows the effect of dissolution temperature on the final particle size (d_{∞}) (as shown as line graphs) as compared to the results of sedimentation test (as shown as column charts). It can be observed that the d_{∞} decreased from 20-50 ℃ and appeared to increase at 60 ℃ for fresh powders with relatively short storage duration. This result implied that 50 ℃ favored the dissolution of relatively fresh MPC powders. When the temperature were raised to 60 ℃, the final particle size increased accordingly, suggesting that the solubility of MPC became deteriorated at 60 ℃. The data indicated that the final particle size (an indication of final solubility) was sensitive to the testing temperature only when the powder was fresh. When the powder were stored for long duration at high temperature (e.g. 35 ℃ for 2 months), the d_{∞} did not show significant changes over the tested dissolution temperatures. Meanwhile, d_{∞} and the sedimentation test result exhibited similar trends over the range of tested dissolution temperatures, suggesting good correlation between these two sets of results. The correlation has added significance as the sedimentation test was adapted and modified from the standard insolubility test, and therefore can be used as an indication of the solubility of the tested powder. This indirectly inferred that the final particle size (d_{∞}) can be utilized as an alternate indication of the solubility of the tested powder.

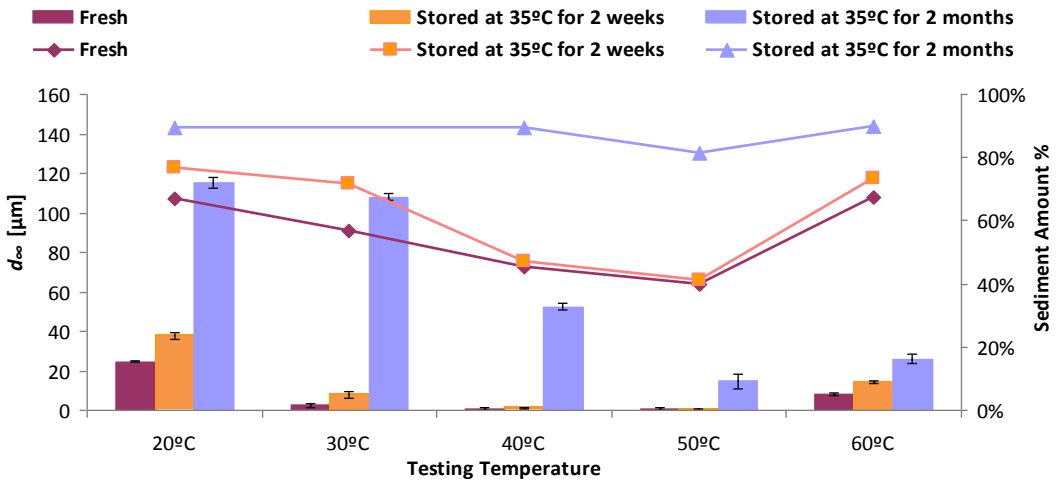

Figure 4-9 Testing temperature effect on d_∞
(◆: fresh MPC; ■: MPC stored at 35 ºC for 2 weeks; ▲: MPC stored at 35 ºC for 2 months)

Figure 4-10 shows the effects of storage temperature and storage duration on the final particle size d_∞ (shown as line graphs) and the results of sedimentation test (shown as colum charts). It can be seen that for powders stored at lower temperatures, (e.g. 10 ℃), d_∞ was similar to that of fresh powder regardless of the storage duration. However, it is clear that d_∞ increased with increasing storage temperature. When the powder was stored at 35 ℃, the d_∞ was significantly higher than that for powders stored at lower temepratures (e.g. 10 and 20 ℃). This suggest that a higher temperature would accelerate the aging process of MPC powder, leading to a more insoluble material as compared to other storage temperatures. In addition, with an increase in the storage duration, the d_∞ increased accordingly, implying that a prolonged period of storage can further deteriorate the powder and decreases the solubility at all storage temperatures. It is noted that by comparing Figure 4-10a and Figure 4-10b, a higher dissolution temeprature (e.g. 50 ℃) significantly reduced the effect of storage temperature and duration when the powder were still 'relatively fresh'. However when the powder underwent an extreme aging process (e.g. stored at 35 ℃ for 2 months), the final particle size d_∞ was much higher than that for the rest of the tested powders (Figure 4-10b). In general, the final particle size d_∞ and the results of sedimentation test showed very good correlation over the range of storage period and temperatures analysed.

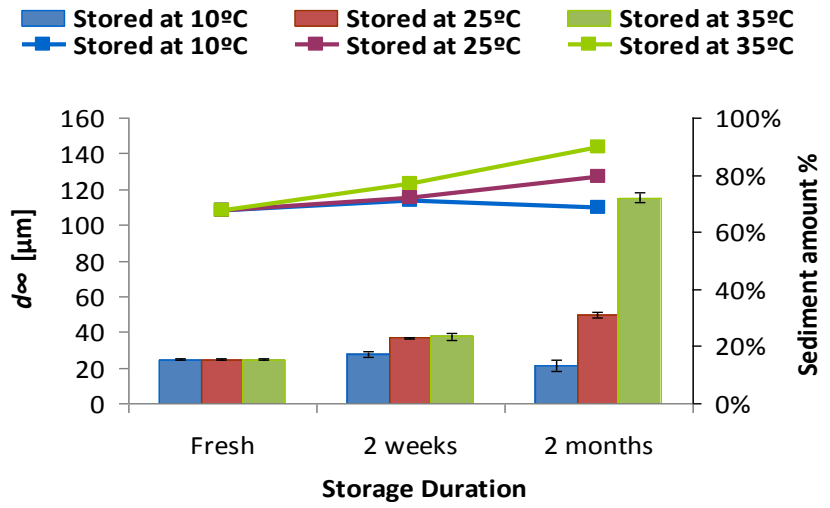

(a)

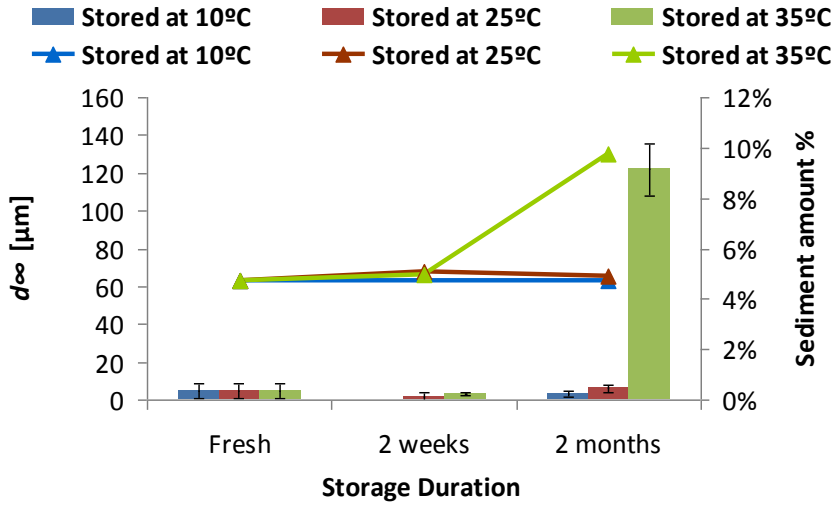

(b)

Figure 4-10 Storage temperature and duration effects on d_∞ (a: tested at 20 ℃; b: tested at 50 ℃)

4.4. Further discussion

The dissolution process consists of two independent processes: the dispersion of agglomerated particles and dissolution of primary particles (Figure 4-1). The proposed model translates these two processes into two phases: **initial dissolution** and **equilibrium dissolution**. The former described large particles de-agglomeration, showing a rapid drop in chord length indicated by the dissolution rate constant (k). The latter was predominantly dissolution of primary particles, showing an incremental drop in measured chord length and represented by the final particle size (d_∞). These two dissolution phases can be observed from the particle counts for different size groups from FBRM (Figure 4-11). For

large particle population (150-300 um), the particle counts decreased rapidly at the initial dissolution process (0-300 seconds) before gradually reaching a plateau with time. On the other hand, the fine particle population (1-10 um) increased steadily throughout the dissolution duration (0-1800 seconds). Looking at the different phases (Figure 4-11) the dispersion and dissolution processes took place simultaneously with dispersion being the dominant process at the initial dissolution stage. At the equilibrium dissolution stage, the dispersion of large particles was near completion so that the dissolution of primary particles became the dominant process. It is noted from Figure 4-11 that the de-agglomeration of large particles contributed most to the reduction of chord length (i.e. the decrease in chord length corresponded with drop in large particle count population in the early stages), while the dissolution of primary particles had insignificant impact on size reduction (i.e. increase in small particle counts did not translate to a drop in particle size at the later stages). These observations were in agreement with Mimouni *et al.* (Mimouni et al., 2009) where de-agglomeration of large particles was observed to take place within the first 10 minutes of dissolution while the dissolution of primary particles (or the release of micelles from primary particles) was the rate-limiting stage of MPC particle dissolution (Mimouni et al., 2009).

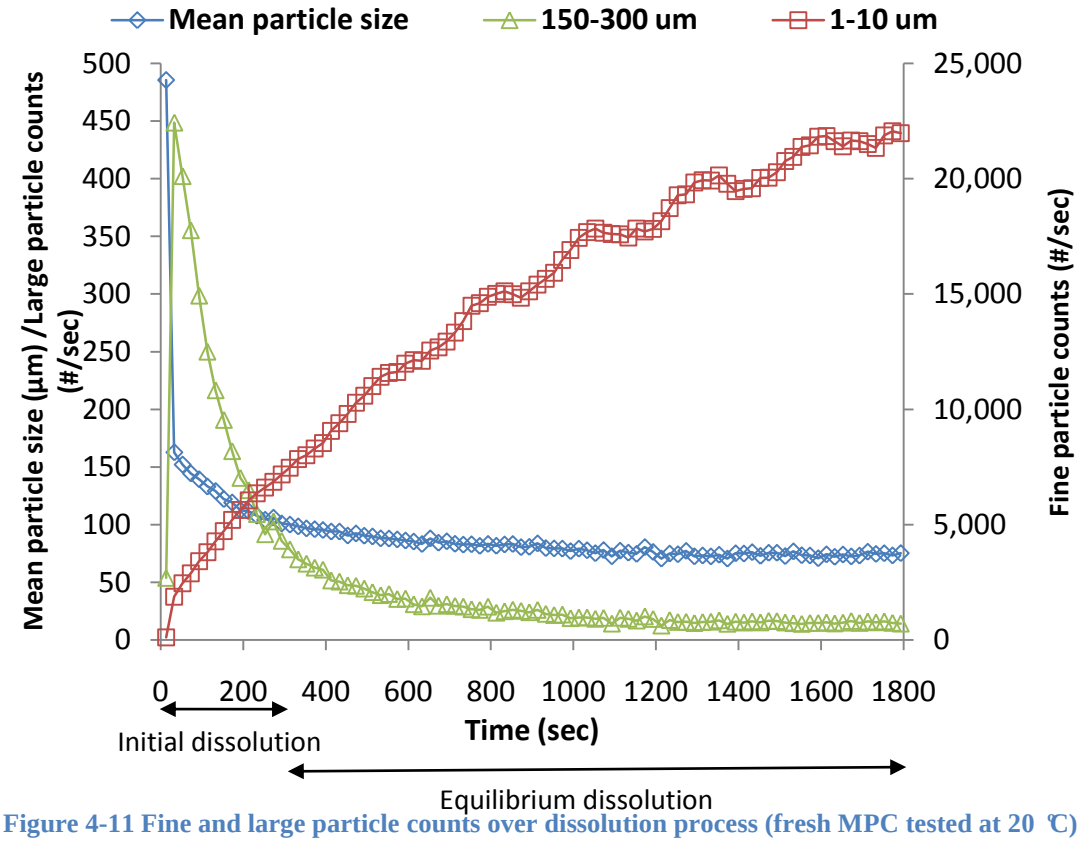

Figure 4-11 Fine and large particle counts over dissolution process (fresh MPC tested at 20 ℃)

(◇: mean particle size; △ : large particle counts (150-300 µm); □: fine particle counts (1-10 µm)

Specifically, the dissolution rate constant *k* was significantly influenced by storage duration and temperature. When the powder was stored at 10 ^{o}C for 2 weeks, *k* remained at same level as that of fresh powder, however, *k* decreased significantly after storing at 35 ^{o}C for two months. However, the powder size analysis result showed that the particle sizes distributions of fresh and aged powders (e.g. stored at 35 ℃ for 2 months) were similar (Figure 4-12). This insignificant changes in MPC particle size before and after storage appeared to dismiss the possiblity of increasing agglomeration with storage. Evidence of similar degrees of agglomeration between fresh and aged powder can also be seen visually *via* SEM images (Figure 4-13). This discrepancy may therefore not be a case of increased agglomerations but rather a change in the binding conditions between existing particles in the agglormerates. This change in conditions may be due to the formation of surface crosslinks between the particles during storage. In this case, increasing the storage duration or temperature may therefore accelerate the rate of cross-links formation (Anema et al., 2006, McKenna, 2000, Havea, 2006). As such, when the number of inter-particle cross-links reached a certain critical threshhold, the solubility dramatically decreased, as shown by the decrease of *k*, making aged powders harder to disperse in solution (Anema et al., 2006). The aging process did not increase agglomeration but rather altered the way particles interacted with their neighbouring particles that usually happened *via* loosely formed crosslinks to maintain the inter-particle structure. The number of crosslinks could increase with time or energy (e.g. *via* an increase in temperature) which rendered the particles sub-structures harder to break up. Hence, it may explain the apparent decrease in solubility without noticeable changes in particle size.

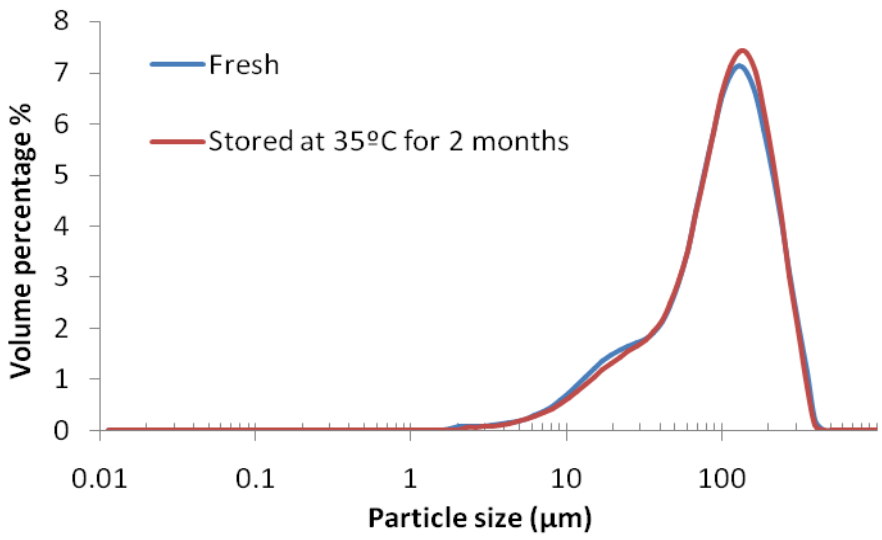

Figure 4-12 Particle size distributions of fresh powder and aged powder

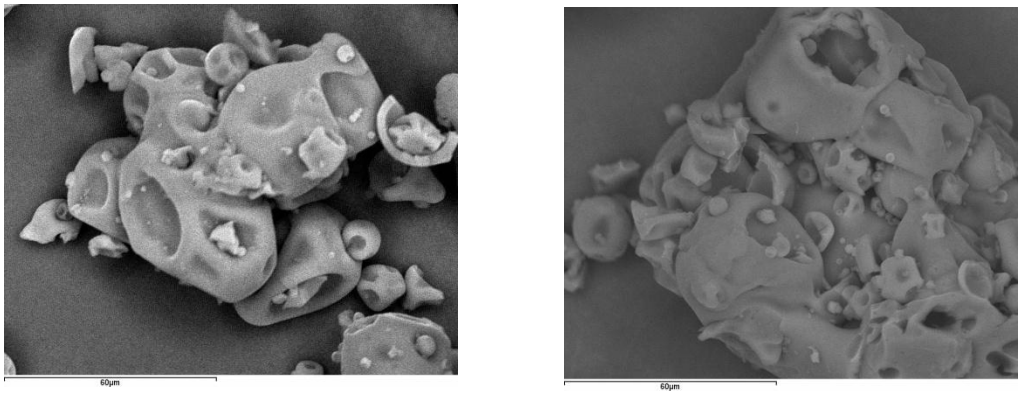

a. Fresh powder

b. Aged powder

(Stored at 35 ℃ for 2 months)

Figure 4-13 SEM images of fresh powder and aged powder

The final size d_∞ was also significantly influenced by the storage conditions. With increasing storage duration or temperature, d_∞ increased considerably. This might be due to increasing difficulty for the primary particles to release casein micelles into the surrounding aqueous phase possibly caused by casein molecules forming inter-micellar linkages during storage. Previous studies showed that particles could potentially develop shell structures during storage, making it hard for water to penetrate (Havea, 2006, McKenna, 2000), so that the materials released from primary particles became the rate limiting step during the dissolution process.

4.5. Conclusion

In both this study and in Chapter 3, FBRM has been demonstrated as a useful tool to characterise MPC solubility (Fang et al., 2010). By applying a modified Noyes-Whitney model on the data, the dissolution rate constant k and the final particle size d_∞ could be obtained. k represented the dynamic solubility related to the de-agglomeration of large particles, whereas d_∞ indicated the final solubility influenced by the release of casein micelles from primary particles. The dynamic dissolution profile of MPC undergoing various dissolution and storage conditions could be established. These results showed that the dissolution temperature had significant effects on k and d_∞ for fresh powder but not so much on aged powders. More significantly, this study identified d_∞ as a dissolution parameter with good correlations with the sedimentation test results. Therefore, the proposed model can potentially be used to analyse the dissolution kinetics and mechanisms of MPC, while also assisting in the benchmarking of other powders by

identifying relevant parameters for dairy powder processing. It is however noted that the proposed model is an idealised model taking the surface area of the solute as a constant. From the microscopic point of view and in practice, this is not true which implies a need to further develop the model. Nonetheless, this model provides a reasonable first estimate which can be further refined with the availability of more dynamic data and fine-grained techniques. The next step is to produce mono-dispersed MPC particles using a specially designed laboratory-scale dryer for dissolution testing to address the issues of difference in particle sizes and shapes found in common industrial powders. Uniform particles will also allow the initial surface area to be estimated and help to validate the model with a more 'ideal' system.

4.6. References

AMBROSE GRIFFIN, M. C. & GRIFFIN, W. G. 1985. A simple turbidimetric method for the determination of the refractive index of large colloidal particles applied to casein micelles. *Journal of Colloid and Interface Science,* 104**,** 409-415.

ANEMA, S. G., PINDER, D. N., HUNTER, R. J. & HEMAR, Y. 2006. Effects of storage temperature on the solubility of milk protein concentrate (MPC85). *Food Hydrocolloids,* 20**,** 386-393.

BELLOQUE, J. & RAMOS, M. 1999. Application of NMR spectroscopy to milk and dairy products. *Trends in Food Science & Technology,* 10**,** 313-320.

CARSTENSEN, J. T. & DALI, M. 1999. Determination of Mass Transfer Dissolution Rate Constants from Critical Time of Dissolution of a Powder Sample. *Pharmaceutical Development and Technology,* 4**,** 1 - 8.

COSTA, P. & SOUSA LOBO, J. M. 2001. Modeling and comparison of dissolution profiles. *European Journal of Pharmaceutical Sciences,* 13**,** 123-133.

DAVENEL, A., SCHUCK, P., MARIETTE, F. & BRULÉ, G. 2002. NMR relaxometry as a non-invasive tool to characterize milk powders. *Lait,* 82**,** 465-473.

DOKOUMETZIDIS, A. & MACHERAS, P. 2006. A century of dissolution research: From Noyes and Whitney to the Biopharmaceutics Classification System. *International Journal of Pharmaceutics,* 321**,** 1-11.

FANG, Y., SELOMULYA, C. & CHEN, X. D. 2008. On Measurement of Food Powder Reconstitution Properties. *Drying Technology,* 26**,** 3 -14.

FANG, Y., SELOMULYA, C. & CHEN, X. D. 2010. Characterization of milk protein concentrate solubility using focused beam reflectance measurement. *Dairy Science and Technology*.

HAVEA, P. 2006. Protein interactions in milk protein concentrate powders. *International Dairy Journal,* 16**,** 415-422.

HU, X., CUNNINGHAM, J. C. & WINSTEAD, D. 2008. Study growth kinetics in fluidized bed granulation with at-line FBRM. *Int. J. Pharm.,* 347**,** 54-61.

KEMPKES, M., EGGERS, J. & MAZZOTTI, M. 2008. Measurement of particle size and shape by FBRM and *in situ* microscopy. *Chem. Eng. Science,* 63**,** 4656-4675.

KOUGOULOS, E., JONES, A. G. & WOOD-KACZMAR, M. W. 2005. Modelling particle disruption of an organic fine chemical compound using Lasentec focussed beam reflectance monitoring (FBRM) in agitated suspensions. *Powder Technol.,* 155**,** 153-158.

KOVALSKY, P. & BUSHELL, G. 2005. *In situ* measurement of fractal dimension using focussed beam reflectance measurement. *Chem. Eng. J.,* 111**,** 181-188.

KRAVTCHENKO, T. P., RENOIR, J., PARKER, A. & BRIGAND, G. 1999. A novel method for determining the dissolution kinetics of hydrocolloid powders. *Food Hydrocolloids,* 13**,** 219-225.

LARSEN, C. K., GÅSERØD, O. & SMIDSRØD, O. 2003. A novel method for measuring hydration and dissolution kinetics of alginate powders. *Carbohydrate Polymers,* 51**,** 125-134.

MARABI, A., MAYOR, G., BURBIDGE, A., WALLACH, R. & SAGUY, I. S. 2008a. Assessing dissolution kinetics of powders by a single particle approach. *Chemical Engineering Journal*, 139**,** 118-127.

MARABI, A., MAYOR, G., RAEMY, A., BAUWENS, I., CLAUDE, J., BURBIDGE, A. S., WALLACH, R. & SAGUY, I. S. 2007. Solution calorimetry: A novel perspective into the dissolution process of food powders. *Food Research International,* 40**,** 1286-1298.

MARABI, A., RAEMY, A., BAUWENS, I., BURBIDGE, A., WALLACH, R. & SAGUY, I. S. 2008b. Effect of fat content on the dissolution enthalpy and kinetics of a model food powder. *Journal of Food Engineering,* 85**,** 518-527.

MCKENNA, A. B. 2000. *Effect of Porcessing and Storage on the Reconstitution Properties of Whole Milk and Ultrafiltered Skim Milk Powders.* Ph.D. thesis, Massey Univeristy.

MIMOUNI, A., DEETH, H. C., WHITTAKER, A. K., GIDLEY, M. J. & BHANDARI, B. R. 2009. Rehydration process of milk protein concentrate powder monitored by static light scattering. *Food Hydrocolloids,* 23**,** 1958-1965.

NIEBERGALL, P. J., MILOSOVICH, G. & GOYAN, J. E. 1963. Dissolution rate studies II. Dissolution of particles under conditions of rapid agitation. *Journal of Pharmaceutical Sciences,* 52**,** 236-241.

NIRO. September 2006a. *Niro Method A 1 b : Powder Moisture Routine Method* [Online]. Available: http://www.niro.com/ndk_website/NIRO/cmsdoc.nsf/WebDoc/ndkw6u9bbd [Accessed 20th January, 2010].

NIRO. September 2006b. *Niro Method A 3 a: Insolubility Index* [Online]. Available: http://www.niro.com/ndk_website/NIRO/cmsdoc.nsf/WebDoc/ndkw74jjk8 [Accessed 12th January, 2010].

SAGGIN, R. & COUPLAND, J. N. 2002. Ultrasonic Monitoring of Powder Dissolution. *Journal of Food Science,* 67**,** 1473-1477.

SIEPMANN, J. & PEPPAS, N. A. 2001. Modeling of drug release from delivery systems based on hydroxypropyl methylcellulose (HPMC). *Advanced Drug Delivery Reviews,* 48**,** 139-157.

SKRDLA, P. J. 2007. A simple model for complex dissolution kinetics: A case study of norfloxacin. *Journal of Pharmaceutical and Biomedical Analysis,* 45**,** 251-256.

VINESS, P. & REZA, F. 1999. Unconventional dissolution methodologies. *Journal of Pharmaceutical Sciences,* 88**,** 843-851.

YOON, S.-Y. & DENG, Y. 2004. Flocculation and reflocculation of clay suspension by different polymer systems under turbulent conditions. *Journal of Colloid and Interface Science,* 278**,** 139-145.

Monash University

Declaration for Thesis Chapter Five

In the case of Chapter 5, the nature and extent of my contribution to the work was the following:

Name	% contribution	Nature of contribution
Yuan Fang	80%	Initiation, Key ideas, Experimental works, Development, Data analysis, Writing up
Samuel Rogers	5%	Experimental works, Data analysis
Dr. Cordelia Selomulya	5%	Initiation, Results Interpretation, Review
Dr. Palatasa Havea	5%	Experimental works
Prof. Xiao Dong Chen	5%	Initiation, Key ideas, Development

Declaration by co-authors

The undersigned hereby certify that:

(1) they meet the criteria for authorship in that they have participated in the conception, execution, or interpretation, of at least that part of the publication in their field of expertise;

(2) they take public responsibility for their part of the publication, except for the responsible author who accepts overall responsibility for the publication;

(3) there are no other authors of the publication according to these criteria;

(4) potential conflicts of interest have been disclosed to (a) granting bodies, (b) the editor or publisher of journals or other publications, and (c) the head of the responsible academic unit; and

(5) the original data are stored at the following location(s) and will be held for at least five years from the date indicated below:

Location(s)	**Department of Chemical Engineering, Monash University Clayton campus, Australia**

Signature		
Signature		
Signature		
Signature		
Signature		

Chapter 5

Functionality of Milk Protein Concentrate: Effect of Spray Drying Temperature

5.1. Introduction

Spray drying is a common method used in the food processing industries, particularly the dairy industry. Powder, granulate, or agglomerate particles are formed during spray drying by removing the water content from the liquid feedstock (Niro, 2010). There are several significant advantages of the spray drying process. It rapidly removes the liquid from solid (within seconds) without excessively heating the product. This minimizes the degree of degradation of the protein and fat contents, which helps extend the shelf life of the powdered products without affecting nutritional value and functionalities. Spray drying also lowers the density of food products (as compared to the liquid form), so that the shipment and storage costs can be greatly reduced (Gaiani et al., 2010).

It is well known that protein is a heat sensitive material. During the heating process, there are various reactions that take place, such as denaturation, aggregation of whey protein, and formation of complexes between whey proteins, caseins and fat globules (Corredig and Dalgleish, 1999, Morr, 1985, Anema and Li, 2003, Anema and McKenna, 1996, Guo et al., 1999, Augustin and Udabage, 2007). It is also known that the surface of spray-dried dairy particles is generally dominated by proteins (Gaiani et al., 2006, Millqvist-Fureby et al., 2001). Therefore, there is a need to develop a better understanding of protein

interactions under different processing conditions such as drying, storage and testing conditions. McKenna conducted an intensive investigation on the formation of the insoluble material in milk protein concentrates (MPC) with different protein contents, subjected to different storage durations and temperature treatments (McKenna, 2000). The casein micelles appeared to be fused together and formed an insoluble material in direct relationship with increasing storage duration and temperature. Protein content was also a determining factor in this degradation process, with higher protein content leading to formation of more insoluble material within shorter storage duration. Guo *et al*. looked into the protein-protein and protein-lipid interactions in infant formula (Guo et al., 1999) and found that fat globules and casein micelles were well-defined discrete spheres in raw milk. They further found that after pasteurization, casein micelles showed rough irregular surfaces which could be a result of casein and whey protein interactions while after homogenization, casein-whey protein aggregates were found on the fat globules surfaces. However, there was little change in microstructure after condensation and spray drying. These results suggested that the major changes in microstructure and component interactions occur during pasteurization and homogenization (Guo et al., 1999).

To understand how proteins interacted to form the insoluble material, Havea conducted an experiment on a batch of MPC that were subjected to different storage durations and investigated the protein interactions using polyacrylamide gel electrophoresis (PAGE) and transmission electron microscopy (TEM) (Havea, 2006). The insoluble material formed during storage was found to be predominantly composed of hydrophobic casein molecules, with insignificant contribution from whey proteins. In addition, numerous studies have investigated the effects of different drying conditions on the functionalities of resulting powders. DeCastro and Harper found that an outlet temperature range of between 65 and 90 ℃ had no obvious effect on protein denaturation, but the moisture content and rehydration rate of the resulting particles were affected (DeCastro and Harper, 2001). Gaiani *et al.* studied the relationship between surface composition of high milk protein powders and the different drying air temperatures (Gaiani et al., 2010). They observed that fat and protein were preferably located on the surface of particles whereas lactose was enclosed at the core, in agreement with a previous study conducted by Kim *et al.* (Kim et al., 2003). Gaiani *et al.* also found that a lower outlet temperature led to increased fat and protein content on the surface of particles. A direct correlation between the powder's functionality (e.g. wettability) and the powder's surface composition was proposed in

order to relate functionality with the drying conditions (Gaiani et al., 2010). In another study, Millqvist-Fureby *et al.* conducted a series of experiments to examine the surface composition of whey protein insolate (WPI) particle with different heat treatment using Electron Spectroscopy for chemical Analysis (ESCA) (Millqvist-Fureby et al., 2001). It was found that the fat and lactose coverage slightly increases on the particle surfaces with increasing degree of insoluble protein along with an insignificant decrease of protein content on the particle surface with increasing heat. In the pharmaceutical industry, the dynamics of drying and the resulting functionalities of pharmaceutical protein particle are of particular interest. Maa and colleagues investigated the effects of different outlet temperatures and different protein composition on protein morphology (Maa et al., 1997). They concluded that the outlet temperature (an indicator of the drying speed) was the single most important parameter in the drying process, whereas difference in protein composition strongly influenced the resulting particles' morphology.

In this study, the relationship between spray drying air temperature and the resulting powder functionality was investigated. Mono-dispersed MPC particles were spray dried under different temperatures *via* a laboratory-scale drier. Using mono-dispersed particle to study the drying effect provides several advantages: firstly, each resulting particle underwent the same heating treatments (same history) and drying durations, implying that the population properties can be expected to be similar with that of the individual particle. Secondly, this unique drying process eliminates the wide variation in size and morphology of the dried particles, thus providing a much more reliable assessment of dissolution behaviour which consequently assisting in the establishment of the dissolution kinetics based on existing dissolution models (Chapter 4).

As previously done in Chapter 4 (Fang et al., 2010) and in other works (Kim et al., 2005) , focused beam reflectance measurement (FBRM) could be used to characterize powder dissolution with good reproducibility. In this study, the dissolution property of MPC powder was monitored using FBRM, the micro-structural changes of proteins from different drying air temperatures examined using TEM and degree of protein denaturation quantified using SDS-PAGE. The current study aims to establish a relationship between the drying air temperature and the functionality of the resulting products so as to provide comprehensive insights into the microstructure changes caused by differing drying conditions that may influence functionality.

5.2. Materials and methods

5.2.1. Materials

Fresh MPC 85 powder was provided by a local manufacturer immediately after production. Powder was sealed in airtight bag and stored at 4 ℃ in a fridge after manufacture. The industrially dried powder was used as control for all comparison.

5.2.2. Laboratory-scale production of MPC powders

MPC powder was first reconstituted to specific concentrations (10 and 20 wt %) before drying. The reconstitution was carried out at 50 ℃ for 30 minutes at 400 r.p.m. stirring rate and the extent of MPC powder dissolution monitored using FBRM. After reconstitution, the resulting solution was spray-dried using a single stream mono-dispersed droplet drier at the following temperatures (Table 5-1) with the orifice diameter of the nozzle being 75 μm. The droplets and hot air were introduced into the drying chamber with co-current direction. The temperature profile inside the drier was monitored by five thermocouples along the drying chamber. After spray drying, the powders collected were stored in desiccators at room temperature before functionality tests were performed. The drying temperatures in this paper referred to the inlet air temperature readings from the thermocouple at the inlet of hot air in the drier. However, the inlet air temperature was not directly controllable, depending on a combination between the temperature setting, the feeding flow rate, the flow rate of the dispersion air, and the external environmental conditions (e.g. temperature and relative humidity).

Table 5-1 Drying conditions of 10% and 20% solids concentration

Inlet air temperature (ºC)	80 ± 3.0		106 ± 1.0		156 ± 1		177 ± 0.5	
Concentration (wt%)	10%	20%	10%	20%	10%	20%	10%	20%
Setting temperature (ºC)	90		130		190		220	
Outlet temperature (ºC)	57	54	68	68	95	93	100	103
Flow rate (g/min)	1.72	1.96	2.68	2	1.84	2	2	2
Droplet size (μm)	197	201.2	191	230	220	201	195	207

5.2.3. Physical characterization

Moisture content measurement was conducted immediately upon collection of the powder from the drier. The measurement was modified and scaled down based on Niro method

No. A 1 b (Niro, September 2006). 0.2 g of MPC powder was dried in the oven at 102 ℃ for 3 hours. The difference in weight before and after drying was recorded.

The powder particle size and particle size distribution were analysed using light microscope. Morphology of powder samples was observed using a Scanning Electron Microscope (JEOL 840A) operated at 20 kV in a low vacuum mode and equipped with a backscatter detector. Sample coated with platinum (~4nm thickness) was placed on a double-sided carbon tape for analysis.

5.2.4. Dissolution test

The dissolution test was conducted using the Focused Beam Reflectance Measurement (FBRM) with the measuring protocol based on work done in Chapter 3 (Fang et al., 2010). 3 ± 0.1 g of powder was weighted and poured onto 150 mL deionised water which was preheated to 50 ℃ before commencement of the experiment to make up a 2 wt% solution. An overhead stirrer was immediately started and stirred continuously at a stirring rate of 400 r.p.m. The data from the FBRM was collected using the iC FBRM^{TM} program (Mettler Toledo). The dissolution duration was 30 minutes while the data-collecting interval was set to 5 seconds.

5.2.5. Polyacrylamide gel electrophoresis

The sodium dodecyl sulphate polyacrylamide gel electrophoresis (SDS-PAGE) technique was employed using a Bio-Rad mini-gel slab electrophoresis unit (Bio-Rad Laboratories) to determine the level and composition of protein in solution and their supernatant. This protocol was based on the previous work conducted by Anema *et al.* under reducing conditions (with 2-mercaptoethanol) and non-reducing conditions (without 2-mercaptoethanol) (Anema and Li, 2003, Anema et al., 2006). 0.1 g powder was poured into 20 mL deionised water and stirred for 30 minutes while maintaining the temperature at 50 ℃ using a magnetic stirring plate. The solution was centrifuged at 5000 r.p.m. for 10 minutes. 10 µL of the resulting supernatant was added to 10 µL Lamile sample buffer for non-reducing SDS-PAGE and 10 µL Lamile sample buffer with 5% 2-mercaptoethanol for reducing SDS-PAGE. The resulting sample mixtures were homogenized for 10 seconds with a vortex meter. For reducing SDS-PAGE, the sample mixture was further heated in a 95 ℃ water bath for 5 minutes. The mixed sample solution was then loaded into the respective wells of a 10 well precast gel (Bio-Rad Laboratories). After the electrophoresis,

the resulting gel stained using 2x Amino Black for 1 hour and de-stained in 10% acetic acid overnight.

5.2.6. Micro XCT

The sample's structural and internal morphology were examined using the micro XCT technique and was conducted by collaborators in Fonterra Research Centre (Palmerston North, New Zealand).

5.2.7. Transmission electron microscope (TEM)

Samples were prepared according to the method described by McKenna (McKenna, 2000) and were imaged using a transmission electron microscope (TEM). This work was conducted by collaborators in Fonterra Research Centre (Palmerston North, New Zealand).

5.3. Results and discussion

5.3.1. Physical characterization

The changes in moisture content and particle size of spray-dried powders under different inlet air temperatures were shown in Figure 5-1. It can be seen that the moisture content decreased and corresponding particle size increased with increasing inlet temperature. This trend was exhibited for both 10 and 20 wt% concentrations over the range of drying air temperatures tested. The moisture content was shown to be dependent on the inlet air temperatures, with higher inlet air temperature removing moisture content from the droplets more rapidly. The resulting particle sizes were relatively smaller when dried at a low inlet air temperature (e.g. 80 ℃) with a somewhat narrow distribution. The resulting particle sizes increases with increasing inlet air temperature along with a wider size variation. The phenomena of shrinking and puffing on the particle surface were observed at high inlet air temperature, leading to formation of irregular particle shapes with a wide particle size distribution. During drying, water was rapidly removed from the surface, creating a diffusion gradient and causing water movement towards the surface. As the droplet was drying, the droplet surface receded into the centre, forming a solid 'skin' on the surface. This skin trapped the water inside, and the outbound moisture movement was consequently dependent on the property of the 'skin'. With a rapid increase in internal temperature, vaporization of water in the porous interior exerted a force outwards and

caused the expansion of the 'skin' or 'puffing' of the droplet, and thus increased the resulting particle size.

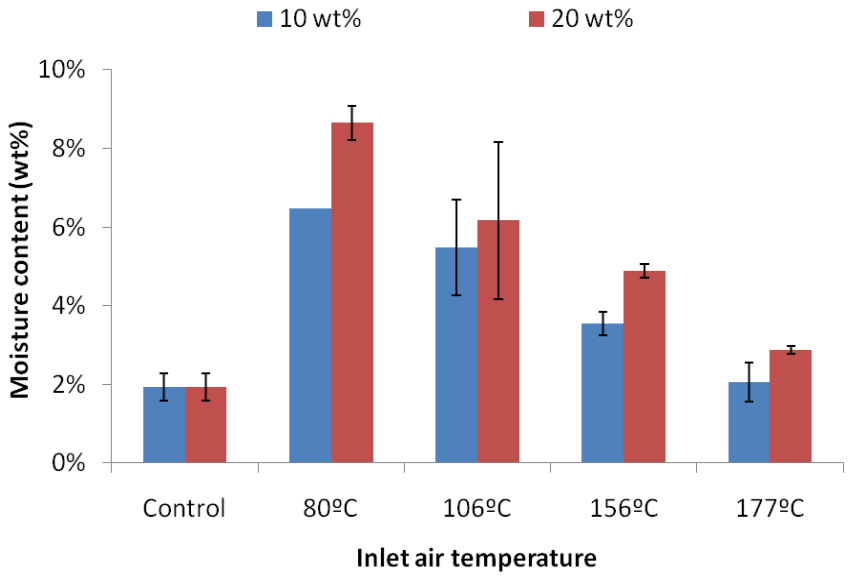

a. Moisture content of particle spray dried at different temperatures

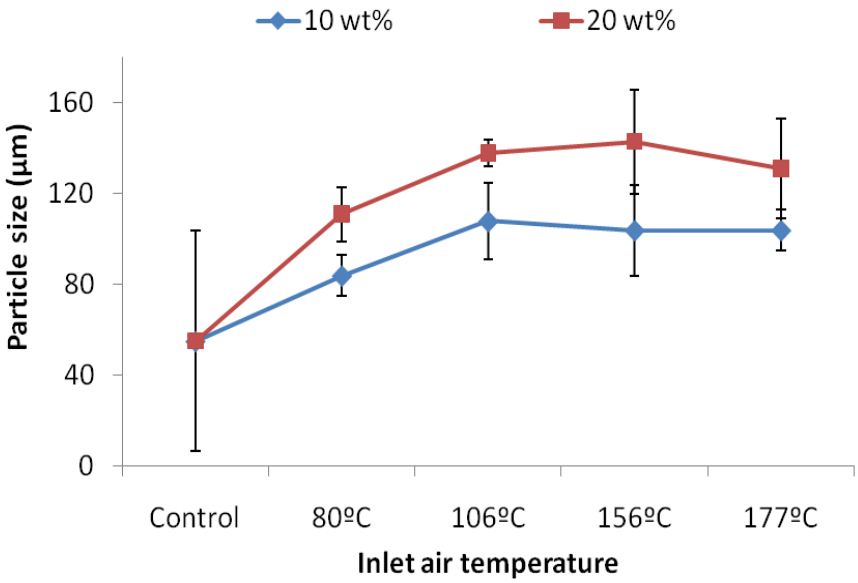

b. Particle size of powder spray dried at different temperatures

Figure 5-1 Moisture content and particle size of powders spray dried at different temperatures

Another observation was that the control powder had a smaller particle size and a much broader size variation as compared with those dried *via* the laboratory-scale drier. This was due to the fact that when the control powder was produced, the particles were milled to reduce the particle size in order to increase the bulk density.

These results were verified using light microscope as shown in Figure 5-2. The images acquired were of dry particles just before dissolution and after 5 minutes of dissolution.

For the control powder, the dry particle appeared to agglomerate with a wide particle size distribution. After dissolution, the majority of the agglomerated particles appeared to have dissolved with only a small portion remained that had a relatively small average particle size. As for powders dried at higher temperatures (e.g. 156 ℃ and 177 ℃), the dried particles appeared to consist of both puffed and shrunken particles. After dissolution, the powders remained un-dissolved and continue to exist as whole particles with reasonably similar particle size. For powder dried at lower temperatures (e.g. 80 ℃ and 106 ℃), the dry particles were close to spherical with reasonably uniform size. After dissolution, only a small number of sediments appear to remain in solution.

	Dry particles	In solution (dissolved after 5 min)
Control	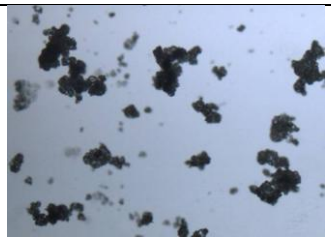	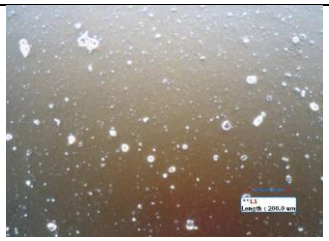
177 ℃	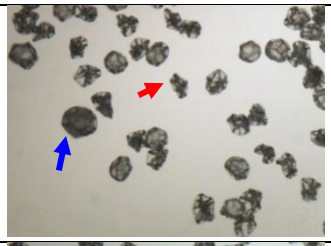	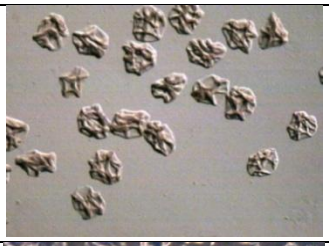
156 ℃	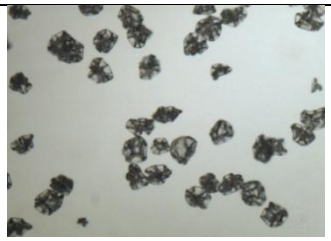	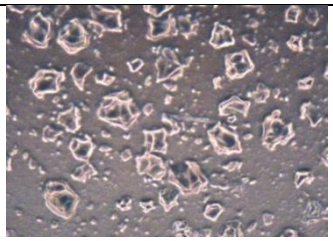
106 ℃	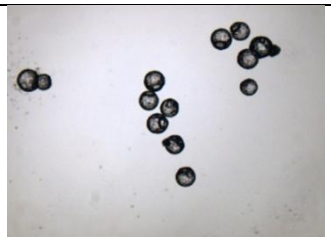	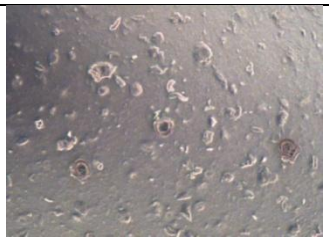
80 ℃	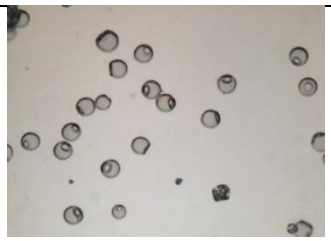	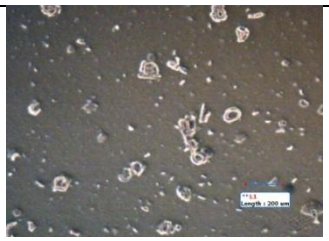

Figure 5-2 Light microscopy images of powders spray dried under different temperatures before dissolution and after dissolution (10 wt%, reference bar: 200 μm)

In terms of solid contents, 10 wt% and 20 wt% MPC were dried under different drying air temperatures. It was noted that at the same drying temperature, 20 wt% solid content powders exhibited higher moisture content and particle size than those at 10 wt% (Figure 5-1a and Figure 5-1b). From the SEM images (Figure 5-3), 20 wt% powders clearly had a thicker wall compared to the 10 wt% powders. Thicker crust reduced water molecule diffusion rate during drying process, consequently increased moisture content.

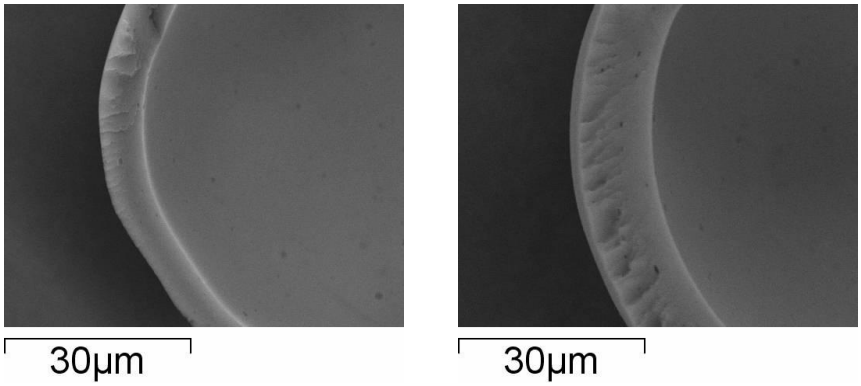

a. 10 wt% **b. 20 wt%**

Figure 5-3 SEM images of 10 wt% and 20 wt% particles (dried at 90 ℃)

5.3.2. Particle morphology

The internal morphologies of the powders from different drying temperatures were also of interest in this study. It was noted that the powders spray dried at different temperatures had very distinct cross-sectional appearances (Figure 5-4). Powders dried at lower inlet air temperatures (e.g. 80 ℃ and 106 ℃) were spherical and smooth while those dried at a higher inlet air temperature (e.g. 156 ℃ and 177 ℃) had crumpled looking surfaces. It was noted that a low inlet air temperature led to formation of relatively uniformly wall with a near circular cross-sectional area (Figure 5-4a). On the other hand, a high inlet air temperature led to irregular, non-hollow structures (Figure 5-4b). From the reconstructed images (Figure 5-4c and d), the powders spray dried at lower temperatures appeared to be mono-dispersed particles.

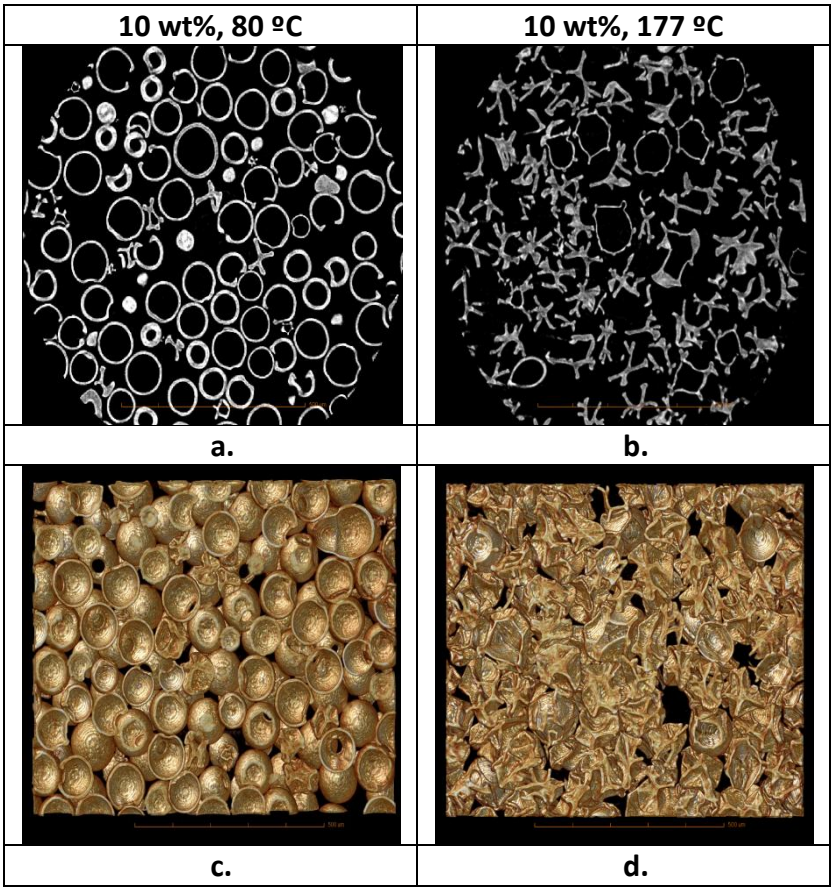

Figure 5-4 Micro XCT images of powder spray dried at 90 ℃ and 177 ℃

(a and b are the cross-section of powder dried at 80 ℃ and 177 ℃ respectively; c and d are the reconstruction images of powder dried at 80 ℃ and 177 ℃ respectively)

Previous studies had investigated the formation and surface composition of particles during spray drying (Kim et al., 2003, Maa et al., 1997, Millqvist-Fureby et al., 2001, Vehring, 2008, Vehring et al., 2007). It was known that particle formation was not only determined by the composition but was also dependent on the relationship between surface recession and diffusion of the solutes during the spray drying process (Maa et al., 1997, Vehring, 2008). For formation of particle surface composition, there were several theories on how the surface of the drying droplet was formed during the drying process. Kim *et al.* investigated the surface composition and components distribution of dairy powder during spray drying process. They confirmed that the solute segregation during drying was the most likely mechanism behind surface formation (Kim et al., 2003). This finding could be used to approximate the radial distribution of all components prior to solidification, and thus helped to predict the structure of the dry particles and estimate the likelihood of specific component(s) forming the shell. Vehring *et al.* identified a dimensionless parameter (Peclet number) which was proposed to influence the particle formation during the drying process (Vehring et al., 2007). It was defined as the ratio of the diffusion

coefficient of the solute and the evaporation rate. Proteins having low diffusion coefficient fall into the high Peclet number category. Vehring pointed out that if the rate of surface shrinking was faster than the rate that dissolved or suspended components moved inwards towards the centre of the droplet, the components would be 'left behind' near the surface shrinking frontage, causing the surface to be enriched with these components, e.g. protein (with low diffusion coefficient), which have a high Peclet number (Vehring, 2008). Upon the formation of the surface shell, the resulting particles exhibited a range of different morphologies, depending on their size and shell properties in the final stages of the drying process. Charlesworth and Marshall conducted a study observing the drying behaviour of droplets using a single droplet method (Charlesworth and Jr., 1960). Using a wide range of drying conditions and materials, different morphologies of droplets were observed. For rigid and less porous material, with the air temperature below that of the boiling point of the solution, the solid on the surface of the droplet forms a stiffened and thickened skin and eventually rupture by implosion (as shown in Figure 5-5a). If the air temperature was above the boiling temperature of the solution, the internal particle temperature would gradually approach the temperature of the surrounding air. Eventually the internal temperature reached the boiling point of the solution leading to vapour formation and creation of a positive pressure within the particle. The resistance of the skin prevented the liquid from forcing through the surface and therefore pressure built up within the particle. With this internal stress, the particle could either fracture or become inflated. Inflated particle could either collapse or stretch which will increase the permeability of the skin. A schematic of a proposed particle formation process is as shown in Figure 5-6 (Charlesworth and Jr., 1960, Handscomb et al., 2009).

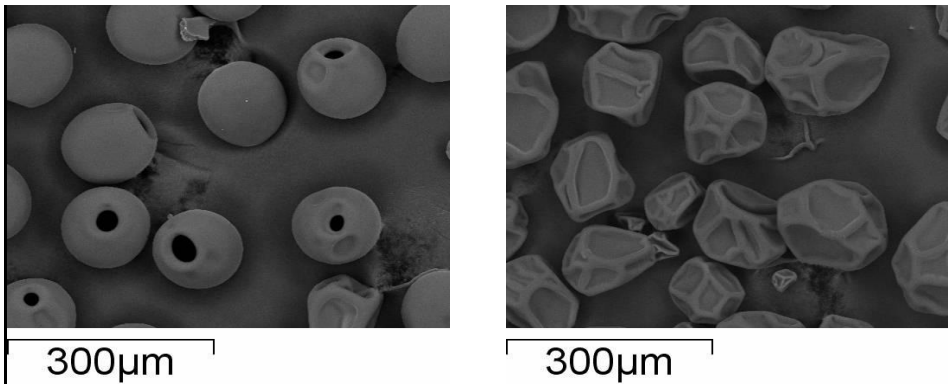

Figure 5-5 SEM images of particles with different morphology as a result of different drying conditions

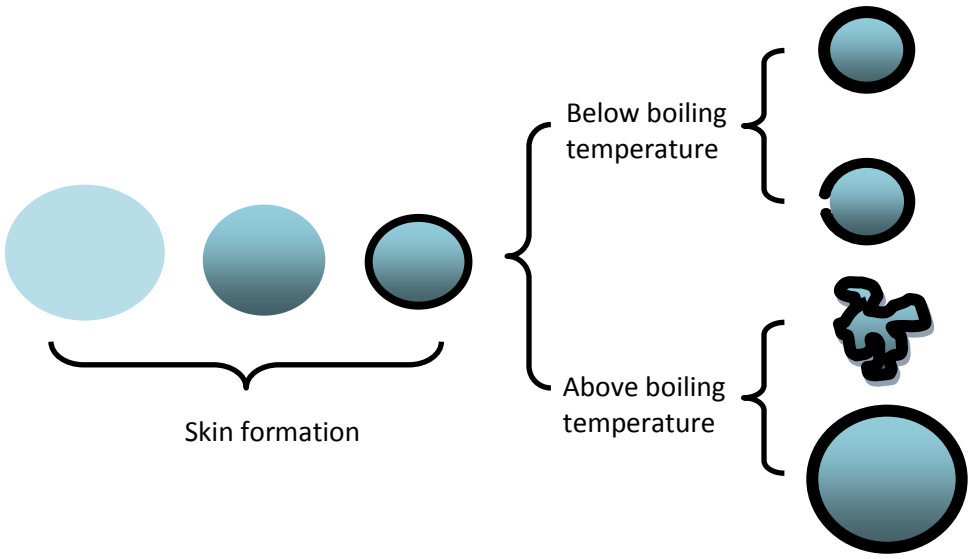

Figure 5-6 Schematic showing some of the different particle morphologies that may result when drying from different temperatures

5.3.3. Particle solubility characterization

To observe the solubility of different powders produced under different temperatures, FBRM analysis was conducted on 2 wt% concentration solution tested at 50 °C for 30 minutes. The dissolution profiles of MPC powders are as shown in Figure 5-7. The dissolution profiles were represented as changes in chord length of the powder particles. Given the same dissolution period, a smaller chord length would suggest a better solubility (Fang et al., 2010). Figure 5-7 showed that the chord lengths of MPC particles dried at lower temperatures (e.g. 80 ℃ and 106 ℃) decreased rapidly to reach a plateau within 200 seconds, as compared to that of MPC powders dried at higher temperatures (e.g. 156 ℃ and 177 ℃). It was noted that for both 80 °C and 106 ℃ dried MPC, the resulting chord lengths decreased to a final particle size of 80 μm, similar to that of the control. This implied that both samples spray died under different temperatures were able to obtain the same extent of dissolution as the control powder. On the other hand, for particles dried at higher temperatures (e.g. 156 ℃ and 177 ℃), the chord lengths decreased slowly and did not reach an equilibrium even after 30 minutes. This indicated that the solubility of resulting powders deteriorated at high drying temperatures.

From the above results, the rate of decreasing chord length appeared to be a function of the inlet air temperature, with the fastest rate occurring for the particles dried at a lower inlet air temperature. Given the same drying duration, higher drying air temperatures rapidly

overheated the particles and induced protein structural changes, thus increasing the amount of insoluble content and reduced solubility. The results from FBRM clearly suggested that the solubility of MPC particles were strongly affected by the inlet air temperature. In addition, the drop in chord length of powders dried at lower temperatures were faster than the control when comparing the dissolution curves between control and lower temperatures (e.g. 80 ℃ and 106 ℃ in Figure 5-7). Since the control powder had relatively smaller particle size and a higher degree of agglomeration, upon coming in contact with water, the control powder took longer to de-agglomerate and dissolve, whereas for the mono-dispersed particles, there was no de-agglomeration such that the only behaviour observed was solely that of similar size particles.

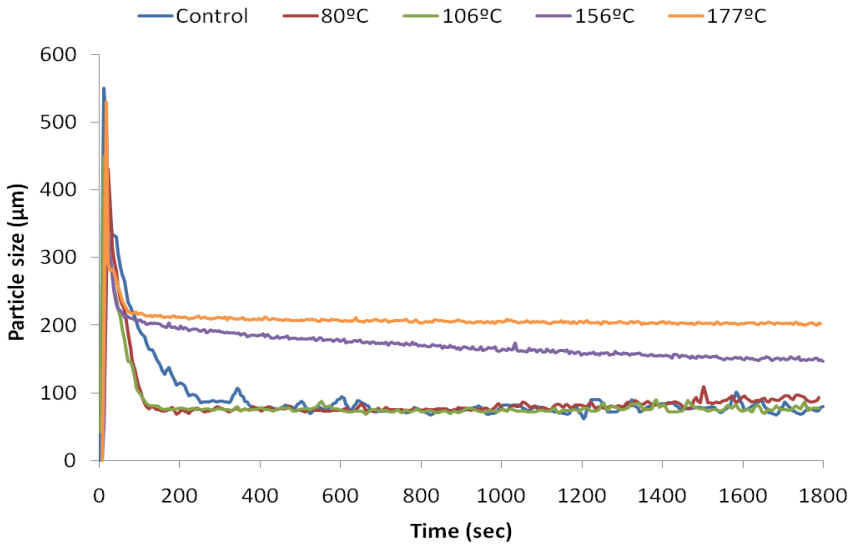

a. FBRM results of powders with 10 wt% solids content

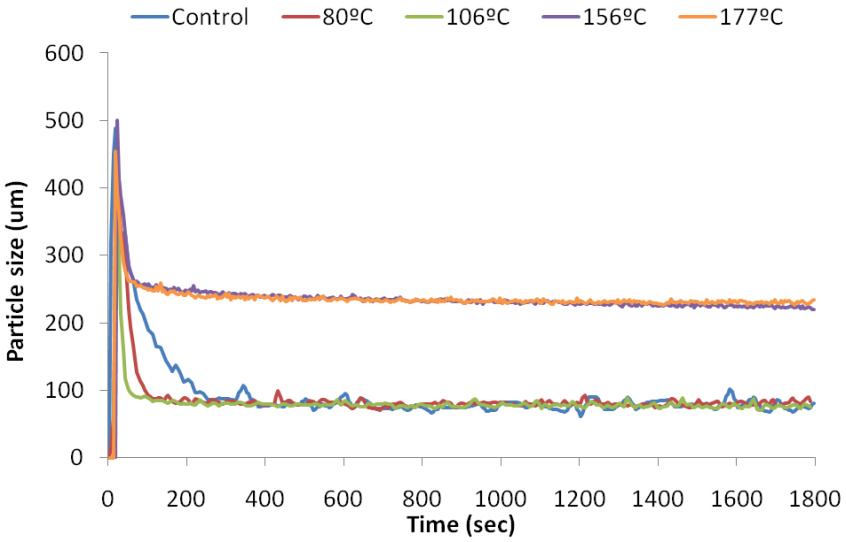

b. FBRM results of powders with 20 wt% solids content

Figure 5-7 Dissolution profile of MPC particles spray dried at different temperatures tested at 50 ℃

5.3.4. Degree of protein denaturation

Reducing and non-reducing SDS-PAGE analyses were conducted on MPC powders dried at different temperatures (Figure 5-8). The analyses were done on the supernatant of MPC solution for each corresponding MPC powder sample. MPC powders dried at different temperatures were expected to have different degrees of denaturation. Higher degrees of denaturation should exhibit higher amount of insoluble denatured protein, which would be retained in the sediment during centrifugation. Thus the amount of soluble protein in the supernatant would decrease. By investigating the differences in the supernatant protein content, the amount of protein denaturation could be quantified. In addition, by examining the position of the bands on the SDS-PAGE gel, the identity of the proteins involved in the formation of the insoluble material in the sediment could be determined. Visual inspection of the gel indicated that with increasing drying air temperature, the protein bands became more diffused and less defined (Figure 5-8). It should be noted that non-reducing SDS-PAGE (Figure 5-8b) was performed immediately after the protein powders been spray dried while reducing SDS-PAGE (Figure 5-8a) was carried out 2 month after the protein powders been spray dried. Therefore, it was not unexpected that the control powder protein band appeared weaker and less defined in the reducing SDS-PAGE in comparison with the non-reducing SDS-PAGE (Figure 5-8). In view of this, the protein band for 80 ℃ was used as a reference in the following intensity analysis.

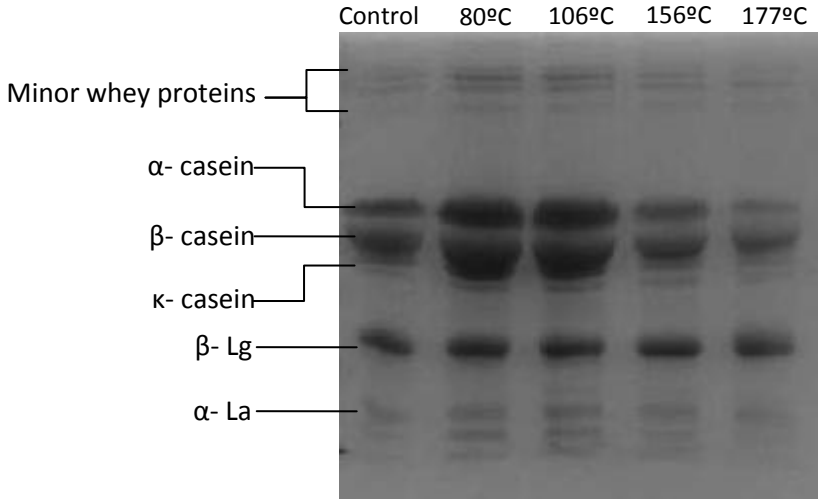

a. reducing SDS-PAGE gel image

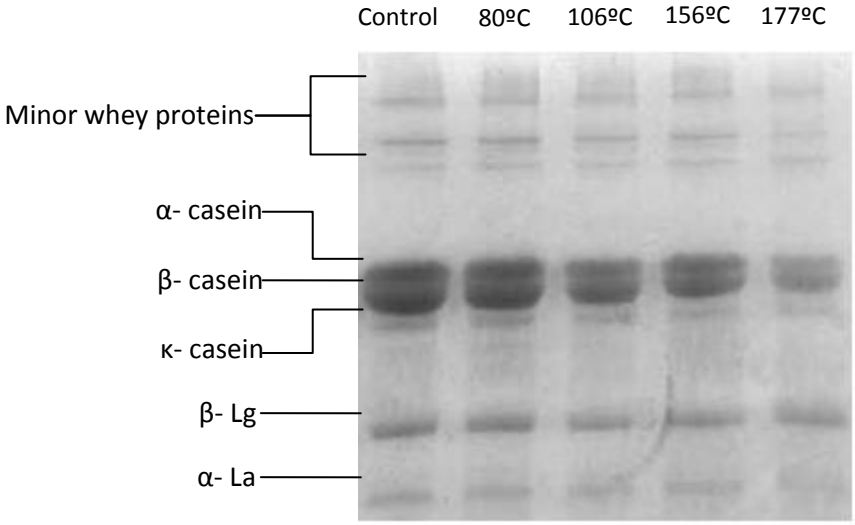

b. non-reducing SDS-PAGE gel image

Figure 5-8 Reducing and non-reducing SDS-PAGE gel

Figure 5-9 shows that the relative change in solubility over the range of drying temperatures based on the integrated band intensities of the major protein bands (α-casein, β-casein, κ-casein, β-lactoglobulin, α-lactalbumin and the total protein) from the SDS-PAGE results. Both the reducing and non-reducing methods exhibited the same trends whereby all the different protein types decreases with increasing inlet air temperature. At relatively low drying temperatures (e.g. 80 ℃ and 106 ℃), the loss of proteins were insignificant (within 20%) whereas for high drying temperatures (e.g. 156 ℃ and 177 ℃), the loss of proteins were highly significant (e.g. less than 40% of total protein remained in supernatant for powder spray dried at 177 ℃). Among these proteins, it should be noted that the loss of casein proteins were more significant than the loss of whey proteins under

all drying temperatures (Figure 5-9). This implied that the insoluble materials in MPC powder were mainly made up of casein rather than whey proteins, in agreement with the study by Corredig and Dalgleish (Corredig and Dalgleish, 1999). They identified two main interactions between casein micelle and whey proteins: (a) a direct interaction of β-Lg with casein micelles, *via* κ-casein binding; (b) a reaction between α-La and β-Lg with the micelles, through an intermediate complex formed between the two whey proteins in solution (Corredig and Dalgleish, 1999, Donato and Guyomarc'h, 2009). In addition, Havea reported that the disulphide-linked proteins consist of κ-casein and β-lactoglobulin (Havea, 2006).

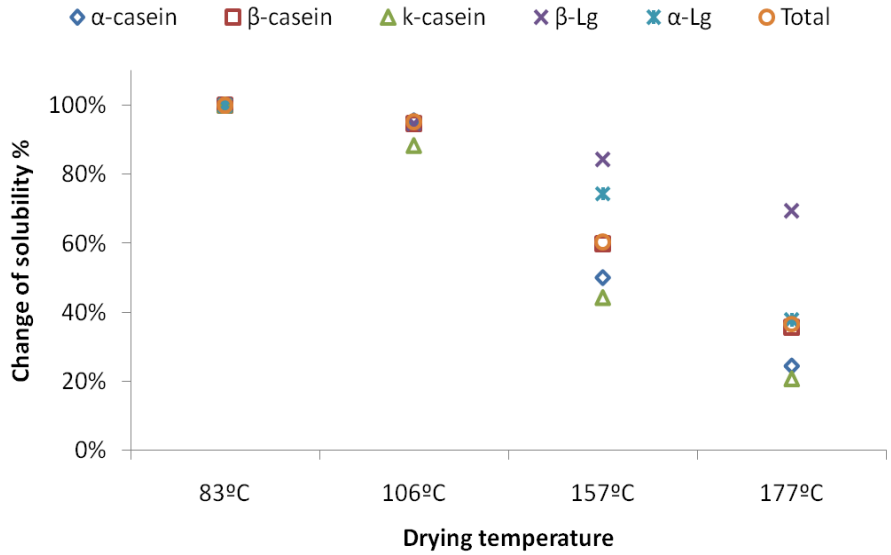

a. Reducing SDS-PAGE gel

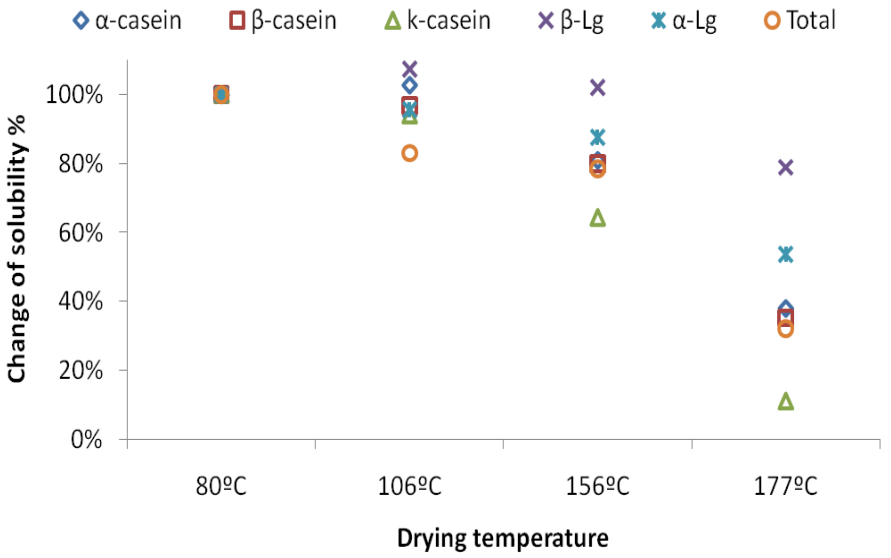

b. Non-reducing SDS-PAGE gel

Figure 5-9 Relative change in solubility measured from integrated band intensities for the major caseins and whey proteins in the supernatants

FBRM results (Figure 5-7) suggested that drying at lower temperatures (e.g. 80 ℃ and 106 ℃) did not affect the dissolution property, whereas higher drying temperatures (e.g. 156 ℃ and 177 ℃) caused deterioration of solubility. The SDS-PAGE results showed that less than 20% of total protein solubility change would not cause any detectable changes in FBRM. When greater than 20% of total protein were lost, significant differences in FBRM results were observed, indicated by the much higher chord length of un-dissolved particles compared with that of the control powder.

5.3.5. Protein-Protein Interaction

TEM microscopy was conducted on three different 10 wt% MPC samples dried at different temperature. Figure 5-10 shows the TEM images of the 3 MPC samples with key observable differences between the samples. For the sample dried at a lower temperature (83 ℃), the casein micelles clearly appeared to be that of individual spheres with variable sizes. When dried at median temperature (156 ℃), the casein micelles boundaries became less distinct as low degree cross-links started to form with the neighbouring micelles; at this point, the individual casein micelles were still distinguishable from one another. However, as drying temperature further increased till a high temperature (177 ℃), the individual casein micelles were no longer visible as they had fused together to form a strong network with each other. No distinct boundaries between each micelle could be observed. In general, TEM result demonstrated an increase in the micelle size with increasing inlet air temperatures and was in agreement with previously reported studies indicating that the resulting micelle size increased with increasing inlet temperature (de Castro-Morel and Harper, 2003) or heating duration (Anema and Li, 2003). At all the heating temperatures, there was an increase in size of the casein micelle. However, the rates of size increment were different and were directly related to the heating temperatures (Anema and Li, 2003).

The increase in casein micelle size could be due to the increasing interactions and cross-links among denatured whey proteins and casein micelles (Jeurnink and De Kruif, 1993). McKenna used TEM to observe the number of fused casein increasing with storage for MPC powders (McKenna, 2000). He postulated that the cross-linking of micelles by whey proteins together with the close association between the micelles at the surface led to the increasing number of cross-linked micelles on the surface. In summary, the results from both SDS-PAGE and TEM suggested that the number of cross-links increased with

increasing inlet air temperature, and the cross-links were attributed to both casein and whey proteins.

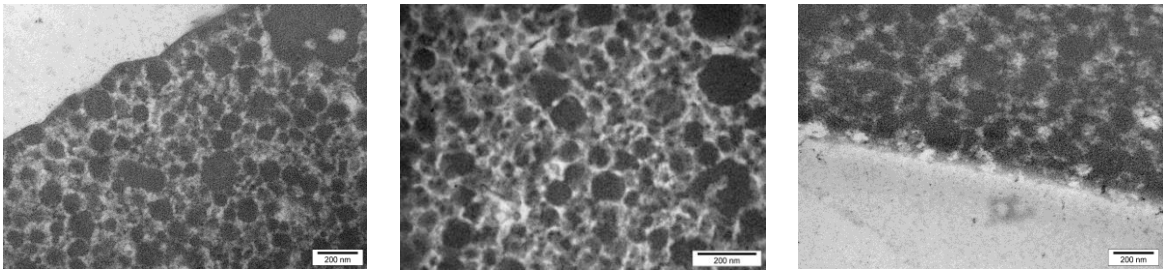

a. b. c.

Figure 5-10 TEM results of 10 wt% MPC dried at (a). 80 ℃; (b). 156 ℃; (c). 177 ℃

5.4. Conclusion

Quantitative analysis and micro-structural analysis to investigate the effect of spray drying temperature on MPC powder functionality were carried out in this study. By using mono-dispersed particles to eliminate the effects of size variation or uneven drying conditions, the outcomes contributed to the current understanding on (i) how spray drying conditions affected the resulting powder functionality; (ii) how spray drying conditions changed the micro-structure of proteins; and consequently (iii) how particle micro-structure could be related to powder functionality. Higher drying temperatures led to lower moisture contents and broader particle size distributions, while higher weight percentage (wt%) of solid concentrations gave higher moisture contents and larger particle sizes. Solubility as determined *via* FBRM deteriorated with increasing inlet air temperature, and this decrease in solubility could be attributed to both the casein and whey proteins, while TEM results confirmed that the number of cross-links clearly increased with inlet air temperature.

This study conclusively showed that there was a direct relationship between drying conditions and the resultant powder functionality and microstructure, and also the formation of protein network during drying which consequently affected powder morphology and functionality. This study also identified the techniques to quantify these changes with different drying temperatures, which can be further used to elucidate the potential mechanisms of powder drying kinetics *via* modelling.

5.5. References

ANEMA, S. G. & LI, Y. 2003. Association of Denatured Whey Proteins with Casein Micelles in Heated Reconstituted Skim Milk and its Effect on Casein Micelle Size. *Journal of Dairy Research,* 70**,** 73-83.

ANEMA, S. G. & MCKENNA, A. B. 1996. Reaction Kinetics of Thermal Denaturation of Whey Proteins in Heated Reconstituted Whole Milk. *Journal of Agricultural and Food Chemistry,* 44**,** 422-428.

ANEMA, S. G., PINDER, D. N., HUNTER, R. J. & HEMAR, Y. 2006. Effects of Storage Temperature on the Solubility of Milk Protein Concentrate (MPC85). *Food Hydrocolloids,* 20**,** 386-393.

AUGUSTIN, M. A. & UDABAGE, P. 2007. Influence of Processing on Functionality of Milk and Dairy Proteins. *In:* STEVE, L. T. (ed.) *Advances in Food and Nutrition Research.* Academic Press.

CHARLESWORTH, D. H. & JR., W. R. M. 1960. Evaporation from drops containing dissolved solids. *AIChE Journal,* 6**,** 9-23.

CORREDIG, M. & DALGLEISH, D. G. 1999. The Mechanisms of the Heat-induced Interaction of Whey Proteins with Casein Micelles in Milk. *International Dairy Journal,* 9**,** 233-236.

DE CASTRO-MOREL, M. & HARPER, W. J. 2003. Effect of Retentate Heat Treatment and Spray Dryer Inlet Temperatrue on the Properties of Milk Protein Concentrated (MPC's). *Milchwissenschaft,* 58**,** 13-15.

DECASTRO, M. & HARPER, W. J. 2001. Effect of Drying on Characteristics of 70% Milk Protein Concentrate. *Milchwissenschaft-Milk Science International,* 56**,** 269-272.

DONATO, L. & GUYOMARC'H, F. 2009. Formation and Properties of the Whey Protein/κ-casein Complexes in Heated Skim Milk - A Review. *Dairy Sci. Technol.,* 89**,** 3-29.

FANG, Y., SELOMULYA, C. & CHEN, X. D. 2010. Characterization of Milk Protein Concentrate Solubility using Focused Beam Reflectance Measurement. *Dairy Science and Technology*.

GAIANI, C., EHRHARDT, J. J., SCHER, J., HARDY, J., DESOBRY, S. & BANON, S. 2006. Surface Composition of Dairy Powders Observed by X-ray Photoelectron Spectroscopy and Effects on Their Rehydration Properties. *Colloids and Surfaces B: Biointerfaces,* 49**,** 71-78.

GAIANI, C., MORAND, M., SANCHEZ, C., TEHRANY, E. A., JACQUOT, M., SCHUCK, P., JEANTET, R. & SCHER, J. 2010. How Surface Composition of High Milk Proteins Powders is Influenced by Spray-Drying Temperature. *Colloids and Surfaces B: Biointerfaces,* 75**,** 377-384.

GUO, M. R., HENDRICKS, G. M. & KINDSTEDT, P. S. 1999. Effect of Processing on Protein-protein and Protein-lipid Interactions and Mineral Distribution in Infant Formula. *International Dairy Journal,* 9**,** 395-397.

HAVEA, P. 2006. Protein Interactions in Milk Protein Concentrate Powders. *International Dairy Journal,* 16**,** 415-422.

JEURNINK, T. J. M. & DE KRUIF, K. G. 1993. Changes in Milk on Heating: Viscosity Measurements. *Journal of Dairy Research,* 60**,** 139-150.

KIM, E. H.-J., CHEN, X. D. & PEARCE, D. 2003. On the Mechanisms of Surface Formation and the Surface Compositions of Industrial Milk Powders. *Drying Technology: An International Journal,* 21**,** 265 - 278.

KIM, Y.-S., R ÍO, J. R. M. D. & ROUSSEAU, R. W. 2005. Solubility and Prediction of the Heat of Solution of Sodium Naproxen in Aqueous Solutions. *Journal of Pharmaceutical Sciences,* 94**,** 1941-1948.

MAA, Y.-F., COSTANTINO, H. R., NGUYEN, P.-A. & HSU, C. C. 1997. The Effect of Operating and Formulation Variables on the Morphology of Spray-Dried Protein Particles. *Pharmaceutical Development and Technology,* 2**,** 213 - 223.

MCKENNA, A. B. 2000. *Effect of Porcessing and Storage on the Reconstitution Properties of Whole Milk and Ultrafiltered Skim Milk Powders.* Ph.D. thesis, Massey Univeristy.

MILLQVIST-FUREBY, A., ELOFSSON, U. & BERGENSTÅHL, B. 2001. Surface composition of spray-dried milk protein-stabilised emulsions in relation to pre-heat treatment of proteins. *Colloids and Surfaces B: Biointerfaces,* 21**,** 47-58.

MORR, C. V. 1985. Functionality of Heated Milk Proteins in Dairy and Related Foods. *J. Dairy Sci.,* 68**,** 2773-2781.

NIRO. 2010. *Spray Drying Information from GEA Niro* [Online]. Søborg, Denmark: GEA Niro. Available: http://www.niro.com/niro/cmsdoc.nsf/WebDoc/ndkk5hmc6zSprayDryersSprayDryers [Accessed 7th July 2010].

NIRO. September 2006. *Niro Method A 1 b : Powder Moisture Routine Method* [Online]. Available: http://www.niro.com/ndk_website/NIRO/cmsdoc.nsf/WebDoc/ndkw6u9bbd [Accessed 20th January, 2010].

VEHRING, R. 2008. Pharmaceutical Particle Engineering via Spray Drying. *Pharmaceutical Research,* 25**,** 999-1022.

VEHRING, R., FOSS, W. R. & LECHUGA-BALLESTEROS, D. 2007. Particle Formation in Spray Drying. *Journal of Aerosol Science,* 38**,** 728-746.

Chapter 6

Conclusions and Recommendations

6.1. Conclusions

This PhD thesis presented a comprehensive and systematic work on establishing the measurement and modelling protocols for dairy powder functionality characterization. The main outcomes from this work are:

i. **Establishment of the measurement protocol to characterise solubility.** The key contribution from this work is the establishment of the protocol to characterize the solubility of MPC powder using FBRM. This protocol could be applied to characterise the solubility of dairy powders in a reproducible and comparable manner in industrial and laboratory settings.

ii. **Investigation and modelling of powder dissolution kinetics.** A dissolution model was developed based on the Noyes-Whitney Equation with two possible scenarios considered, namely complete dissolution and incomplete dissolution. Analysis indicated that the incomplete dissolution model described the MPC powder dissolution kinetics more accurately with two parameters identified, namely the **dissolution rate constant (*k*)** and the **final particle size (d_∞)**. Dissolution rate constant was related to powder dispersibility whereas the final particle size related to powder solubility. The proposed dissolution model can serve as first estimation to characterize powder dissolution kinetics.

iii. **Correlation between effects of drying conditions on resulting powder functionality and microstructure properties.** To better understand the effect of

spray drying condition on resulting powder functionality and microstructure, mono-dispersed MPC particles were produced using a laboratory-scale spray drier. This study: 1) established the relationship between drying conditions (i.e. air temperature), resultant powder functionality (solubility) and microstructure (i.e. protein micelle network, particle shape and morphology); 2) produced mono-dispersed particle without deteriorating the functionality; 3) identified the techniques to elucidate the potential mechanisms of powder dissolution and for model development.

6.2. Recommendations

This PhD thesis has established the first step in generating a 'toolkit' for dairy powder functionality characterization. The future works are grouped into the four main sections as follow:

1) **Further development of the dissolution kinetic model**

   To further improve the dissolution kinetic model, elimination of variables in the model and corresponding experimental system should be considered. One potential variable to consider is the powder surface area. Industrial powders usually have wide particle size distributions and irregular surface areas, which increase the uncertainty when modelling the dissolution kinetics. By producing mono-dispersed particles, the variability in terms of particle size and shape can be eliminated from both experimental systems and model. This simplifies the model to better reflect the powder behaviours for the specified conditions. The experimental data acquired from the investigation of different drying conditions should be applied into the existing dissolution model to improve the dissolution model.

2) **Further investigation on techniques to characterize the full range of functionalities**

   Investigations into other potential techniques should be carried out to develop the characterisation toolkit for the full range of powders functionalities for different powder types. This toolkit will aid in standardising the benchmarking criteria for efficient testing of powder functionality for both manufacturers and end users.

3) **Development of powder characteristic profile library**

   Extensive benchmarking of dissolution profiles for different powder types to create a profile library of their functionalities.

4) **Application of the profile library and characterisation toolkit for product optimisation**. Investigations into the effects of spray drying processes on the powder quality (functionality and microstructure) should be carried out. These investigations should include the modelling of the process based on the characteristic profiles and models previously established for the required powder type, to help optimise the conditions for production. The toolkit should enable the functional properties of the resultant powder to be quickly analysed.

Appendix A

Understanding Wetting Behaviour of Dairy Powder using a Flow Channel

A.1. Introduction

Various techniques have been employed to characterize powder wetting property. One particular method by Freudig *et al.* developed in 1999 has successfully measured the dynamic wettability of milk powder by minimizing the movement of liquid surface (Freudig et al., 1999). They employed a two dimensional observation of wetting distance as a parametric measure of wettability (Figure A-1). In their experimental setup, a flow channel was built with a powder feeder. The testing powder was fed onto the water surface by the powder feeder, and was transported away from the feed point by the water flow, which mimicked the situation on the liquid surface for an un-baffled stirred vessel. The powder wetting behaviour was observed from the top downwards, so that the wettability was defined as the point all the powder sinks below the water surface.

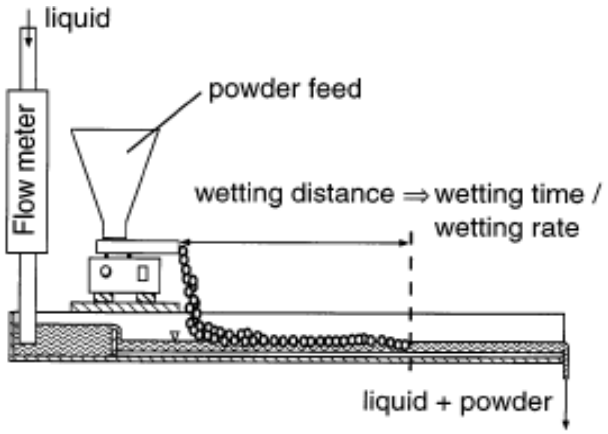

Figure A-1 Two dimensional Wetting Distance Experimental Design by Freudig *et al.* (Freudig et al., 1999)

To further understand the dissolution behaviours of different powders, an experimental setup modified from Freudig's study is proposed (as shown in Figure A-2). The change enabled the observation is extended from two dimensional to three dimensional. It is expected that the powder wetting behaviour can be observed from the top downwards, so that the wettability is defined as the point where all the powder sinks below the water surface (as shown in Figure A-3a). Meanwhile, it is expected to observe the smooth transition curve between water and milk powder solution alone the channel from the side (as shown in Figure A-3b). By this means, the powder wettability can be characterized by the wetting distance (*D*, as shown in Figure A-3) whereas dispersibility can be characterized by the dispersing distance (*d*, as shown in Figure A-3a) and the sinking angle (α, as shown in Figure A-3b).

The basis of the modification is that different powders have different wetting behaviours, with some requiring a shorter wetting time due to good wettability, while others with poor wettability taking a longer duration. By adjusting the flow rate and the powder feed rate, this method can potentially be used to characterize the wetting properties of a powder in a reproducible manner (if the exact flow velocity is known, and the determination of the point where the powder starts to sink can be done accurately). The accuracy can be improved by using more sophisticated imaging tools to determine the sink point, and modifying the channel dimension to reduce the wall effects that affect the velocity distribution.

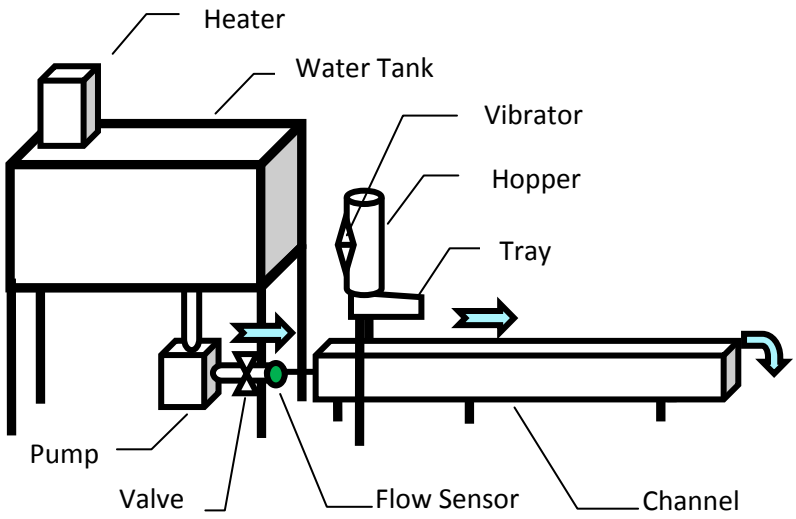

Figure A-2 Schematic setup of flow channel

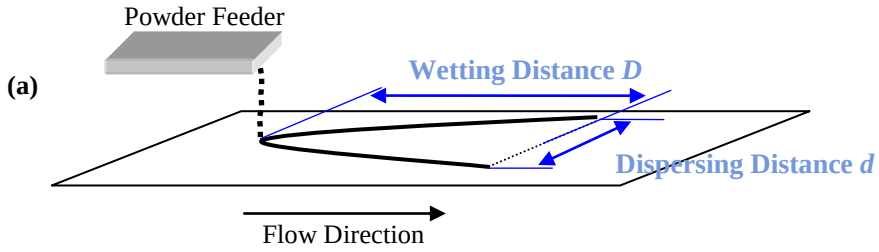

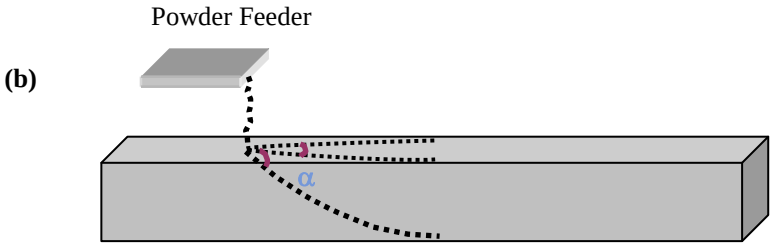

Figure A 6-1

Figure A-3 Extension of experimental setup from 2D (Wetting distance) to 3D observation (Wetting Distance and Dispersing Distance) in addition to observing the dispersion angles α

A.2. Experimental procedure

A.2.1. Proposed experimental setup

The experimental rig is design based on two main assumptions, namely

i. Laminar flow of medium in the flow channel;

ii. Sufficient distance for observation of the wetting behaviours of different powder types.

Therefore, the design of flow channel was carried out based on Reynolds number calculation:

$$\mathrm{Re} = \frac{\rho \cdot u \cdot d_h}{\mu} = \frac{\rho \cdot u \cdot A/p}{\mu} = \frac{\rho \cdot u}{\mu} \cdot \frac{B \cdot D}{(B + 2D)} < 2000$$

Equation A-1

where *Re* is Reynolds Number ,

ρ is mass density of fluid (kg/m^3),

u is mean velocity (m/s),

d_h is hydraulic diameter,

μ is dynamic viscosity (Pa·s),

A is cross-section area (m^2),

p is wetted perimeter (m),

B is the width of channel (m),

D is the depth of liquid in the channel (m).

There were two assumptions made in this calculation:

- Only trace of milk powder is fed and dissolved in water, thus the density and viscosity approximately remain the same, which is equal to that of water ($\rho_{water} \approx 1.0$ g/cm^3 and $\nu_{water} \approx 1.0 \times 10^{-3}$ Pa·s at 25 ℃) (ThermExcel, June 2003).
- Powder should travel far enough to be observed before sinking into water. For some instant powders, they have very good wettability and can sink into water within 2 seconds. Therefore, it is assumed that the $u_{max} \approx 0.05$ m/sec.

In this way, a relationship between the width *B* and depth *D* can be obtained.

$$\frac{B \cdot D}{B + 2 \times D} < 0.04 \qquad (B>0,\ D>0)$$

Equation A-2

To maintain an appropriate balance between the width and depth of the channel, and taking the water consumption into consideration, a compromise of B=6 cm and D=10 cm was made. In terms of the channel length, it has to be long enough for powder to wet and sink, while keeping the water turbulence minimal. The channel length was set to be 150 cm whereas the powder feed point start at 50 cm after the reservoir (to minimize the turbulence from the water entrance).

As mentioned before, the velocity is assumed to be $u_{max} \approx 0.05$ m/s, as such, the maximum flow rate can be deduced from:

$$Q = u \times A = u \times B \times D = 18 \text{ L/min}$$

Equation A-3

Thus, if each experiment lasts 3 minutes, the maximum water consumption is approximately 50 L, which decides the capacity of the water tank. On the other hand, from the flow rate, the working range of pump and flow sensor can thus be chosen.

The final setup and major component are shown in Figure A-4.

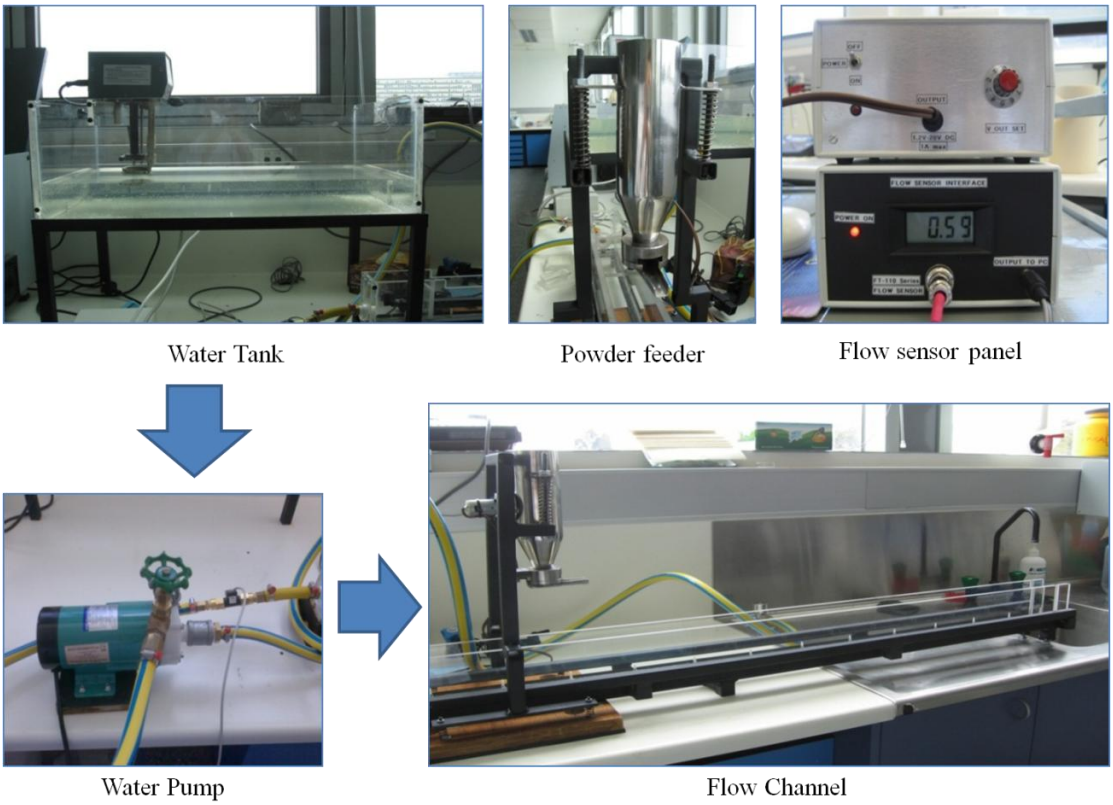

Figure A-4 Major component setup of designed flow channel

A.2.2. Calibration of Flow Sensor

The readout from flow sensor (which detects the flow rate of the water pump) is in voltage. Therefore, it is necessary to determine the relationship between the voltage reading and actual flow rate.

A flow sensor with working range 1 ~ 15 L/min was installed. The calibration results are shown as plots (Figure A-5) of voltage against calculated average flow rate. From this plot, the readout from the sensor is relatively consistently linear and an equation which represents the relationship between voltage and flow rate can be presented.

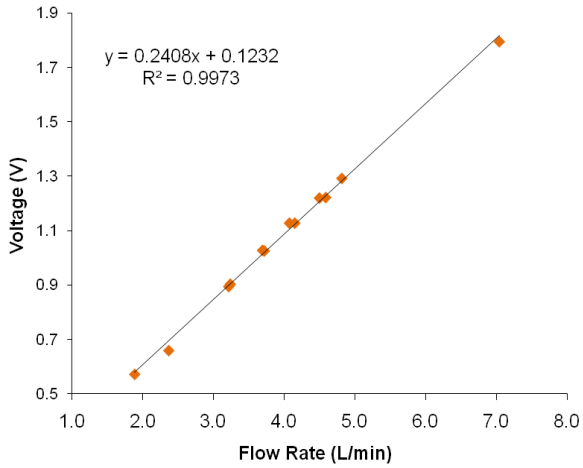

Figure A-5 Calibration plot for flow sensor with has an inconsistent output

A.2.3. Calibration of Powder Feeder

This powder feeder is powered by a motor which is a high torque DC motor with voltage range from 12 to 30V. The speed which the powder is fed onto the channel is another important component of the rig as it has to be consistent and stable for experimental consistency. Therefore, it is necessary to calibrate the powder feed rate.

The results of the calibration are shown in Figure A-6, which shows a plot of average feed rate (g/min) against each sample. Table A-1 shows the average feeding rate, standard deviation and error percentages for different runs conducted, from which it can be seen that the feed rate was relatively stable and repeatability was considerable good (with the average error percentage across the three trial runs was about 16.2%).

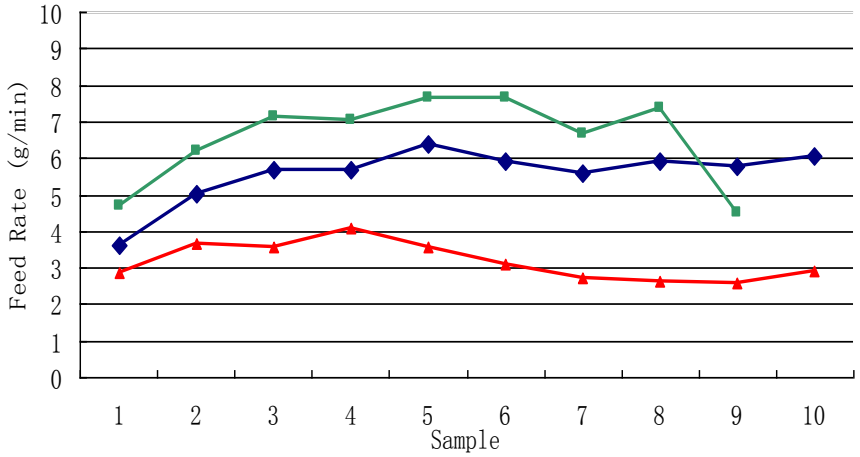

Figure A-6 Calibration results of powder feeder

Table A-1 Mean feed rate, standard deviation and error percentage of the powder feeder

Mean Feed Rate (g/min)	Stand deviation (g/min)	Error percentage

5.56	0.76	13.8%
6.54	1.19	18.3%
3.17	0.52	16.4%
Average Error Percentage		16.2%

A.2.4. Materials and method

Commercial skim milk powder (SMP) and whole milk powder (WMP) were obtained from local supermarket. The samples were sieved into 3 groups according to particle size, namely <100 µm, 100-224 µm and >244 µm using a sieve shaker (AS 200 digit, Retsch®, Germany). The powders were stored at room temperature before conducting each test. However, the amount collected for the group with size below 100 µm was insufficient for the test. The flow rate was maintained at the same level for all the runs, whereas the feed rates were slightly varied between runs. The testing conditions applied were as shown in Table A-2. All tests were carried out at room temperature.

Table A-2 Testing conditions

	Particle Size Range (µm)	Flow Rate (L/min)	Feed Rate (g/min)
SMP	100 < D < 224	6.63	15.46
	D > 224		13.14
WMP	100 < D < 224		9.66
	D>224		11.74
***All measurement were carried out at room temperature**			

A.3. Results and discussion

The following test runs on the rig had been conducted in order to investigate the performance of the rig and its components, assess the initial results of the powder dissolution behaviour and identify potential limitation and issues for improvement to the design of the rig. Different powder types (SMP and WMP) and particle size (D> 224µm and 100µm > D > 224µm) were tested in order to investigate the wetting behaviour of different powders in the flow channel. The visual observation results are shown in Figure A-7 whereas the testing conditions are as shown in Table A-3.

Table A-3 Results of the wetting distance and the calculated wetting time

	Particle	Wetting	Wetting Time (s)

	Size Range (μm)	Distance (cm)	
SMP	100 < D < 224	<80	12.07
	D > 224	80 < D < 100	12.07 < t < 15.08
WMP	100 < D < 224	N/A	N/A
	D>224	N/A	N/A

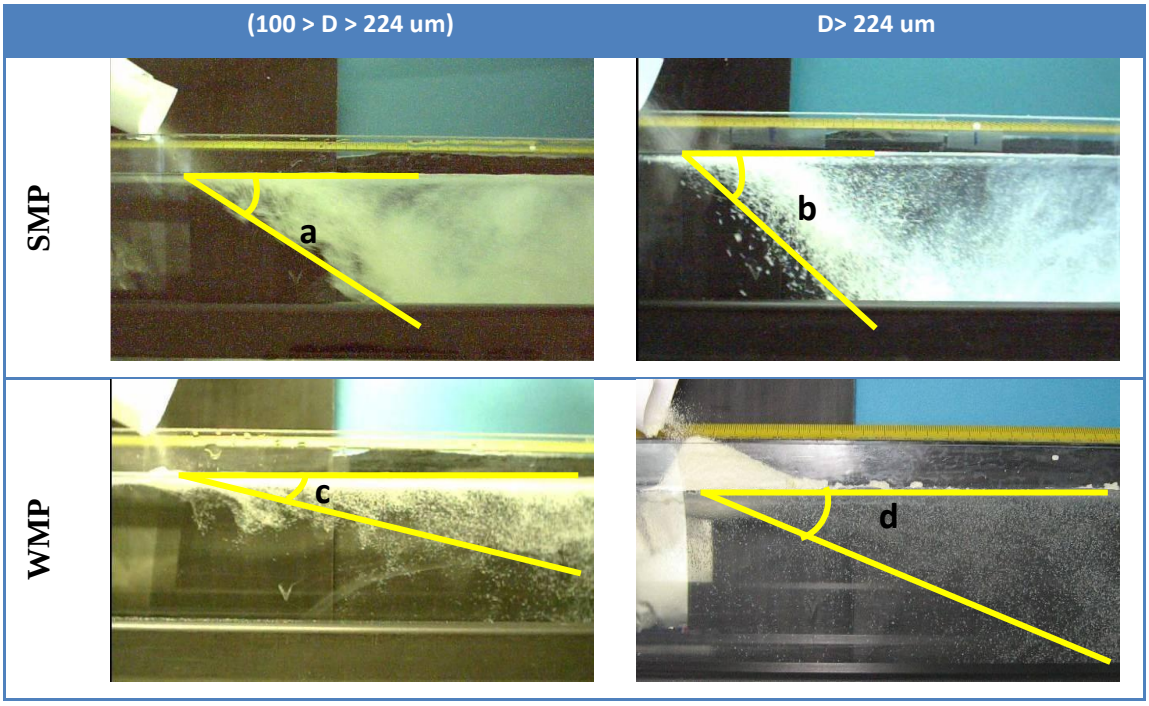

Figure A-7 Preliminary results (side camera recording image stills) of the test run for SMP and WMP at two different particle size sample groups

Observations from Figure A-7 indicated that there were significant differences in terms of the dissolution behaviour between the powder types as well as across the different particle size groups. Under the same flow rate and similar powder feed rate, SMP displayed higher wettability with a larger sinking angle (angles a and b in Figure A-7) and shorter wetting distance as compared to WMP. In terms of particle size groups, the sinking angles of large particles (b and d) were greater than that of the smaller particles (a and c). However, it is worth noting that WMP powders does not wet easily and form a thin layer on the water surface when they touch the water surface. The un-wetted powder eventually run off the channel (fine-tuning of the key input parameters may be required for future experiments). Moreover, for the larger particle size group of WMP, the powder tends to forms lump of powder at the feed point and not many of them sink into the water. From the top down

observation view of the particle dissolution (Figure A-8), it can be found that SMP forms fewer lumps when landing onto the water whereas WMP tend to have a wider spread and back draft.

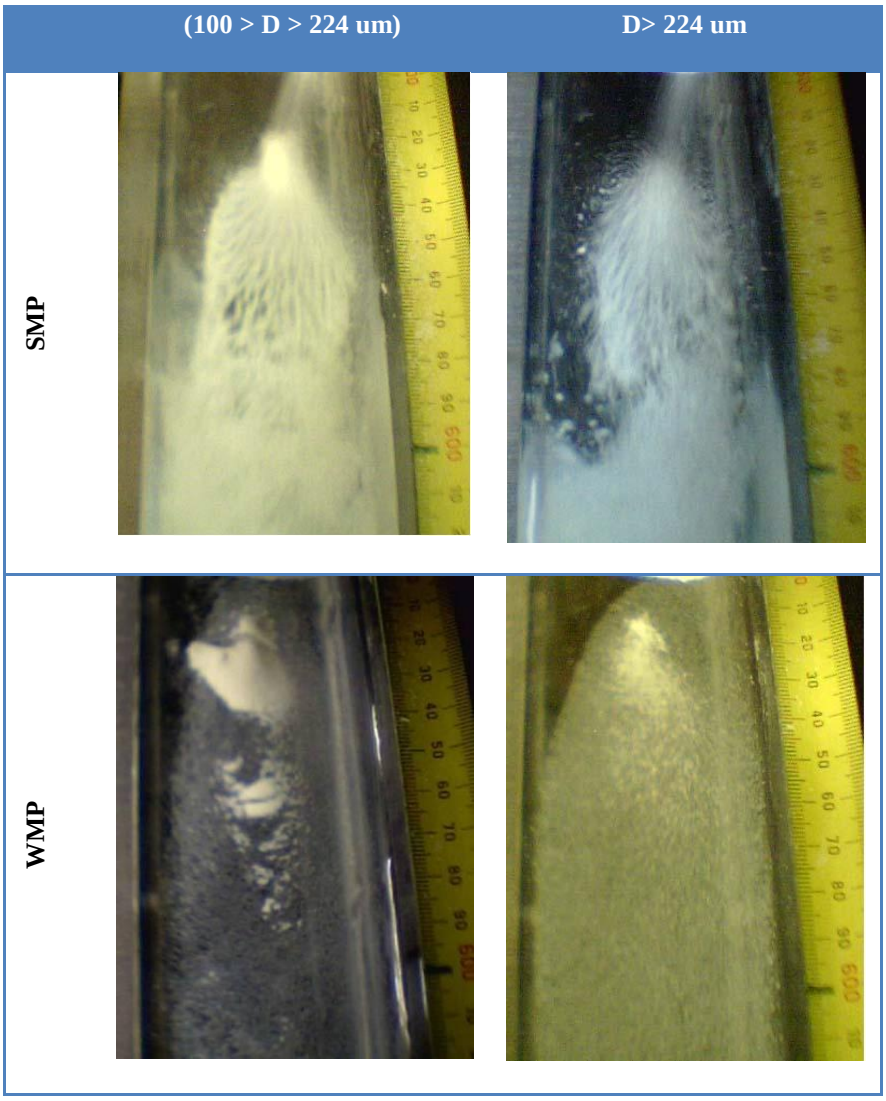

Figure A-8 Preliminary results (top down camera recording image stills) of the trial run for SMP and WMP at two different particle size sample groups

From these results it is clear that the system is able to qualitatively distinguish between the dissolution behaviours of different powders and sizes based on the three dimensional observation monitoring. There are existing issues on the accuracy of the quantitative measures in the setup, for example the determination of the sink point. These are primarily due to instability in the flow channel cause by turbulence. In addition, it is noted that when the powder feed rate is high (powder specific), lumps of powder aggregates tends to form as it falls onto the water surface, causing difficulty in wetting. On the other hand, at a low

powder feed rate; there are difficulty in tracking the characteristic curvature of the powder under the water surface as the small amount of powder was quickly carried away from the feed point (or if the flow rate is too high). Below are potential directions for approaching the key issues in future experiments.

To minimize turbulence, possible solutions should be investigated, two of which are as follows. The first option is to extend the length of the channel to keep the powder feeder and feed point at a considerable distance away from the water reservoir. The other possible option is to install a porous mesh between the powder feed point and reservoir to act as a buffer to smoothen the flow in the channel.

A.4. Conclusion

A pilot in-house flow channel was designed and constructed to characterize the dynamic wettability of various dairy powders. Using this flow channel, it was observed that different powders with different particle sizes behave distinctively different. Agglomerated particles tended to sink faster than the smaller particles, whereas hydrophobic powder like WMP tended to form lumps on the water surface due to the surface tension rather than sinking into water like SMP.

The setup was able to qualitatively distinguish between different powder types and size in the characterization test conducted. This technique is sufficient for qualitative analysis and characterization of powder dissolution behaviour. In order to quantitatively characterize the dairy powder dissolution properties, assistance from complementary techniques and further fine-tuning are required in order to optimize the system for reliable and accurate quantitative analysis.

A.5. References

FREUDIG, B., HOGEKAMP, S. & SCHUBERT, H. 1999. Dispersion of powders in liquids in a stirred vessel. *Chemical Engineering and Processing*, 38**,** 525-532.

THERMEXCEL. June 2003. *Physical characteristics of water (http://www.thermexcel.com/english/tables/eau_atm.htm) Last Access: 25th Feb, 2008* [Online]. [Accessed].

Appendix B

Understanding Milk Powder Dispersion using Turbiscan

B.1. Introduction

Four properties are generally used to classify dairy powder dissolution properties, namely wettability, sinkability, dispersibility and solubility (Chen, 1992). Among these properties, dispersibility can be used to determine the 'instant dissolution' of the dairy powder (Varnam and Surherland, 1994). In many applications, the de-agglomeration/dispersion of powders is of interests as it represents the efficiency of the processes and product quality.

Many techniques/methods have been used to investigate the dispersibility of dairy powders (Galet et al., 2004, Goalard et al., 2006, Chen and Lloyd, 1994). In this study, an optical analyser Turbiscan MA 2000 was employed to characterize powder dispersibility. This technique measures the independent and anisotropic scattering of light of an emulsion or suspension in a glass cylindrical tube which in this study is milk powder suspension. This method has been used in many applications such as sedimentation (Azema, 2006), crystallizations (Ali and et al., 2002), emulsion stability (Grotenhuis et al., 2003) and suspend stability (Ian and et al., 2005).

The key component of the Turbiscan is a moving detection head consisting of a pulsed near infrared light source (λ=850 nm) and two detectors (Sci-Tec, 2008, Mengual et al., 1999) as shown in Figure B-1. The light source emits infrared onto the suspension in the test tube, light that transmits through the suspension is detected by the transmission

detector located on the others side of the test tube (denoted 0 ° angle) while light that is obstructed and backscattered 135 ° along the path of the emitted light beam is detected by a backscattering detector (Sci-Tec, 2008). The intensity of transmission/backscattered light is dependent on the volume fraction of the particles in the suspension (Sci-Tec, 2008). The detection head moves up the length of the test tube to detect light intensity changes at 40 µm intervals, acquiring data on transmission/backscattering light intensity as a function of displacement along the length of the test tube. Transient data of intensity changes with time can be acquired by repeating each scan of the tube length at specific time intervals. In this way, the dynamic changes in the particle size along the length of the suspension with time can be monitored and outlined. Figure B-2 shows a typical readout from the Turbiscan depicting how the light intensity (y-axis) changes with displacement (x-axis) at different time-points (each curve represents one time-point).

In this study, the effects of different powder types, different powder particle sizes, as well as different concentrations on dissolution behaviour were investigated in order to assess the suitability of Turbiscan for characterization of powders dissolution behaviours.

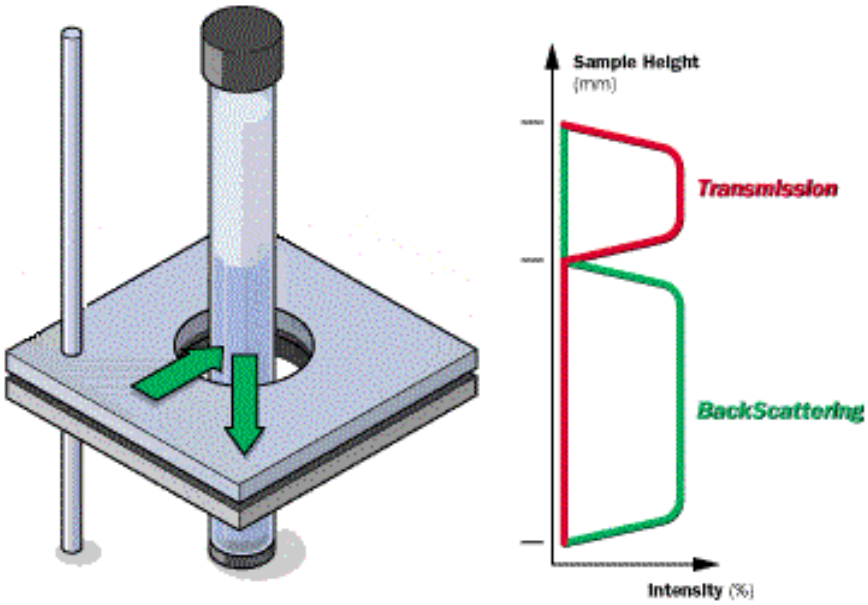

Figure B-1 Working principle of Turbiscan MA 2000 (Sci-Tec, 2008)

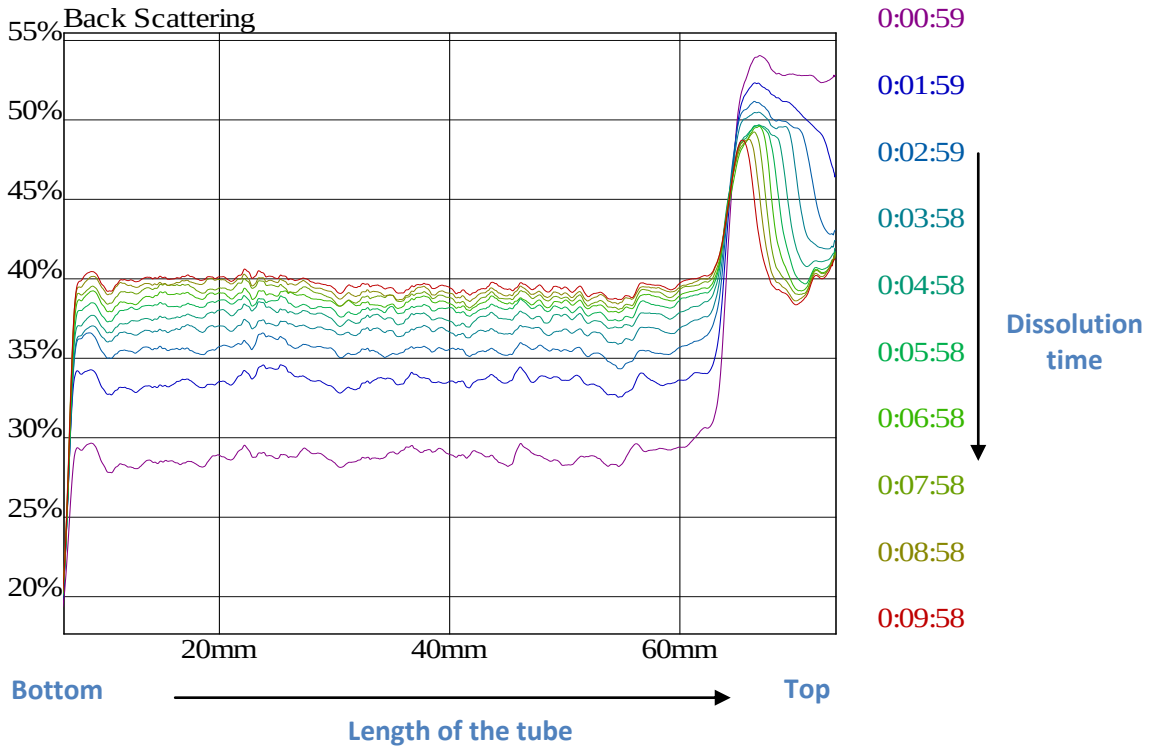

Figure B-2 Typical readout from Turbiscan for backscattering intensities at different time points where the x-axis denotes length of the tube from bottom (left) to top (right), y-axis denotes backscattering intensity reading and individual curves denoting independent scans at specific dissolution time-points.

B.2. Experimental Setup

B.2.1. Materials

Commercial skim milk powder (SMP) and whole milk powder (WMP) were obtained from local supermarket. SMP were sieved into different particle size (D) groups, namely D<100 μm, 100<D<150 μm, 150<D<200 μm, 200<D<250 μm, 250<D<300 μm, D>300 μm.

B.2.2. Dissolution behaviour for different types of powders

To investigate the dissolution dynamics of different powders, the following experiment was carried out: the cylindrical tube was filled with 10 mL of distil water prior to insertion into Turbiscan at room temperature. 0.2g ± 0.01g of powder was measured for each

powder type (WMP and SMP). The stopwatch was started as the powder sample was poured into the tube. The first scan was started after 10 seconds of lag time. The subsequent scan interval was set as 30 seconds, stopping the scan after 5 minutes. The transmission intensities of different powders were collected and compared.

B.2.3. Dissolution behaviour for different particle sizes

To investigate the dissolution behaviour of different particle sizes, the sieved particle size groups for SMP were used. The testing procedure was similar to Section B.2.2 with 0.2 ± 0.01g powder of different size groups weighted and poured into the tube while starting the stopwatch. Scanning started after 10 seconds lag time with interval set as 1 minute for a measuring duration of 10 minutes. Backscattering intensity data was collected and the intensity change with respect to the first scan was calculated for each time-point. The experiment was repeated to acquire triplicate data for each particle size group.

B.3. Results and Discussion

B.3.1. Dissolution behaviour for different types of powders

The dissolution of different powder types were investigated using Turbiscan with the resulting transmission readout for SMP (Figure B-3) and WMP (Figure B-4). For SMP it can be seen that the first scan was around 90% whereas the second scan dropped to less than 10%, subsequent scan gradual increased with time. It was noted that the reading at the bottom of the tube was very low compared with the reading at the top of the tube, and remained almost at zero throughout the testing period. On the other hand, the readouts of WMP were completely different from that of SMP. First of all, it was noted that all the readouts of WMP have significantly more fluctuations and the transmission intensity decreased with time (whereas that of SMP increased with time).

Visual inspection of SMP and WMP powder dissolution behaviours was conducted in parallel with the Turbiscan measurements. When SMP came in contact with the water surface, a layer was formed on the surface which started to sink immediately, dropping quickly and subsequently landed and remained at the bottom of the tube. On the contrary, WMP formed a layer on the water surface upon contact with water, but it took some time to get wetted and sink. Once sunken, WMP immediately started dissolving with little accumulation of WMP particles at the bottom of the tube.

As mentioned in Chapter 2, the dissolution of milk powder comprises of soluble components such as lactose, un-denatured whey protein and salts, as well as dispersible components like casein and fat. In order to verify that the soluble components do not affect the transmission, a baseline verification scan was done by comparing lactose solution (2g/10mL water) with distilled water. As shown in the baseline measurement readout in Figure B-5, the transmission of lactose solution has identical level of transmission readout as distilled water (~90%) which verifies that the soluble components has no influence on transmission readout. Therefore, only the dispersible components affect the transmission.

From the factory report data shown in Table B-1, the dispersible components in SMP takes up about 35%, of which 34.5% are protein. The size of fat globule ranges from 0.1 to 15 μm (Fox and McSweeney, 1998) with an average of 4 μm (Jensen, 2002), whereas the size range of casein is from 0.02 to 0.3 μm (Walstra and Jenness, 1984). The working range of Turbiscan is from 0.05 to 5000 μm (Sci-Tec, 2008) which implies that the Turbiscan might not be sensitive enough to detect casein micelles as compared to the larger fat globule, which fits into the working range. As such, SMP's (with a lower dispersible fraction, smaller particle size and less fat content than WMP) transmission increases as it dissolves.

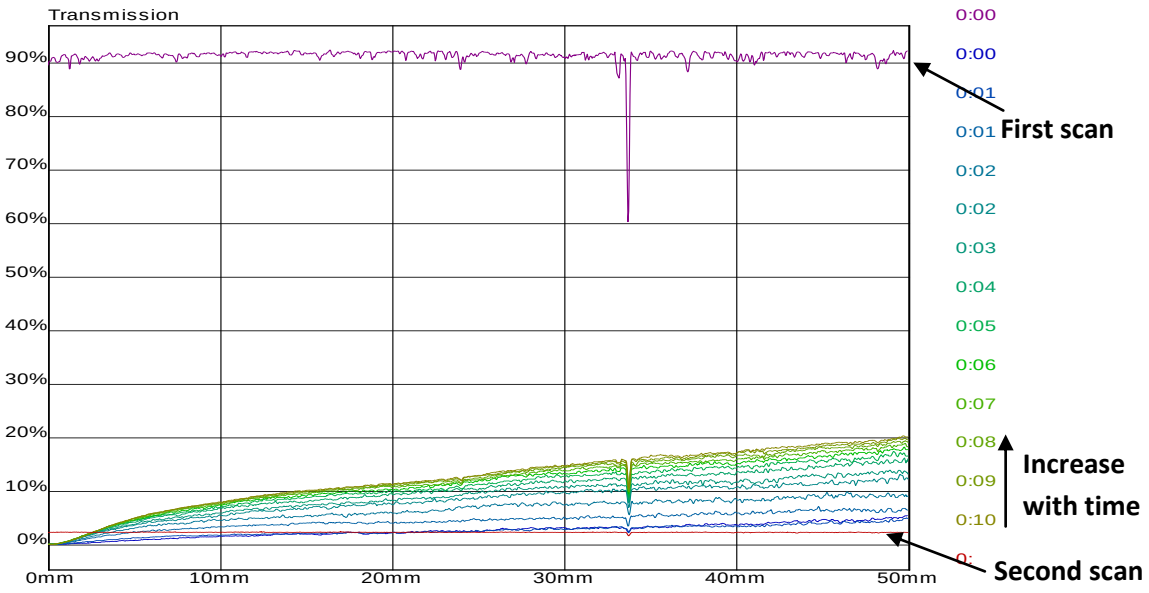

Figure B-3 Turbiscan transmission intensity readout for SMP

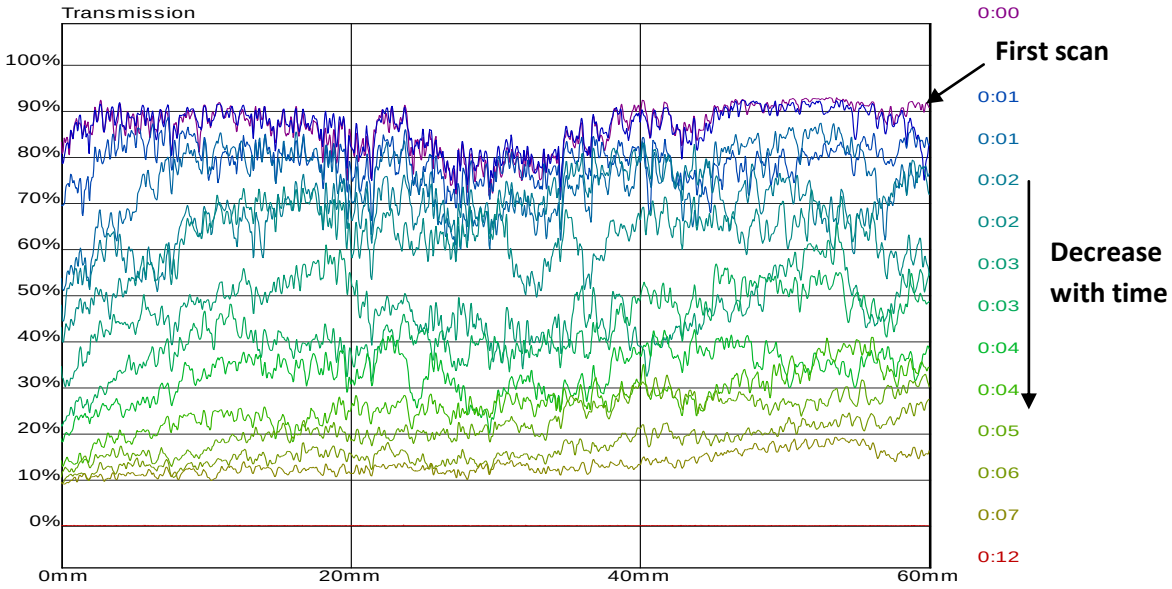

Figure B-4 Turbiscan transmission intensity readout for WMP

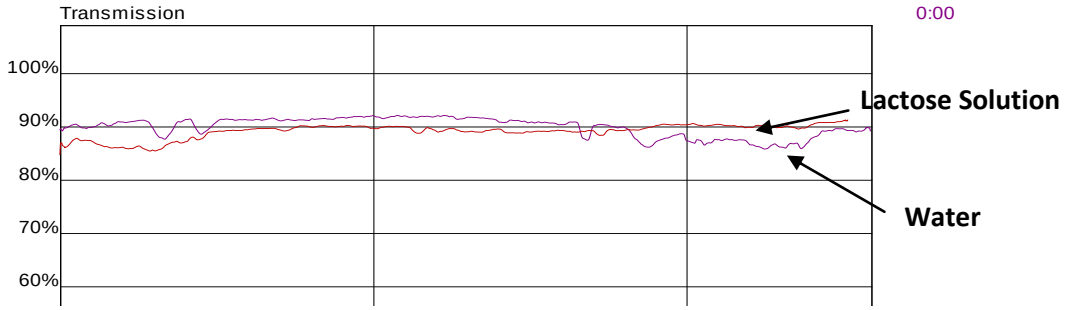

Figure B-5 Transmission intensity of lactose solution compared with water

Table B-1 Dispersible fraction and particle size for different powder types (Fox and McSweeney, 1998) (Walstra and Jenness, 1984) (Sci-Tec, 2008)

	Dispersible Fraction		Total Percentage
	Fat (%)	Protein (%)	
SMP	0.5	34.5	**35%**
WMP	27.3	24.3	**51.6%**
Particle Size	0.1-10 µm	0.02-0.3 µm	
Turbiscan Working Range	**0.05-5000 µm**		

B.3.2. Dissolution behaviour for different particle sizes

The dissolution behaviour for particles with different sizes ranges was investigated. Backscattering intensities readouts for different particle size groups of SMP was collected and the change in backscattering (delta-backscattering) calculated for each time-point. A

steeper delta-backscattering with time implies faster dissolution. Figure B-6 shows the average delta-backscattering for different particle size group with time. With the exception of particle size group <100μm, the rate of increment of delta-backscattering in time decreases with increasing particle size. Particle size group 100-150μm has the fastest rate of increment and had the best dispersibility, with smaller amount of agglomeration. Larger sized particles take longer to de-agglomerate, thus a slower rate of delta-backscattering increment. Particle size group <100μm appears to be behave differently probably as the particle size are too small and fine, making it hard to sink into the water as mentioned in Section 2.2.5.2.

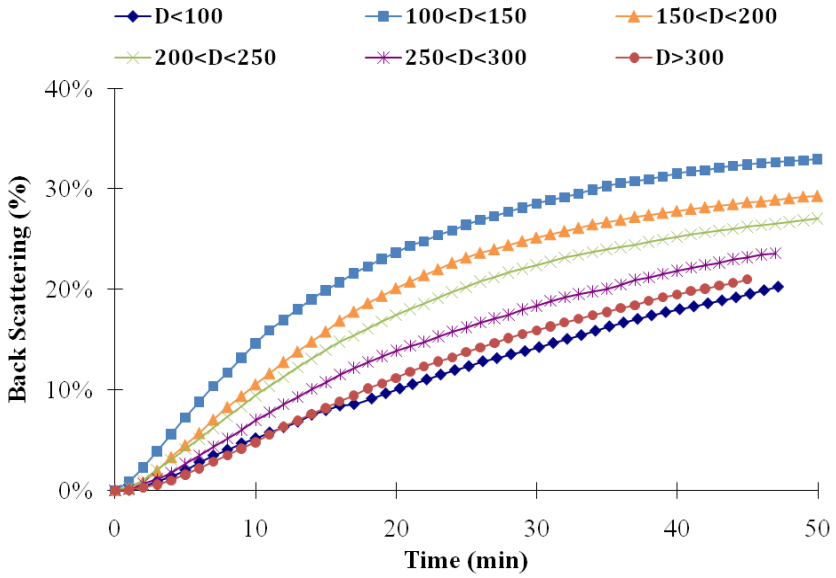

Figure B-6 Average delta-backscattering for different particle size groups in time

B.4. Conclusions

The dissolution behaviours of different powder types and particles size were investigates using the Turbiscan. Results indicated that this Turbiscan technique was able to distinguish between SMP and WMP with the dissolution behaviours of SMP and WMP being significantly different. This study also demonstrated the ability of Turbiscan to qualitatively distinguish between different powder size groups with larger particles having poorer dispersibility compared to smaller particle groups. As such, Turbiscan is able to characterize powder dispersion property qualitatively, however for quantitative

measurements and accuracy, potential complementary techniques or methods will be required.

B.5. References

ALI, A. & ET AL. 2002. Investigation of on-line optical particle characterization in reaction and cooling crystallization systems. Current state of the art. *Measurement Science and Technology,* 13**,** 349.

AZEMA, N. 2006. Sedimentation behaviour study by three optical methods -- granulometric and electrophoresis measurements, dispersion optical analyser. *Powder Technology,* 165**,** 133-139.

CHEN, X. D. 1992. Whole Milk Powder Agglomeration—Principles and Practice. *Milk Powder for the Future.* Palmerston North, New Zealand: Dunmore Press.

CHEN, X. D. & LLOYD, R. J. 1994. Some aspects of measuring the size and rate of dispersion of milk powder agglomerates using the Malvern Particle Sizer 2600c. *journal of Dairy Research,* 61**,** 201-208.

FOX, P. & MCSWEENEY., P. L. H. 1998. Dairy Chemistry and Biochemistry. Springer - Verlag.

GALET, L., VU, T. O., OULAHNA, D. & FAGES, J. 2004. The Wetting Behaviour and Dispersion Rate of Cocoa Powder in Water. *Food and Bioproducts Processing,* 82**,** 298-303.

GOALARD, C., SAMIMI, A., GALET, L., DODDS, J. A. & GHADIRI, M. 2006. Characterization of the Dispersion Behavior of Powders in Liquids. *Part. Part. Syst. Charact.,* 23**,** 154-158.

GROTENHUIS, E. T., TUINIER, R. & DE KRUIF, C. G. 2003. Phase Stability of Concentrated Dairy Products. *J. Dairy Sci.,* 86**,** 764-769.

IAN, A. C. & ET AL. 2005. Determination of Particle Size Distribution by Laser Diffraction of Doped-CeO2 Powder Suspensions: Effect of Suspension Stability and Sonication. *Particle & Particle Systems Characterization,* 22**,** 310.

JENSEN, R. G. 2002. The Composition of Bovine Milk Lipids: January 1995 to December 2000. *J. Dairy Sci.,* 85**,** 295-350.

MENGUAL, O., MEUNIER, G., CAYRE, I., PUECH, K. & SNABRE, P. 1999. Turbiscan MA2000: Multiple light scattering measurement for concentrated emulsion and suspension instability analysis. *Talanta,* 50**,** 445-456.

SCI-TEC. 2008. *TURBISCAN MA 2000 (http://www.sci-tec-inc.com/TurMapr.html?reload_coolmenus) Last Accessed: 18 Feb 2008* [Online]. Sci-Tec Inc. [Accessed].

VARNAM, A. H. & SURHERLAND, J. P. 1994. *Milk Powder Technology: Evaporation and Spray Drying*, Copenhagen, Denmark, NIRO A/S.

WALSTRA, P. & JENNESS, R. 1984. *Dairy Chemistry and Physics*, New York, Chichester, Brisbane, Toronto, Singapore, A Wiley-Interscience Publication.

Appendix C

Application of FBRM to Characterize the Solubility of Different Dairy Powders

C.1. Introduction

In previous work, it has been demonstrated that the capability of focused beam reflectance measurement (FBRM) to characterize dissolution properties of milk protein concentrate (Fang et al., 2010). By on-line monitoring particle size changes with time, FBRM is able to work with a wide range of concentrations. In this section, the suitability of FBRM to characterize the solubility of different dairy powders types was assessed. By applying the protocol developed previously, the dissolution behaviours of different types of powders with varying properties were tested. The expected outcome of this study is the establishment and benchmarking of the dissolution profiles of different types of powders using the data obtained from FBRM as well as ascertain the adequacy of the establish FBRM measurement protocol.

C.2. Experiment

C.2.1. Materials

Different types of powders with very different functional and chemical properties were investigated in this study. Powders investigated include skim milk powder (SMP) and whole milk powder (WMP) which were obtained from the local supermarket, whereas milk protein concentrate (MPC) and whey protein concentrate (WPC) were provided by local manufacturers. Samples were stored at room temperature before the conduct of

solubility test using FBRM. For assessing the reproducibility of the characterization protocol, an independent set of industrial MPC was set aside as a validation dataset.

C.2.2. Experimental procedure

The experimental setup was based on our previous work as described in Chapter 3 (Fang et al., 2010). The procedures are as follows: 3g ±0.01g of powder were weighted and poured into a 250 mL beaker with 150 mL DI water to make up a 2 wt% solution at room temperature (21 ℃). An overhead stirrer was used at 400 r.p.m stirring rate. The data from FBRM was collected using iC FBRM^{TM} program (Mettler Toledo), with the collecting interval set at 5 seconds for 20 minutes duration for WMP, MPC and WPC, and 5 minutes duration for SMP. The chord lengths readouts for the different powders within the first 5 minutes were collected, exported and analysed.

C.3. Results and discussion

C.3.1. Reproducibility of FBRM on characterize dairy powder solubility

One of the key criteria for the suitability of the measurement protocol is that it has to be reproducible and accurate. To do that, the same batch of MPC powder was tested on alternate days for four consecutive days and the chord length readouts analysed as shown in Figure C-1. It can be clearly seen from the readout that the resulting curves for the different days were highly correlated with an average inter-sample error of less than 5%. This indicates and verifies the good reproducibility of this protocol and technique. It was also noted that variations mainly appeared at the later stages of dissolution (500-1800 seconds). As most industrial and consumer applications will look at rapid dissolution behaviors of powders, the initial dissolution kinetics will be of greater interest and importance. As such, the different powders were tested for 300 seconds and the dissolution profiles compared.

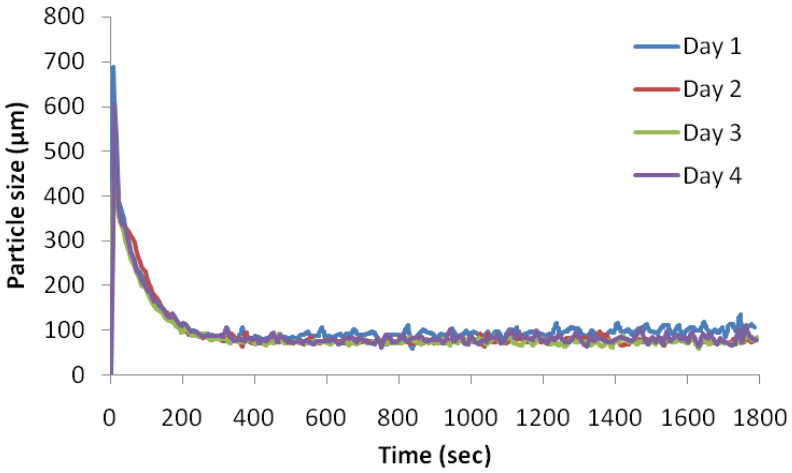

Figure C-1 Reproducibility of measuring the MPC solubility using FBRM

C.3.2. Dissolution profile of skim milk powder (SMP)

The dissolution profile of SMP was obtained based on the chord length reading off the FBRM. The resulting chord length reading of SMP is as shown in Figure C-2. It can be seen that there was a very rapid decrease in chord length reading reaching a minimum (~60 µm) within 50 seconds. This suggested that this commercial SMP had very good dissolution property, as upon contact with water, the powder de-agglomerated rapidly and dissolved within a very short time period.

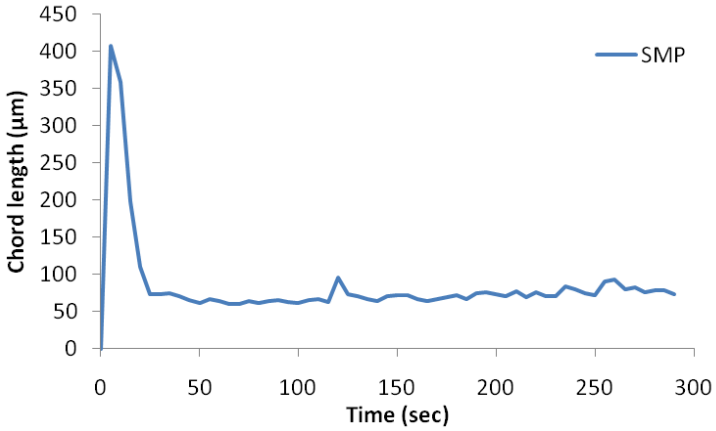

Figure C-2 Dissolution profile of SMP measured by FBRM

C.3.3. Dissolution profile of whole milk powder (WMP)

The dissolution profile of WMP was obtained with corresponding chord length reading from FBRM as shown in Figure C-3. It can be seen that WMP had a relatively poor solubility as it took 400 seconds for the chord length to reach a minimum (~80 µm). From visual inspection, it is clear that it took longer for lumps of WMP which forms upon contact with water, to de-agglomerate and sink under the water surface, even with the aid of stirring.

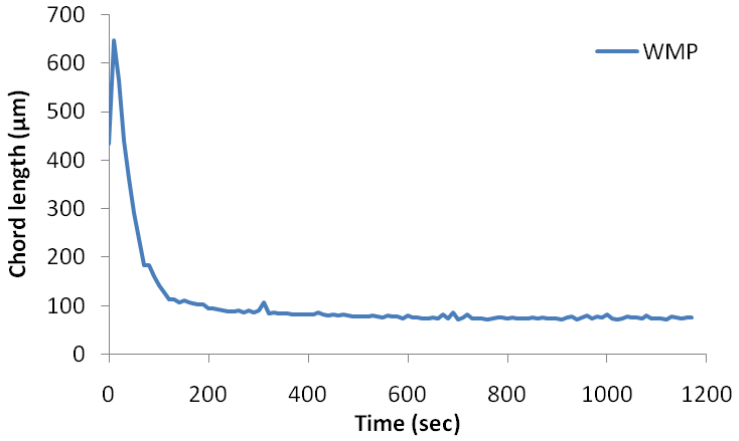

Figure C-3 Dissolution profile of WMP measured by FBRM

C.3.4. Dissolution profile of milk protein concentrate (MPC)

The dissolution profile of MPC was obtained with corresponding chord length reading from FBRM as shown in Figure C-4. It can be seen that upon contact with water, the chord length rapidly decreased to a point (~150 µm) and steadily decreased for the remaining testing duration.

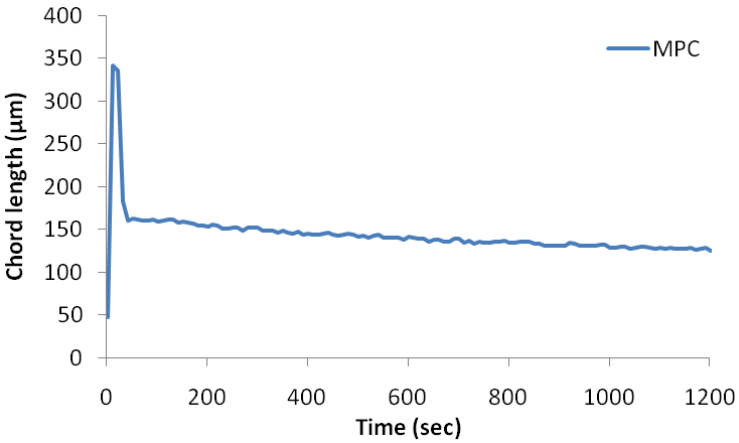

Figure C-4 Dissolution profile of MPC measured by FBRM

C.3.5. Dissolution profile of whey protein concentrate (WPC)

The dissolution profile of WPC was obtained with corresponding chord length from FBRM as shown in Figure C-5. It exhibited similar behavior with MPC, as the chord length rapidly decreases till a chord length of about 140 µm before decreasing slowly for the rest of the test duration with some fluctuations.

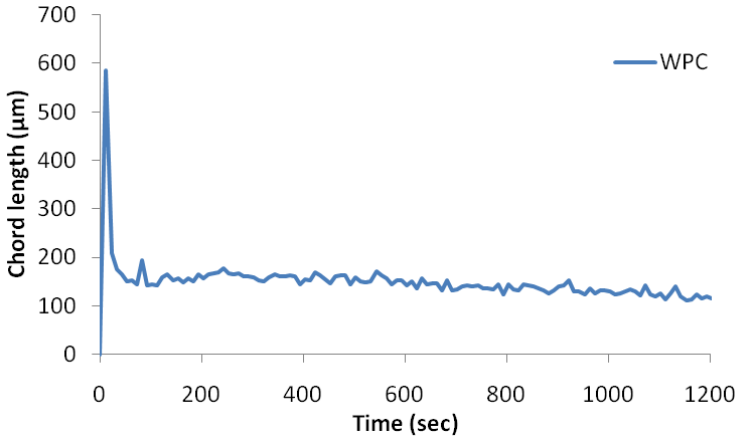

Figure C-5 Dissolution profile of WPC measured by FBRM

C.3.6. Comparison of the dissolution profiles between different powders

Figure C-6 shows the dissolution profiles based on chord length reading for all the tested powders for 300 seconds dissolution period. Although the production and storage history for the powders were unknown, distinct trends were observed for all the tested powders. It is clear that SMP had the best solubility among these powders; with the fastest drop in chord length and the smallest final reading. WMP has the slowest reduction in chord length and did not reach the same level as that of SMP until more than 250 seconds. As WMP had a higher fat content than SMP, it made WMP more hydrophobic. Therefore, when WMP come into contact with water, its individual particles formed lumps due to surface tension and caused WMP to take a longer duration to break up and dissolve.

As for MPC, it had higher final chord length than SMP and WMP primarily due to its relatively higher protein content. Previous studies had suggested that the dissolution rate limiting step for MPC was the release of micelles from the primary particles (Mimouni et al., 2009) and consequently MPC particles remained as whole particles within the testing period instead of dissolving and releasing components into the aqua phase. Therefore, MPC particle size change exhibited a rapid decrease at the beginning (as compared to WMP) and subsequently a very slow decrease till the end of the test.

WPC exhibited similar trend as that of MPC. However, from visual inspection of the WPC solution that resulted from the dissolution test, it was noted that there was no visible particle left in the solution and the solution was relatively translucent when compared with the other powders' solutions. Moreover, the results obtained from sedimentation tests suggested that the sediment amount was 45 wt% for MPC and less than 1 wt% for WPC

(Figure C-7). The sedimentation test result indicated that WPC was very soluble compared with MPC. This optical property of WPC solution could potentially cause readout variation as the low background maybe causes noise to be picked up like for example the air bubbles caused by agitation. Caution should be taken to avoid this like for example for WPC solubility characterization, it is recommended to test with a lower stirring rate.

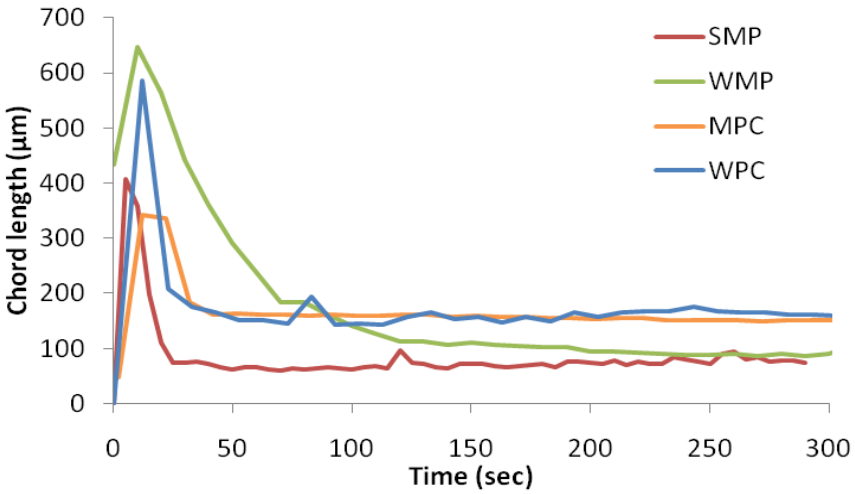

Figure C-6 Comparison of dissolution profiles of different powders measured by FBRM

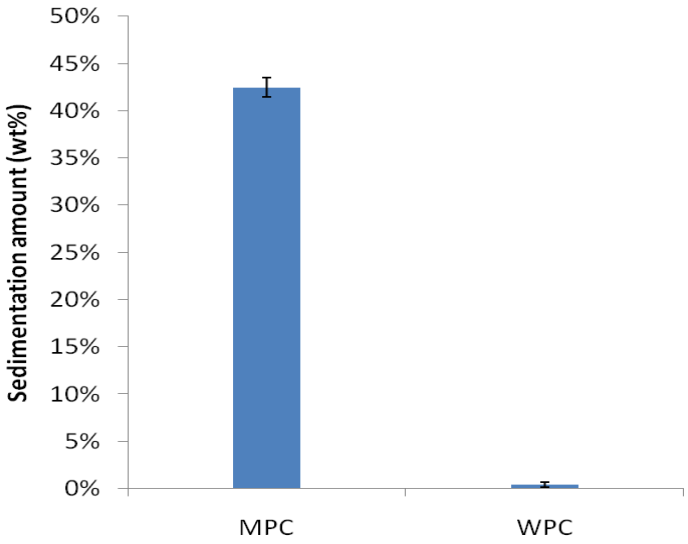

Figure C-7 Sedimentation amounts of MPC and WPC

C.4. Conclusion

In this study, the dissolution profiles of different powder types with varying physical properties were obtained using FBRM. Results indicate that this set of protocol is able and adequate to accurately characterize the different powder solubility in a reproducible

manner whereby dissolution profiles of the different powders can clearly distinguished from one another. With the establishment of this protocol, further analysis and modelling on powder kinetics can be conducted on different dairy powders of interest. It is hoped that this study will aid in the establishment of a standardized testing protocols for both industrial and laboratory testing of dairy powders

C.5. References

FANG, Y., SELOMULYA, C. & CHEN, X. D. 2010. Characterization of Milk Protein Concentrate Solubility using Focused Beam Reflectance Measurement. *Dairy Science and Technology*.

MIMOUNI, A., DEETH, H. C., WHITTAKER, A. K., GIDLEY, M. J. & BHANDARI, B. R. 2009. Rehydration process of milk protein concentrate powder monitored by static light scattering. *Food Hydrocolloids,* 23**,** 1958-1965.